1240180
[0075136H]

WCH-515
Rev. 0

River Corridor Closure Contract

Parameter Uncertainty for the ERDF Performance Assessment Uncertainty and Sensitivity Analysis

February 2013

RECEIVED
SEP 13 2016
EDMC

For Public Release

Washington Closure Hanford

Prepared for the U.S. Department of Energy, Richland Operations Office
Office of Assistant Manager for River Corridor

1540180

TRADEMARK DISCLAIMER

Reference herein to any specific commercial product, process, or service by trade name, trademark, manufacturer, or otherwise, does not necessarily constitute or imply its endorsement, recommendation, or favoring by the United States Government or any agency thereof or its contractors or subcontractors.

This report has been reproduced from the best available copy.

Printed in the United States of America

DOCUMENT CONTROL 03/13/2013 aB

WCH-515
Rev. 0

STANDARD APPROVAL PAGE

Title: Parameter Uncertainty for the ERDF Performance Assessment Uncertainty and Sensitivity Analysis

Author Name: C. Courbet and S. Mehta

Approval: W. A. Borlaug, Waste Operations Project Engineer

W. A. Borlaug
Signature

3/12/2013
Date

The approval signature on this page indicates that this document has been authorized for information release to the public through appropriate channels. No other forms or signatures are required to document this information release.

WCH-515
Rev. 0

River Corridor
Closure Contract

Parameter Uncertainty for the ERDF Performance Assessment Uncertainty and Sensitivity Analysis

February 2013

Authors:
C. Courbet
S. Mehta

For Public Release

Washington Closure Hanford
Prepared for the U.S. Department of Energy, Richland Operations Office
Office of Assistant Manager for River Corridor

EXECUTIVE SUMMARY

This data package provides uncertainty ranges and probability distribution functions of model input parameters that are considered in the uncertainty and sensitivity analyses for the Environmental Restoration Disposal Facility performance assessment. The data package provides the technical basis for the selection of parameter values using the available information regarding conceptual framework of the engineered and natural system; the deep drainage estimates (i.e., recharge rates) at the Hanford Site; and the physical, hydrologic, and contaminant transport properties of the geologic materials below the facility. All of the data and interpreted information were extracted from existing documents and databases. Special attention is given to presenting and justifying the rationale behind appropriate data selection and the assignment of appropriate probability distribution functions for each input parameter in order to properly represent parameter uncertainty without undue conservative bias.

TABLE OF CONTENTS

1.0 INTRODUCTION 1
2.0 METHODOLOGY FOR PROPAGATION OF UNCERTAINTY 2
3.0 RATIONALE FOR ASSIGNING UNCERTAINTY DISTRIBUTION 3
4.0 VADOSE FLOW-FIELD GENERATION USING STOMP-BASED MODEL 6
4.1 CONCEPTUAL MODEL FOR TEMPORAL EVOLUTION OF ERDF 6
4.1.1 Conceptual Timeline 6
4.1.2 ERDF-Specific Subsurface and Hydrogeological Context 10
4.2 RANGES OF FLOW PARAMETERS FOR STOMP 13
4.2.1 Recharge 13
4.2.2 Water-Retention Properties 24
4.2.3 Anisotropy 34
4.3 PROPAGATION OF UNCERTAINTY IN FLOW-FIELD USING PROCESS-LEVEL STOMP MODEL 37
4.4 ABSTRATION OF FLOW-FIELD FOR GOLDSIM-BASED MODEL 37
5.0 SATURATED ZONE FLOW-FIELD 38
5.1 SATURATED HORIZONTAL HYDRAULIC CONDUCTIVITY 38
5.2 ANISOTROPY IN SATURATED HYDRAULIC CONDUCTIVITY 41
5.3 HYDRAULIC GRADIENT 41
5.4 SPECIFIC STORAGE 43
6.0 TRANSPORT PARAMETERS FOR MODELING 43
6.1 AQUEOUS/SOLID PARTITIONING RATIO (K_d) 44
6.1.1 K_d for Sandy and Gravelly Units 46
6.1.2 K_d for Silt-Dominated Cold Creek (CCuz) 48
6.1.3 K_d for Carbonate-Dominated Cold Creek (CCuc) 50
6.2 EFFECTIVE BULK DENSITIES 51
6.3 EFFECTIVE DIFFUSION COEFFICIENT 52
6.4 VADOSE ZONE MACRODISPERSIVITIES 52
6.5 SATURATED ZONE MACRODISPERSIVITIES 53
7.0 POST-CLOSURE ERDF INVENTORY 54
8.0 CONCLUSION 58
9.0 REFERENCES 64
APPENDIX A – PROPAGATION OF UNCERTAINTY IN VADOSE ZONE FLOW PARAMETERS A-1

FIGURES

1. 2008 (Top) and 2009 (Bottom) Aerial Photography of the ERDF Site. 9
2. Soil Types on the Central Plateau (BNWL-243). 11
3. West-East Hydrogeologic Cross-Section through the ERDF (WCH-463). 13
4. Location of Boreholes and Cross Sections Used to Generate the ERDF Hydrogeologic Conceptual Model (WCH-463). 14
5. Triangular Distribution of Recharge Rate (mm/yr) for Vegetated Rupert Sand. 17
6. Triangular Distribution of Recharge Rate for Rupert Sand without Vegetation. 19
7. Triangular Distribution of Recharge Rate (mm/yr) for the Top of the RCRA-Compliant Barrier during the Second Sub-Period (2135-2535) of Early Post-Closure. 22
8. Triangular Distribution of Recharge Rate (mm/yr) for the Top of the RCRA-Compliant Barrier during Late Post-Closure. 24
9. Location of the Samples Selected in WCH-464 to Build the ERDF Data Set of Soil Hydraulic Properties. 26
10. Observed Distributions of the Water-Retention Parameters for Hanford Formation 2 (12 Samples). 30
11. Some Observed Correlations Between Water Retention Parameters for Hf2 (12 samples). 32
12. Water Retention Curves of the Hf1 Unit Obtained (i) by a Fit on Observed Retention Data for Each Hf1 Sample (in Red), (ii) by 50 Realizations of Sampled Parameters (in Gray) and (iii) Composite Water Retention Curve (in Black) Obtained by a Simultaneous Fit on All the Available Retention Data of the Hf1 Unit. 32
13. Unsaturated Hydraulic Conductivity Curves for Hf1 Unit Obtained (i) By a Fit on Observed Retention and Conductivity Data for Each Hf1 Sample (Red), (ii) By 50 Realizations of Sampled Parameters (In Gray) and (iii) Composite Water Retention Curve (In Black) Obtained By a Simultaneous Fit on All the Available Retention and Conductivity Data of the Hf1 Unit. 33
14. Observed Distribution of the Saturated Hydraulic Conductivity of Ringold Formation Unit E Considering Slug Tests and Sediment Sample Analyses for the 200-ZP-1 Model (DOE/RL-2007-28). 39
15. Location of the Tested Wells Near the ERDF and Calibrated Horizontal Hydraulic Conductivity Field Given by the Central Plateau Model V3.4 in the ERDF Area for the Ringold Formation Unit E. 40
16. Comparison of PNNL-19482 Slug Test Results with Central Plateau Model Calibration in the ERDF Area. 40
17. Predictive Heads (m) Below the ERDF Given by the Central Plateau Model Version 3.4 Until 2200. 42
18. Observed and Simulated W-NE Hydraulic Gradient (%) Through the ERDF Given by the Central Plateau Model Version 3.4 Until 2300. 42

TABLES

1. Main Uses of Several Common Distribution Functions (Mishra 2002). 4
2. Guidance for Selection of Probability Distribution Function Considering the Data Constraints (according to Harr 1987). 6
3. Timeline Considered for Representing the Evolution of the ERDF Conceptual Model Over Time. 7
4. Estimates of Recharge Rate Available for Vegetated Rupert Sand in the Central Plateau. 16
5. Estimates of Recharge Rate Available for Rupert Sand Without Vegetation. 18
6. Estimate of Recharge Rate Available for Barrier Side Slopes. 20
7. Estimates of Recharge Rate Available for Side Slopes after the 100-Year Institutional Control Period when they are Expected to Resemble Burbank Loamy Sand with Shrub Steppe. 20
8. Estimate of Recharge Rate Available for Modified RCRA C or Hanford Surface Barrier Top During Its Design Life. 21
9. Estimates of Recharge Rate Available for Vegetated Ephrata Stony Loam Inferred from Vegetated Sandy Loam Estimates. 22
10. Estimates of Recharge Rate Available for Vegetated Warden Silt Loam to Represent the Top Portion of the Surface Barrier After Its Design Life. 23
11. Summary of the Recharge Distribution Functions that will be Considered for the ERDF PA Uncertainty and Sensitivity Analyses. 25
12. Van Genuchten Parameters, Fitted Saturated Hydraulic Conductivity, and Measured Bulk Density Data for the Hanford Formation 1 (Gravel-Dominated) Unit (WCH-464). 27
13. Van Genuchten Parameters, Fitted Saturated Hydraulic Conductivity, and Measured Bulk Density Data for the Hanford Formation 2 (Sand-dominated) Unit (WCH-464). 27
14. Van Genuchten Parameters, Fitted Saturated Hydraulic Conductivity, and Measured Bulk Density Data for the Cold Creek CCuz (Silt-dominated) and CCuc (Caliche) Units (WCH-464). 28
15. Van Genuchten Parameters, Fitted Saturated Hydraulic Conductivity, and Measured Bulk Density Data for the Ringold RFtf Unit (WCH-464). 28
16. Van Genuchten Parameters, Fitted Saturated Hydraulic Conductivity, and Measured Bulk Density Data for the Ringold RFWie Unit (WCH-464). 29
17. Composite van Genuchten-Mualem Parameters for Each ERDF Vadose Zone Unit Based on All Moisture Retention and Unsaturated Conductivity Measurements Available Per Unit (WCH-464). 31
18. Upper and Lower Bounds of the Distributions Selected for Each van Genuchtem/Mualem Parameter of Each ERDF Vadose Zone Unit. 31
19. Upper and Lower Bounds of the Saturated Water Content (θ_s) Used as Diffusive Porosity Estimates for Each ERDF Vadose Zone Unit (WCH-464). 34
20. Macroscopic Anisotropy Parameter (Composite Values) Based on Polmann (1990) Equations for Various Geologic Unitsat the ERDF Site (WCH-464). 35
21. Anisotropy Ratios of Hf1 Calculated Over the Mean Tension Range (700 through 1,000 cm) Considering Range of Unsaturated Hydraulic Conductivity Curves. 37

22. Review of Ringold E Horizontal Hydraulic Conductivity (m/d) (CP-47631). 39
23. Slug-Test Analysis Result (PNNL-19482). 43
24. Waste Stream Designation and Assumed Compositions for Determination of K_d Values (PNNL-14702). 45
25. Aqueous/Solid Partitioning Ratio (K_d in mL/g) Estimates for Low-Organic/ Low-Salt/Near-Neutral Waste Chemistry, not Impacted Sand (<2 mm Size Fraction). 47
26. Average Percent Gravel Measured on Each Unit (According to WCH-464). 48
27. Aqueous/Solid Partitioning Ratio (K_d in mL/g) Estimates Corrected for Gravel for Hf1 and RFwie. 49
28. Aqueous/Solid Partitioning Ratio (K_d in mL/g) Estimates for Low-Organic/Low-Salt/Near-Neutral Waste Chemistry, Not Impacted Silt-Size Sediments. 50
29. Aqueous/Solid Partitioning Ratio (K_d in mL/g) Estimates Given by PNNL-17154 for Low Organic/Low Salt/Near Neutral Waste Chemistry, Not Impacted Carbonate-dominated Sediments. 51
30. Minimum and Maximum Bulk Densities (g/cm^3) Measured for Each Geologic Unit (WCH-464). 52
31. Nonreactive Macrodispersivities Estimates for Various Geologic Units at the ERDF Site (WCH-464). 53
32. Relationship Between Saturated Longitudinal Macrodispersivity (α_L) and Scale of Measurement (L_s). 54
33. Estimates of Saturated Longitudinal Macrodispersivities Deduced from Three Literature Relationships Considering a Length Scale of 100 m. 54
34. Best, Minimum, and Maximum Estimates of Total Mass or Activity for Each Radionuclide Considered in the ERDF PA Uncertainty Analyses. (2 Pages) 56
35. Summary of the Recharge Distribution Functions that will be Considered for the ERDF PA Uncertainty and Sensitivity Analyses. 58
36. Summary of the Vadose Zone Parameter Distributions that will be Considered for the ERDF PA Uncertainty and Sensitivity Analyses. 59
37. Summary of the Polmann Parameters that will be Considered for the ERDF PA Uncertainty and Sensitivity Analyses. 59
38. Summary of the Saturated Zone Parameter Distributions that will be Considered for the ERDF PA Uncertainty and Sensitivity Analyses. 60
39. Summary of the Transport Parameter Distributions that will be Considered for the ERDF PA Uncertainty and Sensitivity Analyses. 60
40. Summary of the K_d (mL/g) Distributions that will be Considered for the ERDF PA Uncertainty and Sensitivity Analyses. (2 Pages) 61
41. Summary of the Radionuclide Inventory (Curies or Metric Tons) that will be Considered for the ERDF PA Uncertainty and Sensitivity Analyses. (2 Pages) 63

1.0 INTRODUCTION

A sensitivity and uncertainty analysis is required as part of the performance assessment (PA) for the Environmental Restoration Disposal Facility (ERDF) per DOE M 435.1-1, *Low-Level Waste Disposal Facility Federal Review Group Manual*. The guidance for completing the sensitivity and uncertainty analyses (DOE G 435.1, *Implementation Guide for Use with DOE M 435.1-1*) states that the dose rates have associated uncertainties and a discussion of uncertainties should be included in expressing the outcomes of any PA. The guidance further states that an estimate of the degree of uncertainty is needed for the analysis that includes the calculation of the maximum impact of the disposal facility beyond the 1,000-year compliance period.

Projections of environmental processes are inherently uncertain. Assessment of uncertainty in model results arising from assumptions and parameter values, for example, is necessary to support the determination that there is reasonable expectation of meeting the performance objectives. The objective of the uncertainty analysis is to estimate the plausible range of potential radionuclide contamination levels in the surrounding environment that results from selecting parameter values within their uncertainty ranges. When sufficient number of parameter combinations is evaluated over their plausible range, the predicted range of potential radionuclide dose can be used to quantify the uncertainty in the dose estimates and meet the requirements of DOE M 435.1-1. The sensitivity of model input parameters can be determined using the calculations performed for the uncertainty analysis.

The objective of this report is to develop uncertainty ranges and probability distributions of input parameter values for the different models used to achieve the ERDF PA. The methodology that will be applied to propagate uncertainty through these models is first presented followed by a discussion of the rationale that has guided the assignment of probability distribution functions of input parameters. Uncertainty in model parameters is subsequently examined considering the following:

- Parameters to be used to generate the vadose zone flow-field through time. This section includes the following:
  - A discussion on temporal changes to soil, vegetation cover, and engineered barriers that influence recharge rates over time
  - A discussion on uncertainty and plausible ranges of hydraulic properties for each vadose zone hydrostratigraphic unit
  - A presentation of the methodology that will be used to propagate uncertainty in the process-level model and abstraction of the vadose zone flow-field for subsequent use.
- Parameters that will be used to generate the saturated zone flow-field. This section includes a discussion of uncertainty in hydraulic properties of hydrostratigraphic unit(s) in the saturated zone below the ERDF.

- Parameters that will be used in contaminant transport calculations in both vadose zone and saturated zone. This section includes a discussion on uncertainty and parameter ranges for each hydrostratigraphic unit.
- Uncertainty in post-closure radionuclide inventory.

2.0 METHODOLOGY FOR PROPAGATION OF UNCERTAINTY

One of the primary expectations of the PA modeling is to provide sufficient explanation of the uncertainty in the dose estimates. A probabilistic uncertainty analysis is proposed that intends to quantify, where possible, the uncertainty in the results associated with uncertainties in the conceptual model, input parameters, and assumptions about current or future events. The intent of these analyses is to improve understanding of what uncertain factors exert the greatest influence on the model results.

Uncertainty analysis will be conducted using a model that is developed by abstracting the results derived from the process-level models. The process-level models are defined as those that are specifically developed using appropriate software to rigorously solve the governing equations of flow and transport with appropriate boundary conditions at the scale of the processes that can incorporate changes to physical, chemical, and hydrologic properties. The abstraction-based approach is adopted because exercising the process-level models to adequately cover all combinations of parameter values across their full ranges of uncertainty would be very time consuming. Furthermore, coupling various process-level models and propagating uncertainties in a consistent manner can also be very challenging. For example, predicting uncertainties in waste form degradation and release mechanisms and coupling these processes to vadose zone and saturated zone flow and transport model with their own set of uncertain parameters, and exercising the coupled model over its full range of uncertainty followed by the dose calculations over various exposure pathways can become excessively complicated.

To simplify the methodology, an abstraction-based PA approach is adopted for performing uncertainty analysis. For this purpose GoldSim™ software (GoldSim Technology Group 2009) is chosen. GoldSim is specifically designed for performing PA analyses. GoldSim provides the platform for coupling various processes through its unique set of specialized tools and provides the method for propagation of uncertainty. Furthermore, GoldSim has tools to develop a finite-difference grid for performing fate and transport calculations based on the user-specified flow rates.

To develop the vadose zone flow rates as a function of time the results will be abstracted from the process-level models (WCH-462, *ERDF Performance Assessment Modeling Approach*). For the purpose of performing the uncertainty analysis, the flow models developed using the STOMP code are considered to be the process-level models (PNNL-12030, *STOMP Subsurface Transport over Multiple Phases Theory Guide*). The STOMP-based model output will be used to generate the flow-field (e.g., spatially and temporally varying velocity vectors and water content), which will be abstracted along with their uncertainty estimates for use in GoldSim-based models. Because uncertainty in input parameters that influence the vadose zone flow rates need to be propagated through STOMP-based models, those parameters are

identified separately in this report from the ones that can be used directly in both STOMP- and GoldSim-based models. The uncertainty in vadose zone flow-field can be determined, for example, by setting the parameter values at their high, low, and mean values in the STOMP-based model and then evaluating the results to determine the uncertainty range in flow velocities and water contents. It is our intent to simplify the flow abstractions, when possible, and perform transport calculations using GoldSim-based models for the purpose of uncertainty analysis.

3.0 RATIONALE FOR ASSIGNING UNCERTAINTY DISTRIBUTION

The lack of knowledge about the appropriate value to use in a modeling approach for a quantity that is assumed to have a fixed value in the context of a particular analysis (e.g., base case) is generally called epistemic uncertainty.

Conceptually, epistemic uncertainty is considered to be distinct from variability, which arises from heterogeneity or an inherent randomness in the behavior of the system under study. The knowledge of experts cannot be expected to reduce stochastic uncertainty due to variability although their knowledge may be useful for quantifying it (Helton 1993). Both uncertainty and variability may be quantified using probability distributions. They can be tracked and evaluated separately during an analysis or they can be analyzed within the same computational framework. However, *Guiding Principles for Monte Carlo Analysis* (EPA/630/R-97/001) recommends that variability and uncertainty are tracked and evaluated separately in order to identify parameters where additional data are needed (i.e., to identify reducible uncertainty through further study).

The evaluation of the uncertainty through a modeling approach requires answering the following two questions (Helton 1993):

- How uncertain are the model results given the uncertainty in the inputs?
- How important are the individual elements of the inputs (i.e., the different parameters) with respect to the uncertainty in the results?

Uncertainty analysis, which refers to the determination of the uncertainty in results that derives from uncertainty in analysis inputs, answers the first question; whereas sensitivity analysis, which refers to the determination of the contributions of individual uncertain inputs, answers the second question.

Among the different uncertainty and sensitivity analysis approaches available, the sampling-based method that corresponds to the so-called "Monte Carlo" method has been widely used for PA of radioactive waste disposals. Among its main assets, this method is conceptually simple, able to cover the full range of parameter uncertainties, and, more importantly, allows obtaining the predictive uncertainty results without using surrogate models to map relations between uncertain inputs and analysis results (Helton 1993).

The Monte-Carlo approach involves the following steps (Mishra 2007, "Uncertainty and Sensitivity Analysis Techniques for Hydrologic Modeling"):

- Selecting model input parameters
- Assigning probability distributions to input parameters to quantify uncertainty
- Generating many sample sets (realizations) through sampling of probability distribution
- Propagating the uncertainty (via realizations) through the analysis
- Determining parametric and nonparametric estimates of the reliability in the model output once an appropriate sample size is reached that ensures stable estimates of the output distribution.

A Monte Carlo approach will be developed for the ERDF PA using the GoldSim software, which allows a practical handling of stochastic variables that will represent the parameter inputs of the ERDF model.

Although an infinite number of theoretical distributions can be used to fit an empirical data set, only a handful of distributions are considered in practice (Mishra 2002, "Assigning Probability Distributions to Input Parameters of Performance Assessment Models"). The key features of these distributions are described in Table 1.

Table 1. Main Uses of Several Common Distribution Functions (Mishra 2002).

Distribution	Useful for Representing
Uniform (log-uniform) Triangular (log-triangular)	Low state of knowledge and/or subjective judgment
Normal	Errors due to additive processes
Log-normal	Errors due to multiplicative processes
Weibull	Component failure rates
Poisson	Frequency of rare events
Beta	Bounded, unimodal, random variables

Several studies have tried to assess the impact of a chosen distribution function on the sensitivity analysis results. For instance, the results obtained by Hoffman (1996) can be used as a rule of thumb for focusing the attention on parameter distributions that will have a relevant impact. Hoffman's conclusions are summarized in the following:

- As long as the uncertainty of a given parameter is small (coefficient of variation ≤30%), it makes very little difference which distribution is chosen.
- As the coefficient of variation approaches and exceeds 30%, the use of distributions of log-transformed values is recommended.
- The choice of distribution shape will be important if the analyst is interested in extreme values.

However, no framework for distribution selection has been described and/or utilized in the PA literature according to Mishra (2002) who recommends using, as a starting point, the guidelines given by EPA/630/R-97/001, *Guiding Principles for Monte Carlo Analysis,* the context of probabilistic health risk assessment. In selecting a distributional form, EPA/630/R-97/001 recommends that the analyst considers first the quality of the information in the database and answers a series of questions including, but not limited to, the following:

- Is there any mechanistic basis for choosing a distribution family?
- Is the shape of the distribution likely to be dictated by physical or biological properties or other mechanisms?
- Is the variable discrete or continuous?
- What are the bounds of the variable?
- Is the distribution skewed or symmetric?
- If the distribution is thought to be skewed, in which direction?
- What other aspects of the shape of the distribution are known?
- How well do the tails of the distribution represent the observations?

Although it is more desirable to generate probability distributions for uncertain parameters on the basis of observed and/or simulated data, probability distributions are often inferred on the basis of only a limited amount of information and are also subject to rather ad-hoc assumptions. In that case, Mishra (2002) recommends choosing a probability distribution function by considering the principle of maximum entropy that preserves the maximum uncertainty about the data, similar to the well-known concept of thermodynamic entropy related to the degree of disorder or randomness. The principle of maximum entropy seeks to choose a probability distribution function that maximizes the entropy, subject to known constraints. Uncertainty is reduced as much as possible by using all information (i.e., satisfying all constraints), but no further by unnecessary assumptions. This ensures that ignorance is preserved and one is maximally uncertain with respect to the unknown information.

From a practical perspective, the use of the maximum entropy principle in assigning a distribution function implies the following considerations:

- If all the samples are equally likely because no constraint on the plausible parameter values is available, the maximum entropy is reached and corresponds to the uniform distribution.
- If some information is available, uncertainty is reduced as much as possible by using all information (i.e., by satisfying all constraints) but no further by unnecessary assumptions. This ensures that ignorance is acknowledged and forces the analyst to retain maximum uncertainty in the distribution developed from the data. In that case, the distribution function will have a concentration of probability away from the extreme values, leading to a reduction of uncertainty and hence a reduction of entropy in comparison to the uniform distribution.

The constraints that can be used for selecting a distribution function in accordance with the maximum entropy principle are summarized in Table 2.

These guidelines will be used in this report for assigning a distribution function to all the parameters in accordance with the maximum entropy principle.

Table 2. Guidance for Selection of Probability Distribution Function Considering the Data Constraints (according to Harr 1987).

Constraint	Distribution
Upper bound, lower bound	Uniform
Minimum, maximum, mode	Triangular
Mean, standard deviation	Normal
Range, mean, standard deviation	Beta
Mean occurrence rate	Poisson

4.0 VADOSE FLOW-FIELD GENERATION USING STOMP-BASED MODEL

Prior to the discussion of flow-related parameters, it is important to understand the conceptual framework of ERDF since the conceptual model influences the choice of parameters. Because ERDF is a man-made feature that is designed to store and isolate radionuclides from the geosphere, it is conceptualized as an engineered barrier system. Outside this is the natural system, which includes the vadose zone and saturated zone. Because the performance of a fully-functioning engineered barrier system cannot be tested prior to it being built and monitored over a long period of time, an educated estimate of the lifetime of some of the engineered barriers to flow is considered along with the conceptualization of how and when the barriers might fail and how might they affect the recharge of meteoric water over time. To reduce the uncertainty from lack of knowledge on the failure times and mechanisms of failure, a conceptually stylized evolution of ERDF is considered that is purposely conservative, leading to early failure of the engineered barrier and, thereby, earlier transport of radionuclides to the natural system. Because the temporal evolution of ERDF is stylized, the timings for degradation and failure of barriers are fixed for the purpose of uncertainty analysis.

4.1 CONCEPTUAL MODEL FOR TEMPORAL EVOLUTION OF ERDF

4.1.1 Conceptual Timeline

The ERDF construction began in 1996. Since then nearly 10 million tons of solid waste materials (approximately 60% of the expected final capacity) have been emplaced into different disposal areas called "cells" (WCH-479, *Inventory Data Package for ERDF Waste Disposal*). Multiple layers of plastic and other impermeable materials have been used to build a liner in each cell with the overall purpose of collecting and removing liquids that drain through the waste materials. A temporary cap is placed over cells as they are filled and the leachate collection

liner is gradually extended. At the completion of the operation period, a *Resource Conservation and Recovery Act of 1976* (RCRA) compliant barrier (as designed by DOE/RL-93-33, *Focused Feasibility Study of Engineered Barriers for Waste Management Units in the 200 Areas*) is assumed to be in place over the whole facility to provide long-term containment and hydrologic protection for a performance period of 500 years.

With expected changes to the land cover over time and its continued degradation due to such things as growth of vegetation, creep, and changes in confining stress due to possible erosion and subsidence, several time periods have been conceptualized (Table 3) to represent the changes in recharge rates and hydrologic conditions at ERDF. Each of these time periods is characterized by a different recharge rate that will be discussed in Section 4.2.1.

Table 3. Timeline Considered for Representing the Evolution of the ERDF Conceptual Model Over Time.

Phase	Conditions	Duration	Conceptual Half Cross Section of the ERDF Area
Pre-operations	Before construction of ERDF	Until steady-state moisture conditions are achieved for the year	
Operations	Current conditions	1996 to 2035	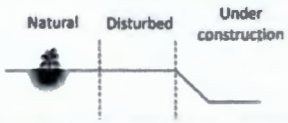
Early Post-Closure	Transition to conditions of restricted recharge due to RCRA-compliant barrier and intact liner during the first 100 years of institutional control	2035 to 2135	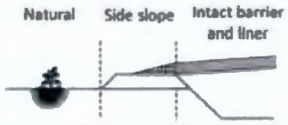
	Intact surface barrier and degraded liner after its assumed service life of 100 years	2135 to 2535	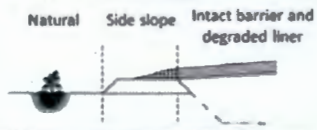
Late Post-Closure	Degraded surface barrier conditions	Time needed to reach the groundwater table. At least 2535 to 3035 (possible extension to 12035)	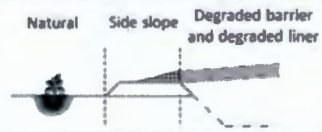

4.1.1.1 Conceptual Timeline Rationale. The hydrologic conditions prior to the facility construction (1996) control the initial moisture content and the matric potential in the vadose zone. To estimate the initial conditions, a pre-operations phase is considered, which will be used to produce initial moisture conditions for subsequent temporal changes conceptualized at ERDF. A long-term transient calculation will be run with pre-operational period recharge rates until moisture profile reaches equilibrium with the boundary conditions. A vegetation cover representative of pre-ERDF construction is assumed over the whole domain during this period.

The current condition (construction) period is considered to represent the ERDF construction phase with a gradually extended liner over the ERDF area. This period starts in 1996 and is assumed to end in 2035 when a surface barrier is placed over the facility. A distinct recharge rate will be assigned to the following three different zones during this period:

- The undisturbed zone around the facility characterized by a vegetation cover representative of this area.
- The disturbed zone around the facility, which has no vegetation cover. This zone can be observed on aerial photographs (Figure 1).
- The construction zone that corresponds to different cells under construction or equipped with a leachate collection liner but still not covered by vegetation.

At the end of the construction period, an early post-closure period is considered to represent the functioning of the RCRA-compliant barrier along with the underlying leachate collection liner. The *Assessment and Recommendations for Improving the Performance of Waste Containment Systems* (EPA/600/R-02/099) states the life expectancy is likely to be about 160 years for a primary liner at 35°C and greater than 600 years for a secondary geomembrane, provided the temperature is lower than 20°C. According to the methodology suggested by the article "Long-Term Performance of Contaminant Barrier Systems" (Rowe 2005), to assess the long-term performance of contaminant barrier system, a 1.5-mm-thick high-density polyethylene (HDPE) liner has a life expectancy of 970 years for classical landfill conditions (aqueous anaerobic environment). The Proceedings from the Association of State Dam Safety Officials (Koerner and Husan 2003) report lifetime predictions of HDPE geomembranes at elevated field temperatures, which range from 109 years at 40°C to 712 years at 20°C. The longevity of a double (HDPE) geomembrane liner depends mainly on temperature and chemical aggressiveness of leachates (mainly driven by their oxygen content, which controls HDPE oxidation). For the purpose of this PA, a conservative assumption is made about the life expectancy of the double liner. It is assumed that the double liner at ERDF will have a service life of 100 years corresponding to the institutional control period. This is a conservative assumption.

Because the expected design life of the RCRA-compliant surface barrier (500 years according to DOE/RL-93-33) is assumed to be longer than the double liner (100 years), the early post-closure period is split in the following two sub-periods: (1) beginning in year 2035 (assumed closure of ERDF) and ending at year 2135 (completion of the assumed 100-year service life of the double liner), and (2) starting in year 2135 and ending in year 2535 (the end of the 500-year assumed life expectancy of the surface barrier).

Figure 1. 2008 (Top) and 2009 (Bottom) Aerial Photography of the ERDF Site.

For each of these two sub-periods, a distinct recharge rate is assigned to three spatially distinct zones:

- The undisturbed zone, away from the surface barrier, and the surrounding berm, characterized by a vegetation cover.
- The zone under the stabilizing side slopes of the surface barrier as it tapers on the berm (Table 3). The berm is built using silt derived from on-site soil and then 95% compacted. The recharge through this material is expected be to be low.
- The zone beneath the extent of surface barrier, which is designed to minimize infiltration of meteoric waters.

A late post-closure period is finally considered to represent the functioning of a degraded surface barrier with an underlying degraded liner. This period will start at the end of its assumed design life expectancy of surface barrier (year 2535) and will continue through the rest of the simulated time period. A distinct recharge rate will be assigned to three different zones during this period:

- The undisturbed zone away from the barrier characterized by a vegetation cover representative of the area
- The side slopes of the barrier (compacted silt)
- The degraded surface barrier fully covered with vegetation, which will have undergone soil and ecological processes.
- It is possible that the conceptualized time evolution may be perturbed by fire cycles, which could affect the recharge rates due to removal of vegetation. The impact of these events on the ERDF barrier performance will be evaluated by considering stochastic events in an independent sensitivity analysis that will not be part of the base case. Fires can be simulated as discrete events characterized by a specified rate of occurrence that follow a Poisson process (distribution function widely used to represent stochastic variables only characterized by a mean occurrence rate, cf. Table 2).

4.1.2 ERDF-Specific Subsurface and Hydrogeological Context

4.1.2.1 Soil and Vegetation. Holocene deposits and exposed sediments have undergone soil development processes in the Hanford area. Figure 2 shows a map of the soil types in the Central Plateau based on the soil survey conducted around 1910 to 1915 (BNWL-243, *Soil Survey Hanford Project in Benton County*). According to this map, the soil type present in the majority of the ERDF area is Rupert sand. The Burbank loamy sand may be found to the north of ERDF. Because the Rupert/Burbank contact falls outside the main ERDF footprint area, the only naturally-occurring soil type that will be considered for the ERDF PA modeling will be Rupert sand.

BNWL-243 defines the Rupert sand type as follows:

> "This mapping unit represents one of the most extensive soils on the Hanford Project. The surface is a brown to grayish brown (10YR5/2) coarse sand, which grades to a dark grayish brown (10YR4/2) sand at about 36 inches. Rupert soils developed under grass, sagebrush, and hopsage in coarse sandy alluvial deposits, which were mantled by wind-blown sand. Relief characteristically consists of hummocky terraces and dune-like ridges. This soil may be correlated as Quincy sand, which was not separated here. Active sand dunes are present. Some dune areas are separated; however, many small dunes, blow-outs, and associated small areas of Ephrata and Burbank soils are included."

This description tends to confirm that too much attention should not be paid to the contact between Rupert/Burbank sand, as some areas of Burbank soil have been included into the Rupert sand mapping.

Figure 2. Soil Types on the Central Plateau (BNWL-243).

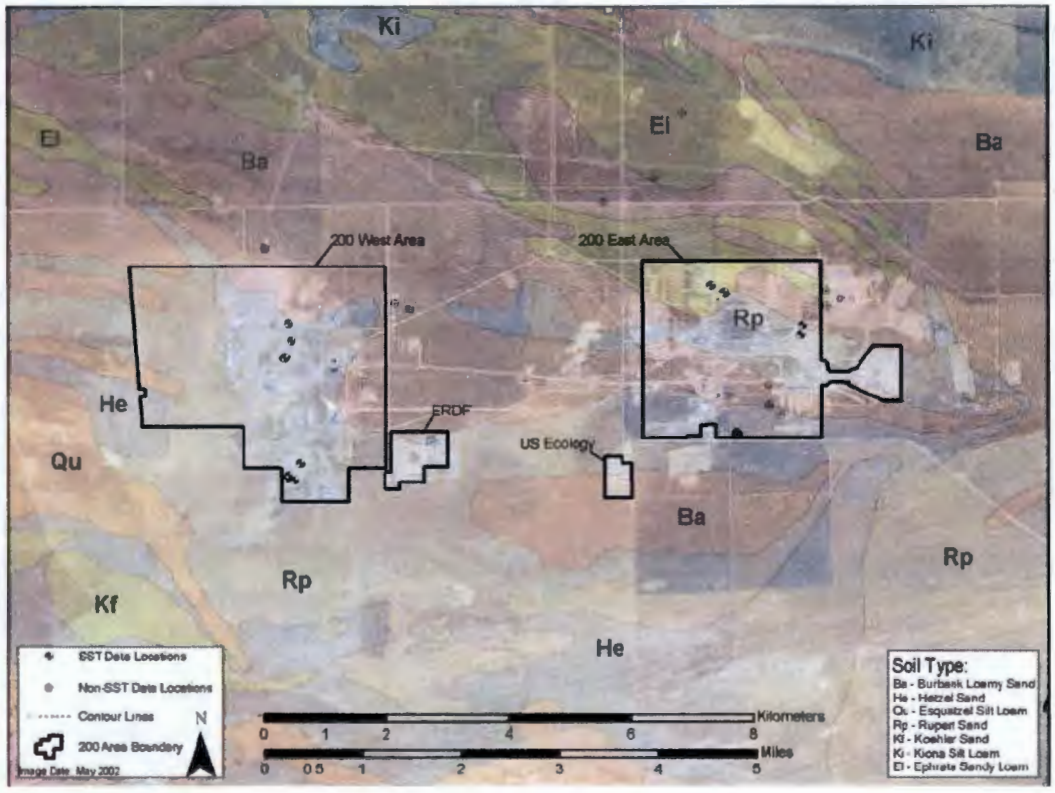

With regards to the vegetation, the Central Plateau portion of the Hanford Site is characterized as a shrub-steppe ecosystem that is adapted to the region's mid-latitude semiarid climate of hot summers, cold winters, and low precipitation (PNNL-6415, *Hanford Site National Environmental Policy Act [NEPA] Characterization*). Consequently, a mature shrub-steppe plant community will be considered as the most representative vegetation cover of the ERDF area under natural conditions (i.e., undisturbed conditions or after the reestablishment of vegetation).

Range fires that historically burned through the Hanford area during the dry summers were found to eliminate fire-intolerant species (e.g., big sagebrush) and allow more opportunistic and fire-resistant species to establish. According to PNNL-6415, approximately 25% of the vascular plant species recorded for the Hanford Site are non-native. Among the dominant non-native species, cheatgrass is an aggressive shallow-rooted colonizer that has become well established across the site. However, there is no basis for assuming that cheatgrass will entirely replace the pre-existent shrub-steppe plant community over the whole ERDF area after a fire. "Geochemical Estimates of Paleorecharge in the Pasco Basin: Evaluation of the Chloride Mass-Balance Technique" (Murphy et al. 1996) reported that past range fires may have resulted in a sparse cover of shrub. Consequently, fire effects on the portions of the ERDF that will be covered by vegetation when a fire randomly occurs will be analyzed by considering first a no vegetation cover and then a young plant community, prior to the reestablishment of a mature shrub-steppe plant community. PNNL-14702, *Vadose Zone Hydrogeology Data Package for Hanford Assessments* has reported that the reestablishment of vegetation after a fire is generally less than 1 year.

4.1.2.2 Hydrostratigraphic Units. Most stratigraphic units typically associated with the Central Plateau portion of the Hanford Site have been recognized beneath ERDF (WCH-463, *Hydrogeologic Model for the Environmental Restoration Disposal Facility, Hanford Site*). For the purpose of this PA the hydrostratigraphic units (HSUs) are deemed equivalent to the stratigraphic units. The following 10 HSUs are present at ERDF, ordered from top to bottom in a cake-layer geometry:

- Recent (Holocene) backfill material (Hdb)
- Hanford formation-unit 1 – gravel-dominated sequence (Hf1 unit)
- Hanford formation-unit 2 – sand-dominated sequence (Hf2 unit)
- Cold Creek unit silt – fine grained (CCuz)
- Cold Creek unit calcic geosol – coarser grained (CCuc)
- Ringold Formation member Taylor Flat-fine grained (RFtf)
- Ringold Formation Unit E – silty sandy gravel (RFwie)
- Ringold Formation lower mud unit – fine-grained sequence (RFlm)
- Ringold Formation Unit A – silty sandy gravel (RFwia)
- Columbia River Basalt Group.

The ERDF hydrogeological conceptual model is described in WCH-463 in order to provide the framework for evaluating general stratigraphic and structural controls on moisture and waste fluid movement through the vadose zone to the water table. The conceptual model was based on data obtained from all available wells and boreholes (35 wells) located within 610 m (2,000 ft) of the ERDF area. The analysis focused on the information from the deepest and most recently drilled boreholes. Combining geologist or driller log information with borehole geophysical log plots provided complete information on the suprabasalt stratigraphy and lithology of the site.

Detailed geologic cross-sections are presented in WCH-463 based on the borehole data collected in the vicinity of ERDF. An east-west geologic cross-section through ERDF is presented in Figure 3 and shown on the map in Figure 4. The ERDF is underlain by 159 to 177 m (521.7 to 580.7 ft) of suprabasalt sediments. The water table is located within the Ringold Unit E and the vadose zone is approximately 80 to 100 m thick (262.4 to 328.1 ft). Groundwater flows to the east-northeast beneath the site and is known to contain dissolved contaminants derived from liquid discharge at waste sites in the 200 West Area located upgradient from ERDF. Perched groundwater has not been observed in the vicinity of the facility.

The ERDF waste disposal cells are constructed in the near-surface sediments within the thick vadose zone, which consists primarily of unconsolidated Pleistocene-aged Hanford formation and Cold Creek unit sediments. The ERDF disposal cell floors (bottom of cells) penetrate through the Hf1 unit and lie within the sand-dominated Hf2 unit. The Cold Creek unit lies directly beneath the Hanford formation and is subdivided into two sub-units, the silt-dominated CCuz and carbonate-dominated CCuc. Cold Creek unit silt and CCuc were found laterally continuous throughout most of the 200 West Area but are truncated to the east within the ERDF footprint either because of paleo-flood erosion or by depositional thinning (Figure 3). East of this truncation, the Hf2 sediment directly overlies Ringold Formation sediment. The deepest and oldest geologic units within the vadose zone consist of the Ringold Formation upper fine-grained unit (RFtf) and the upper portion of the fluvial-silty sandy gravel unit (RFwie).

Figure 3. West-East Hydrogeologic Cross-Section through the ERDF (WCH-463).

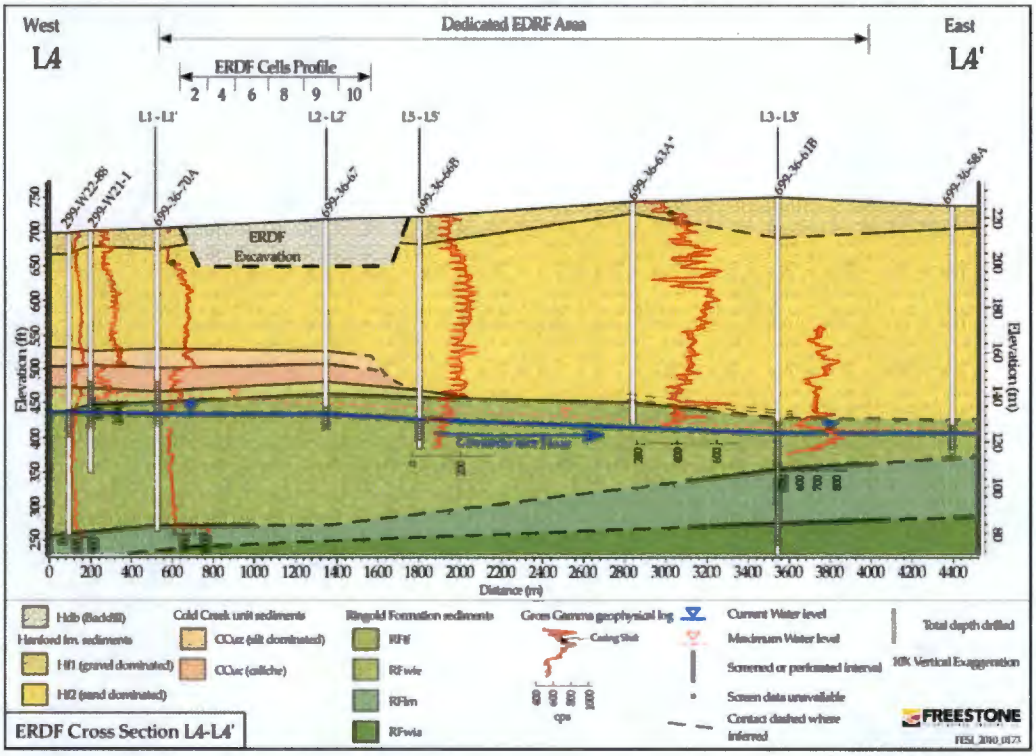

4.2 RANGES OF FLOW PARAMETERS FOR STOMP

4.2.1 Recharge

4.2.1.1 Data Sources and Methodology. Recharge rates (i.e., fluxes of water reaching the water table after leaving the evapotranspiration zone) need to be estimated for each zone of the ERDF conceptual model in order to simulate the assumed hydrologic evolution of the ERDF through time (presented in Section 4.1.1).

Many other projects have collected recharge data that are relevant to assess ERDF-specific estimates and their associated uncertainty. The following reports and databases have been examined to retain some of the material that is pertinent to the ERDF PA.

Figure 4. Location of Boreholes and Cross Sections Used to Generate the ERDF Hydrogeologic Conceptual Model (WCH-463).

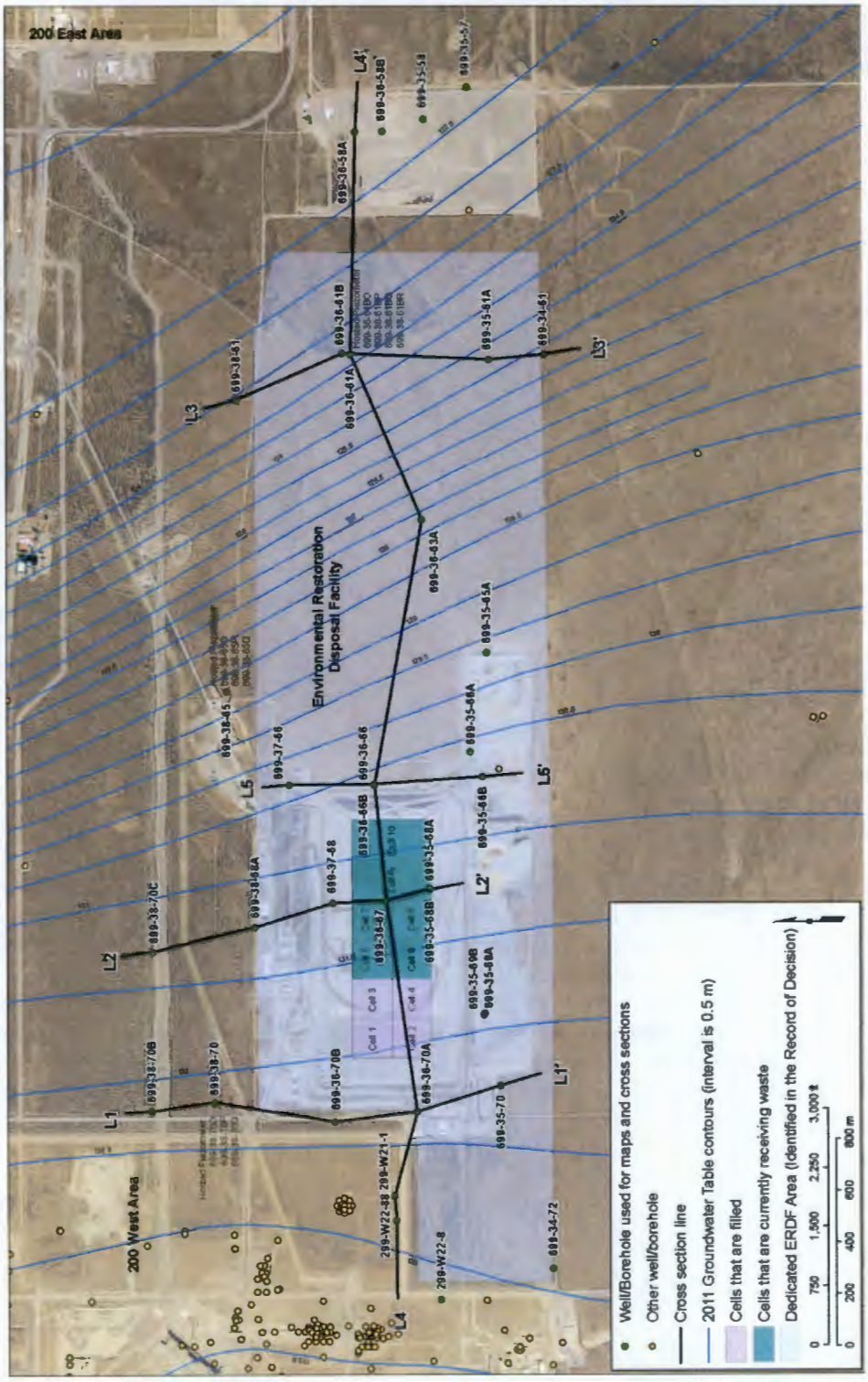

- PNNL-14702 provides recharge (deep drainage) estimates for use in Hanford Site assessments. Their recharge estimates were derived from a suite of available field data and computer simulation results. The estimates do not account for overland flow from roadways or roofs, subsurface drainage from water line leaks, or any other manmade additions of water, the impacts wrought by future climate change or land-use alterations, variations within soil types, or dune-sand deposition. The estimates were developed for fairly large geographic areas and may not represent the local recharge rates at specific locations. Estimates were provided for natural and disturbed soils and for surface barriers for different periods (pre-operations, operations, post-remediation, and final state). The conditions during these periods include natural soil and shrub-steppe plant communities, disturbances that alter the surface soil and vegetation, emplacement of surface barriers, and long-term changes that occur as the waste sites stabilize and return to natural conditions. PNNL-14702 also suggests probability distributions of the recharge estimates that can be used to represent the expected range of recharge rates.

- The recharge estimates provided by PNNL-16688, *Recharge Data Package for Hanford Single-Shell Tank Waste Management Areas* update and supplement the estimates provided by PNNL-14702 for the Hanford Site using additional field measurements and simulations considering weather data through 2006. This updated data package was published to provide recharge estimates for the scenarios being considered in the RCRA Facility Investigation for the single-shell tank (SST) waste management areas (WMAs). Consequently, probability distributions to represent the range of updated recharge rates are not suggested in PNNL-16688.

The recharge estimates suggested by these reports are based on three methods (lysimetry, tracer tests, and computer simulations) judged to be able to cover the whole range of recharge rates at the Hanford Site, which can range from near 0 to more than 100 mm/yr according to "Variations in Recharge at the Hanford Site" (Gee et al. 1992). However, these sources have provided only limited, relevant data for recharge-rate estimation at ERDF from which it was only possible to determine a best estimate and reasonable bounds.

To quantify uncertainty in the recharge estimates, PNNL-14702 recommends using a triangular probability distribution approach in which the low value is equal to the mean recharge rate minus the standard deviation, and the high value is equal to twice the mean value. When the number of recharge estimates is too small to calculate adequate statistics, recharge standard deviations can be estimated using statistics from winter precipitation, which is considered to be the primary source of recharge water. Data from Hanford Site precipitation records were used by PNNL-14702 to obtain the mean and standard deviation of the extended winter precipitation for the period from November 1946 to March 2004. The record yielded a mean value of 101 mm/yr (3.94 in./yr) and standard deviation of 40 mm/yr (1.56 in./yr), or roughly 40% of the mean value. Because the available recharge data were limited, PNNL-14702 estimated the standard deviation for each surface as equal to half the mean recharge rate. This choice was deemed slightly conservative based on the statistic for the extended winter precipitation. For sites with very high recharge rates, the triangular distribution resulted in unreasonably high upper limits. In that case, PNNL-14702 reasoned that, because winter precipitation was the primary source of recharge, recharge would seldom, if ever, exceed winter precipitation. Therefore, all recharge-rate distributions were truncated to the mean extended winter precipitation rate of 101 mm/yr (3.94 in./yr). As more data are collected for various surface conditions, the actual standard deviations in recharge can be substituted.

However, as only limited data were available for ERDF-specific rate estimation, the method suggested by PNNL-14702 was not rigorously applied. Instead a simplified triangular distribution was used to represent uncertainty in recharge, considering only the mean, highest, and lowest available values. The sections below presents the selected recharge data and the associated distributions assigned to each ERDF zone for each time period conceptualized during the evolution of ERDF (Section 4.1.1).

4.2.1.2 Pre-Operation Period. During the pre-operation period (before 1996), the area currently occupied by ERDF is conceptualized to be a uniform zone of Rupert sand soil covered by a mature shrub-steppe plant community. These features are assumed to correspond to the best representative conditions prior to the ERDF construction (Section 4.1.2.1).

For this type of soil (Rupert sand) and vegetation cover (mature shrub-steppe plant community), only three recharge estimates are currently available in the literature (Table 4).

Table 4. Estimates of Recharge Rate Available for Vegetated Rupert Sand in the Central Plateau.

Recharge Estimate (mm/yr)	Method of Measurement and Location	Description of the Vegetation Cover at the Measurement Site	Reference
4	Based on chloride data collected from a borehole near the Wye Barricade (about 11 km [6.8 mi] southeast of the 200 East Area)	Stabilized dune area with low shrub cover dominated by cheatgrass and Sandberg's bluegrass	Reported by PNNL-14702 citing Murphy et al. (1996)
0.26	Derived from measurements of temperature, matric potential gradients, and soil hydraulic properties measured at the 200 East Area deep well site (located about 2 km (1.2 mi) south of the Integrated Disposal Facility, southeast portion of the 200 East Area.	Cover dominated by sagebrush and cheatgrass	Reported by PNNL-16688 citing Enfield et al. (1973)
0.9	Derived by averaging recharge estimates determined using deep chloride data from seven boreholes at the Integrated Disposal Facility site (south-central portion of the 200 East Area.	Healthy mature shrub-steppe	Reported by PNNL-16688 citing PNNL-14744

PNNL-14702 recommended using the Wye Barricade data (4 mm/yr [0.36 in./yr]) as the best estimate value for vegetated Rupert Sand soil. PNNL-16688 revised the best estimate of PNNL-14702 by considering an average of the three available estimates (4, 0.26, and 0.9 mm/yr [0.36, 0.01, and 0.03 in./yr]). They considered the averaged value given by *Recharge Data Package for the 2005 Integrated Disposal Facility Performance Assessment* (PNNL-14744) from seven boreholes at the Integrated Disposal Facility site (0.9 mm/yr [0.03 in./yr]) as a single value in order to avoid weighting that site too heavily (since the soil at this site does not exactly fit the description of official soil type). Moreover, they reported a good agreement between their suggested mean value (1.7 mm/yr [0.06 in./yr]) and their modeling results that yielded a rate of 1.8 mm/yr (0.07 in./yr) considering a 50-year weather record (including the two wettest years: 1995 and 1996). Consequently, they recommended using an estimate of 1.7 mm/yr (0.06 in./yr) for vegetated Rupert sand soil.

In order to keep the mean value at 1.7 mm/yr (0.06 in./yr), the following triangular distribution is considered (Figure 5):

- The maximum will be fixed at 4 mm/yr (0.36 in./yr) as it corresponds to the maximum value of the data set.
- The minimum will be fixed at 0.26 mm/yr (0.01 in./yr) as it corresponds to the minimum value of the data set.
- The mode is calculated to be 0.9 mm/yr (0.03 in./yr).

As this distribution is based on the best available estimates of recharge rates through vegetated Rupert sand representative of the 200 Area, this recharge distribution (Figure 5) will be applied to the ERDF domain for the duration of the pre-operational period.

Figure 5. Triangular Distribution of Recharge Rate (mm/yr) for Vegetated Rupert Sand.

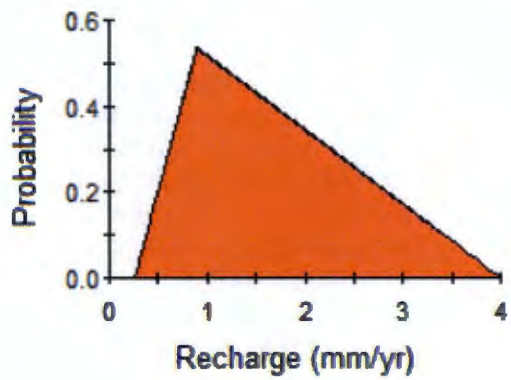

4.2.1.3 Operation Period. During the operation period, which started in 1996 and is assumed to last till 2035, the following three recharge zones have been conceptually defined:

- The undisturbed zone characterized by a vegetation cover representative of this area
- The disturbed zone around the facility that has no vegetation cover
- The construction zone that corresponds to the different ERDF cells that are under construction or equipped with a leachate collection liner but still not covered by vegetation.

4.2.1.3.1 Undisturbed Zone. As the undisturbed zone is conceptualized to be under the influence of the initial natural conditions observed prior to the ERDF construction (vegetated Rupert Sand), the recharge estimate over this zone will be the same as the pre-operation period previously described in Section 4.2.1.2. Consequently, the recharge rate distribution presented in Figure 5 will be used over this zone during the operation period.

4.2.1.3.2 Disturbed Zone. The disturbed zone corresponds to a disturbed Rupert sand zone without vegetation (bare soil). Two recharge estimates are currently available in the literature to describe the case in which vegetation was removed and plants were prevented from reestablishing in Rupert sand soil (Table 5).

Table 5. Estimates of Recharge Rate Available for Rupert Sand Without Vegetation.

Recharge Estimate (mm/yr)	Method	Reference
44	Simulation estimate for the period 1957 to 1997	Reported by PNNL-14702 citing PNNL-13033
45	Simulation estimate for the period 1957 to 2006	PNNL-16688

PNNL-16688 revised the best estimate of 44 mm/yr (1.7 in./yr) given by PNNL-14702 by considering a more extended weather record for their simulation, which yielded a value of 45 mm/yr (1.75 in./yr).

To our knowledge, 45 mm/yr (1.75 in./yr) corresponds to the best estimate of recharge rate currently available for Rupert sand without vegetation. As this estimate is a simulation result, the uncertainty on this value can be assessed using statistics for precipitation, which is the main input parameter for recharge simulations. Consequently, we have chosen the probability distribution function proposed by PNNL-14702 based on statistics from winter precipitation. PNNL-14702 found that the weather record yielded a standard deviation corresponding roughly to 40% of the mean precipitation value at the Hanford Site and finally suggested estimating the standard deviation of recharge distribution as equal to half the mean recharge rate and recommended using the following triangular distribution function:

- The lowest value is equal to the mean recharge rate minus the standard deviation, which corresponds in our case to 45-(45/2)=22.5 mm/yr

- The highest value is equal to twice the mean value, which corresponds in our case to 45x2=90 mm/yr. This maximum is in good agreement with the highest plausible recharge rate over the whole Central Plateau, which was estimated at 100 mm/yr by Gee et al. (1992).

This distribution leads to a mode of 22.5 mm/yr (0.87 in./yr), and the final triangular distribution is presented in Figure 6. This distribution will be applied to the disturbed zone during the operation period, which starts in 1996 and ends in 2035 when a RCRA-compliant surface barrier is assumed to be in place over the facility.

Figure 6. Triangular Distribution of Recharge Rate for Rupert Sand without Vegetation.

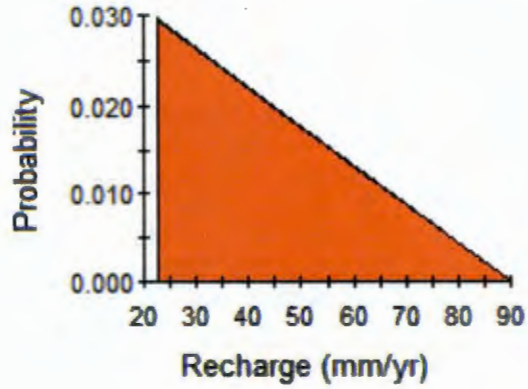

4.2.1.3.3 Under Construction Zone. The recharge rate estimate underneath the ERDF cells (construction area) is expected to be negligibly small as a double liner with leachate collection system is emplaced during the construction phase and gradually extended over the facility to collect any precipitation. Consequently, a recharge rate of zero is applied to this zone.

As the pre-operation period is relatively short (only 39 years) compared to the simulation duration (at least 1,000 years and up to 10,000 years), this input parameter is not likely to have a significant impact on contaminant transport below the facility.

4.2.1.4 Early Post-Closure.

4.2.1.4.1 Undisturbed Zone. As the undisturbed zone is assumed to remain under the influence of the natural conditions observed prior to the ERDF construction (vegetated Rupert sand), the recharge estimate over this area is assumed to be the same as the pre-operation period previously described in Section 4.2.1.2. Thus, the recharge rate distribution presented in Figure 5 will be used over this zone during the early post-closure period.

4.2.1.4.2 Side Slopes of the Surface Barrier. The ERDF surface barrier is expected to slope gradually toward the sides and taper off on top of 4.6 m (15 ft) of compacted silt loam that forms a surrounding berm. Although the ERDF surface barrier is not yet designed, it is not expected to have gravel or basalt rip-rap side slopes like those present at the prototype Hanford surface barrier. The current intent is to extend and taper the surface barrier silt loam to the silt loam of the berm, and revegetate the side slopes and berm. Table 6 presents the recharge estimates for surface barrier side slopes based on 15 years of observation on the Hanford prototype surface barrier (PNNL-18845, *200-BP-1 Prototype Hanford Barrier – 15 Years of Performance Monitoring*). The general trend in the ratio of drainage to precipitation appears to be decreasing, and 13 of the 20 possible side slope drainage measurements between 2005 and 2009 have been less than 5 mm/yr (0.20 in./yr) (PNNL-18845), indicating that the side slopes are functioning somewhat like a native soil, even though neither side slope incorporates any plant-promoting features. Surveys of the western and northern side slopes of the prototype Hanford barrier indicate that 13 species of plants occupy the side slopes, including sagebrush and rabbitbrush (PNL-10872). PNNL-14702 recommends representing the side-slope recharge rate in a time-dependent fashion, assuming that the side slopes are likely to resemble Burbank loamy sand with a shrub-steppe plant community (Table 7). This estimate appears to be more

representative of what could infiltrate below the ERDF side slopes as compacted silt will drastically prevent infiltration and encourage plant growth. The side slopes are also subject to the institutional controls applied to the ERDF facility that include vegetation surveillance and maintenance.

Table 6. Estimate of Recharge Rate Available for Barrier Side Slopes.

Type of Side Slope	Recharge Estimate (mm/yr)	Method	Reference
Sand and gravel with a 10% slope	29	Based on 15 years (1994-2009) of drainage data from the Prototype surface barrier, with the first three years of the north slope values scaled to ambient precipitation.	PNNL-18845
Basalt with a 50% slope	25	Based on 15 years (1994-2009) of drainage data from the Prototype surface barrier, with the first three years of the north slope values scaled to ambient precipitation.	PNNL-18845

Table 7. Estimates of Recharge Rate Available for Side Slopes after the 100-Year Institutional Control Period when they are Expected to Resemble Burbank Loamy Sand with Shrub Steppe.

Recharge Estimate (mm/yr)	Method	Reference
3	Average of three estimates (0.66, 2.8, 5.5) from deep chloride data collected in three boreholes in a vegetated Burbank loamy sand area	Reported by PNNL-14702 citing Prych (1998)

PNNL-16688 revised the estimate of 3 mm/yr for vegetated side slopes to 1.9 mm/yr by averaging the different tracer-based data for vegetated Burbank loamy sand:

- The five Prych (1998) estimates (2.8, 5.5, 1.8, 1.2, and 0.66 mm/yr)
- The two PNNL-14744 estimates (0.16 and 0.24 mm/yr)
- The Keller et al. (2007) estimate (2.5 mm/yr).

As the zone covered by the side slopes (mostly the berm area made up of compacted silt) is limited in extent and surrounds the excavated cells, the recharge in this zone is not perceived to have a significant impact on contaminant transport below the facility. Therefore, we will consider only a fixed recharge rate below the barrier side slopes to 2 mm/yr (best value of 1.9 mm/yr recommended by PNNL-16688 rounded up to 2 mm/yr) and not include uncertainty in recharge through the side slopes in the analysis.

4.2.1.4.3 Top Portion of the Surface Barrier. As a double liner and a leachate collection system is assumed to be effective until 2135, the recharge rate through the bottom of the liners from 2035 to 2135 will be initially kept fixed at 0 mm/yr as both the double liner and the surface barrier will prevent the deep infiltration of meteoric water. A higher recharge value will be considered after the life expectancy of the liners, which are assumed to fail at 2135 (after 100 years of post-closure). After this time, only the RCRA-compliant surface barrier is assumed

to prevent or limit recharge in this zone. The design criteria of such a barrier are identified in BHI-00007 and DOE/RL-93-33, and include limiting recharge to 0.5 mm/yr (0.02 in./yr).

From the data that are available, recharge is estimated to be 0.1 mm/yr (0.004 in./yr) for the area under a Modified Type C RCRA or Hanford barrier (Table 8). This estimate is based on 15 years of observations of the 200-BP-1 prototype surface barrier and several lysimeter studies. It must be noted that the observed recharge rate is actually much lower than this estimate (e.g., see Fayer and Gee 2006 and PNNL-18845). PNNL-14702 and PNNL-16688 recommend a value of 0.1 mm/yr, and PNNL-14702 mentions that a best value of 0.1 mm/yr (0.004 in./yr) is conservative, more easily defended, and more easily demonstrable than the observed value. However, other DOE O 435.1 performance assessments (e.g., DOE/ORP-2005-01) and guidance (e.g., DOE 2005) identify the value of 0.5 mm/yr (0.02 in./yr) as the best estimate. Thus, the recharge rate through the surface barrier that will be placed over the ERDF in year 2035 is assumed to be 0.5 mm/yr (0.02 in./yr). This value appears to be conservative and possibly bounding because the data that are available indicate that the barriers are capable of limiting recharge to less than 0.1 mm/yr (0.004 in./yr) with or without vegetation (Fayer and Gee 2006). Longevity data must be extrapolated, but lysimeter tests serving as analogues to degraded barrier conditions such as erosion of the silt loam top soil or the loss of vegetation did not produce drainage, and barrier analogue performance has not diminished during the 17 years of testing (Fayer and Gee 2006). The criterion for design life longevity of the Hanford Barrier is 1,000 years, and it is 500 years for the Modified RCRA C Barrier (DOE/RL-93-33). Therefore, it is assumed that design and construction of the barrier placed over the ERDF will at a minimum meet the Modified RCRA C criterion.

Table 8. Estimate of Recharge Rate Available for Modified RCRA C or Hanford Surface Barrier Top During Its Design Life.

Recharge Estimate (mm/yr)	Method	Reference
0.1	Based on Hanford prototype barrier data, lysimeter data, and simulation results considering a variety of scenarios which notably include the complete lack of vegetation	Reported by PNNL-14702 citing PNNL-14744, Fayer and Gee (2006), and PNNL-18845

Because of limited data and the speculative nature of estimating the effectiveness of the surface barrier in reducing recharge over several hundred years, uncertainty is applied to the recharge rates for this period. The design criterion of 0.5 mm/yr (0.02 in./yr) identified in BHI-00007 and applied here as the best estimate is considered as the mode of the probability distribution for the recharge rate through the top portion of the barrier from 2135 to 2535. The lowest value of this distribution is fixed at 0.05 mm/yr (0.02 in./yr), which corresponds to half of the best estimate of 0.1 mm/yr (0.04 in./yr) recommended by PNNL-16688. The maximum value is fixed at 1 mm/yr (0.04 in/yr), which corresponds to twice the mode of 0.5 mm/yr (0.02 in./yr). This distribution (Figure 7) leads to a mean value of 0.5 mm/yr (0.02 in./yr), which is the same as the mode.

Figure 7. Triangular Distribution of Recharge Rate (mm/yr) for the Top of the RCRA-Compliant Barrier during the Second Sub-Period (2135-2535) of Early Post-Closure.

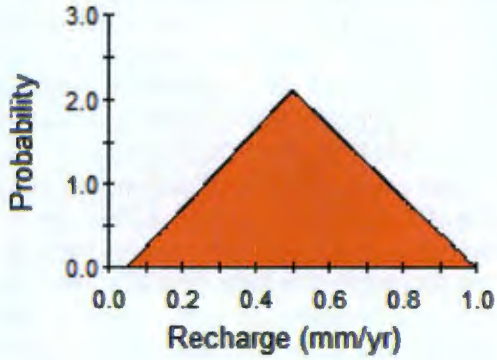

4.2.1.5 Late Post-Closure.

4.2.1.5.1 Undisturbed Zone. As the undisturbed zone is assumed to remain under the influence of natural conditions observed prior to the ERDF construction (vegetated Rupert sand), the recharge estimate over this area will be the same as the pre-operation period previously described in Section 4.2.1.2. Consequently, the recharge rate distribution presented in Figure 5 will be used over this zone during the late post-closure period.

4.2.1.5.2 Side Slopes of the Degraded Surface Barrier. No measurements are available for specifying the barrier slope recharge rate for the time after the design life of the barrier. According to PNNL-14702, the side slopes during the late post-closure period can resemble a vegetated Ephrata stony loam. However, no data are available to date for this particular type of soil, although some analogous information is derived as shown in Table 9.

Table 9. Estimates of Recharge Rate Available for Vegetated Ephrata Stony Loam Inferred from Vegetated Sandy Loam Estimates.

Recharge Estimate (mm/yr)	Method	Reference
1.5	Derived from estimate for Ephrata sandy loam: Average of two estimates, 1.2 and 1.8, from deep chloride data collected from two boreholes	Reported by PNNL-14702 citing Prych (1998)
2.8	Derived from estimate for Ephrata sandy loam and Burbank loamy sand: Average of four Prych (1998) estimates (2.8, 5.5, 1.8, 1.2 mm/yr) from deep chloride data collected from two boreholes and the Keller et al. (2007) estimate (2.5 mm/yr)	Reported by PNNL-16688 citing Prych (1998) and Keller et al. (2007)

PNNL-16688 revised the value given by PNNL-14702 by including data for Burbank loamy sand in their averaging scheme in order to take into account the uncertainty about the soil type at specific borehole locations.

As the side slopes correspond to a limited area compared to the overall area of the barrier and are offset from the waste, the side-slope recharge rate is not expected to have an appreciable impact on contaminant transport below ERDF. Consequently, the recharge rate below the side slopes during the late post-closure will be kept fixed at 2 mm/yr (0.07 in./yr) without considering uncertainty on this parameter. This value is the same as that used for the early post-closure period and is approximately the average of the two estimates (2.15 mm/yr [0.08 in./yr]) available to date for vegetated Ephrata sandy loam (reported in Table 9).

4.2.1.5.3 Top Portion of the Degraded Surface Barrier. No data are available that quantify the performance of the barrier top after its design life. PNNL-14702 assumed that the barrier top would resemble a silt loam soil during the late post-closure period and estimated the recharge rate as analogous to that of Warden silt loam (Table 10). According to PNNL-13033 results, numerical simulations indicate that the surface cover limits recharge to less than 0.1 mm/yr, regardless of presence of any plant type or climate change conditions, whether or not the silt loam layer erodes as expected, or dune sand deposits on the barrier. The ERDF waste compaction requirements minimize the potential for subsidence, and burrowing animals do not typically burrow below 1 m (3.3 ft) (PNNL-14744). The pea gravel admix appears capable of limiting wind erosion to approximately 15 cm (0.5 ft) for a 12,000-year period (PNNL-14744). The recommended post-design barrier recharge rate in PNNL-14744 is the same as that recommended for the design period, indicating that the performance of the barrier is not expected to change throughout time. Conclusions in PNNL-14744 indicate that the possibility of the most likely natural failure mechanisms (i.e., bioturbation of the silt loam layer, wind erosion, and accretion of windblown sand) of these natural systems is quite low with an appropriate design. The emplaced silt-loam soils should continue to perform as long as they remain in place. PNNL-14744 concludes that the long-term effectiveness of the surface barrier would continue to limit recharge rates to less than 0.1 mm/yr for thousands of years. However, because it is difficult to assert that surface barriers remain effective indefinitely, its performance is assumed to degrade after 500 years to permit a recharge rate of 1.0 mm/yr, which is double the value of the design period. The barrier limits recharge to that amount for the remainder of the simulation period.

Table 10. Estimates of Recharge Rate Available for Vegetated Warden Silt Loam to Represent the Top Portion of the Surface Barrier After Its Design Life.

Recharge Estimate (mm/yr)	Method	Reference
0.04	Average of four estimates (0.013, 0.008, 0.024, 0.11) from chloride data collected in silt loam soils	PNNL-14702 citing Prych (1998)
0.1	Value recommended to represent the state of surface barriers after their design life	PNNL-14744; PNNL-16688

In order to be conservative, the mode, maximum, and minimum values of the triangular probability distribution function previously developed for the surface barrier top during the second part of the early post-closure period (Section 4.2.1.4.3) are doubled during the late post-closure period (Figure 8). This leads to a triangular distribution with a mode of 1 mm/yr (0.03 in./yr), a maximum of 2 mm/yr (0.07 in./yr), and a minimum of 0.1 mm/yr (0.003 in./yr). This distribution results in a mean of 1 mm/yr (0.03 in./yr).

Figure 8. Triangular Distribution of Recharge Rate (mm/yr) for the Top of the RCRA-Compliant Barrier during Late Post-Closure.

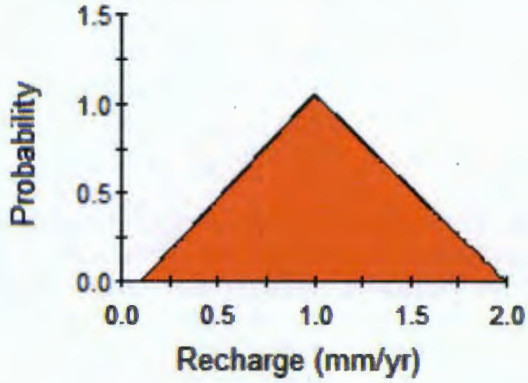

4.2.1.6 Summary of Recharge Rate Distributions Considered for ERDF PA Uncertainty and Sensitivity Analyses. The probability distribution functions representing the uncertainty in the recharge rate estimates evaluated in the ERDF PA analysis are summarized in Table 11. Two distinct recharge rates will be applied during the early post-closure period through the top portion of the surface barrier in order to take credit for the intact double liner, which is assumed to fail in 2135.

Effect of fire cycles on recharge rates will be evaluated in an independent analysis. Vegetation recovers after 1 to 2 years after a fire (PNNL-14744), and native perennial species such as sagebrush began reestablishing themselves on the prototype barrier within 2 to 3 years after the controlled burn there (PNNL-18934). A recharge rate without vegetation will be considered (typically less than 1 year) followed by the reestablishment of a young plant community and a mature plant community.

4.2.2 Water-Retention Properties

Data on physical and hydraulic properties of sediment samples collected in the 200 Area are compiled and reported in WHC-EP-0883, *Variability and Scaling of Hydraulic Properties for 200 Area Soils, Hanford Site*. For the purpose of developing physical and hydraulic properties for ERDF PA, a subset of data is used in WCH-464, *Hydrologic Data Package in Support of Environmental Restoration Disposal Facility*. The sample locations for this data set are shown in Figure 9. Since no ERDF-specific sample was available to estimate the hydraulic properties of the gravel-dominated Hanford sequence (Hf1), surrogates from the 241-T-106 tank site, 200-UP-1 Operable Unit (OU), 200-UP-2 OU in 200 West Area, and 100 Area sandy gravel sediments were used to create an Hf1 data subset, and also to expand other ERDF subsets (Figure 9). Similarly, as no data were available for the RFtf unit, the Hf2 data set was used to evaluate RFtf hydraulic properties, which were deemed similar to that of Hf2 because of similar lithology (sandy layers without gravel).

Table 11. Summary of the Recharge Distribution Functions that will be Considered for the ERDF PA Uncertainty and Sensitivity Analyses.

Period	Zone	Distribution Type	Recharge Rate (mm/yr)
Pre-operation (before 1996)	Undisturbed zone (Rupert sand with vegetation)	Triangular	Mean: 1.7 Min: 0.26 Max: 4 Mode: 0.9
Operation (1996-2035)	Undisturbed zone (Rupert sand with vegetation)	Triangular	Mean: 1.7 Min: 0.26 Max: 4 Mode: 0.9
	Disturbed zone (Rupert sand without vegetation)	Triangular	Mean: 45 Min: 22.5 Max: 90 Mode: 22.5
	Under construction zone (ERDF cells)	Fixed value	Best estimate: 0
Early Post-Closure (2035-2535)	Undisturbed zone (Rupert sand with vegetation)	Triangular	Mean: 1.7 Min: 0.26 Max: 4 Mode: 0.9
	Side slopes (compacted silt)	Fixed value	Best estimate: 2
	Side slopes from 2135 to 2535 (degraded gravel with vegetation)	Fixed value	Best estimate: 2
	Top portion of the barrier from 2035 to 2135	Fixed value	Best estimate: 0
	Top portion of the barrier from 2135 to 2535	Triangular	Mean: 0.5 Min: 0.05 Max: 1 Mode: 0.5
Late Post-Closure (at least 2535-3035, possible extension to 12035)	Undisturbed zone (Rupert sand with vegetation)	Triangular	Mean: 1.7 Min: 0.26 Max: 4 Mode: 0.9
	Degraded side slopes with vegetation	Fixed value	Best estimate: 2
	Degraded top portion of the barrier	Triangular	Mean: 1 Min: 0.1 Max: 2 Mode: 1

ERDF = Environmental Restoration Disposal Facility
PA = performance assessment

Figure 9. Location of the Samples Selected in WCH-464 to Build the ERDF Data Set of Soil Hydraulic Properties.

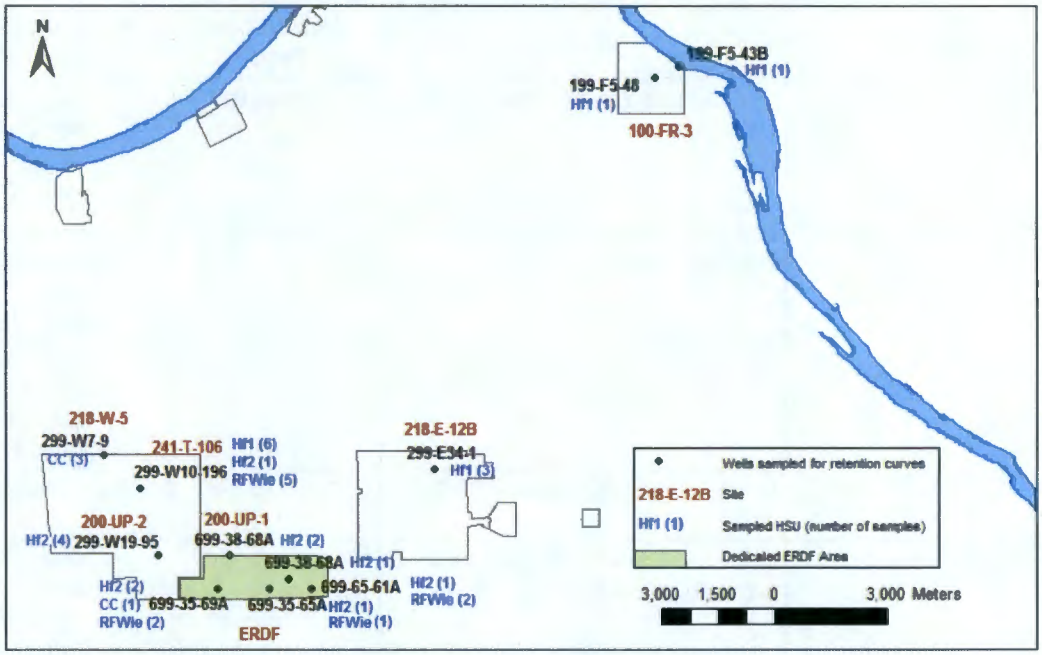

Based on fitting the laboratory measured soil-moisture retention and unsaturated hydraulic conductivity datasets, the following five parameters were estimated (WCH-464):

- The residual water content θ_r
- The saturated water content θ_s
- The van Genuchten fitting parameters α and n (van Genuchten 1980)
- The fitted saturated conductivity K_s.

The pore size distribution factor, ℓ (Mualem 1976), was kept fixed at 0.5 during this fitting. The fitted parameters were estimated for all five stratigraphic units that comprise vadose zone at ERDF. These are presented in Tables 12 through 16.

Table 12. Van Genuchten Parameters, Fitted Saturated Hydraulic Conductivity, and Measured Bulk Density Data for the Hanford Formation 1 (Gravel-Dominated) Unit (WCH-464).

Sample	Site/ Operable Unit	Well Number	Depth (m)	Percent Gravel	θ_s (cm^3/cm^3)	θ_r (cm^3/cm^3)	α (1/cm)	N (-)	Fitted K_s (cm/s)	Bulk Density (g/cm^3)
3-0210	241-T-106	299-W10-196	3.1	48	0.186	0.029	0.014	1.7674	1.96E-04	2.11
3-0572-2	100-FR-3	199-F5-48	8.1	27	0.179	0	0.0031	1.4306	2.38E-05	2.03
3-0576	100-FR-3	199-F5-43B	5.4	20	0.244	0.0166	0.0167	1.5428	3.96E-04	1.95
3-0668	241-T-106	299-W10-196	38.9	62	0.175	0	0.0192	1.6124	1.63E-04	2.13
3-0682	241-T-106	299-W10-196	46.1	51	0.224	0	0.0166	1.6577	2.37E-04	2.14
3-0688	241-T-106	299-W10-196	48.5	49	0.199	0	0.0043	1.5321	2.60E-05	2.17
3-0689	241-T-106	299-W10-196	52.2	28	0.236	0	0.0025	1.4747	4.58E-05	1.93
3-0690	241-T-106	299-W10-196	53.7	53	0.1819	0.0177	0.0046	1.541	4.19E-05	2.19
5-0152	218-E-12B	299-E34-1	65.5	26	0.280	0.0252	0.0438	1.3253	2.43E-03	1.85
5-0153	218-E-10	299-E32-4	10.7	47	0.214	0.0092	0.0099	1.3829	1.41E-04	2.08
5-0158	218-E-10	299-E32-4	71.6	44	0.217	0	0.0104	1.3369	4.47E-04	2.15

ERDF = Environmental Restoration Disposal Facility
Hf1 = Hanford formation 1

Table 13. Van Genuchten Parameters, Fitted Saturated Hydraulic Conductivity, and Measured Bulk Density Data for the Hanford Formation 2 (Sand-Dominated) Unit (WCH-464).

Sample	Site/ Operable Unit	Borehole Number	Depth (m)	Percent Gravel	θ_s (cm^3/cm^3)	θ_r (cm^3/cm^3)	α (1/cm)	N (-)	Fitted K_s (cm/s)	Bulk Density (g/cm^3)
3-0589	241-T-106	299-W10-196	25.5	1	0.429	0.0268	0.0057	1.7173	4.73E-05	1.86
3-1707	200-UP-2	299-W19-95	9.5	15	0.364	0.0742	0.0082	2.0349	1.55E-05	1.86
3-1712	200-UP-2	299-W19-95	43.1	0	0.290	0.0362	0.0156	2.021	2.05E-04	1.71
3-1713	200-UP-2	299-W19-95	46.3	0	0.5026	0	0.0077	1.6087	2.51E-05	1.72
3-1714	200-UP-2	299-W19-95	50.8	2	0.394	0.1301	0.0061	1.535	1.05E-04	1.68
4-0637	ERDF	699-36-63A	74.9	0	0.378	0	0.0153	1.7309	6.89E-05	1.62
4-0642	ERDF	699-35-69A	25.7	0	0.353	0.0286	0.014	1.4821	6.81E-04	1.98
4-0644	ERDF	699-35-69A	49.8	0	0.394	0.0557	0.0076	1.8353	3.24E-05	1.89
4-0791	ERDF	699-35-65A	63.2	0	0.338	0.0256	0.0226	2.2565	6.81E-04	1.60
4-1076	ERDF	699-35-61A	76.4	0	0.357	0	0.0293	1.7015	1.23E-03	1.74
4-1111	200-UP-1	699-38-68A	56.9	1	0.394	0.0497	0.0093	1.4342	5.80E-05	1.69
4-1112	200-UP-1	699-38-68A	66.0	0	0.4346	0	0.0054	1.4985	2.49E-05	1.73

ERDF = Environmental Restoration Disposal Facility
Hf2 = Hanford formation 2

Table 14. Van Genuchten Parameters, Fitted Saturated Hydraulic Conductivity, and Measured Bulk Density Data for the Cold Creek CCuz (Silt-Dominated) and CCuc (Caliche) Units (WCH-464).

Sample	Site/ Operable Unit	Borehole Number	Depth (m)	Percent Gravel	θ_s (cm^3/cm^3)	θ_r (cm^3/cm^3)	α (1/cm)	N (-)	Fitted K_s (cm/s)	Bulk Density (g/cm^3)
4-1011	ERDF	699-35-69A	73.0	0	0.489	0.0608	0.0037	1.6486	2.81E-05	1.72
5-5001	218-W-5	299-W7-9	21.6	4	0.380	0	0.0061	2.3247	2.30E-04	1.60
5-5002	218-W-5	299-W7-9	24.9	2	0.352	0.058	0.0058	1.7911	1.27E-04	1.68
5-5005	218-W-5	299-W7-9	21.1	0	0.374	0	0.0066	2.0076	1.08E-04	1.61

ERDF = Environmental Restoration Disposal Facility
CCuc = Cold Creek Caliche (carbonate-dominated unit)
CCuz = Cold Creek silt-dominated unit

Table 15. Van Genuchten Parameters, Fitted Saturated Hydraulic Conductivity, and Measured Bulk Density Data for the Ringold RFtf Unit (WCH-464).

Sample	Site/ Operable Unit	Borehole Number	Depth (m)	Percent Gravel	θ_s (cm^3/cm^3)	θ_r (cm^3/cm^3)	α (1/cm)	N (-)	Fitted K_s (cm/s)	Bulk Density (g/cm^3)
3-0589	241-T-106	299-W10-196	25.5	1	0.429	0.0268	0.0057	1.7173	4.73E-05	1.86
3-1707	200-UP-2	299-W19-95	9.5	15	0.364	0.0742	0.0082	2.0349	1.55E-05	1.86
3-1712	200-UP-2	299-W19-95	43.1	0	0.290	0.0362	0.0156	2.021	2.05E-04	1.71
3-1713	200-UP-2	299-W19-95	46.3	0	0.5026	0	0.0077	1.6087	2.51E-05	1.72
3-1714	200-UP-2	299-W19-95	50.8	2	0.394	0.1301	0.0061	1.535	1.05E-04	1.68
4-0637	ERDF	699-36-63A	74.9	0	0.378	0	0.0153	1.7309	6.89E-05	1.62
4-0642	ERDF	699-35-69A	25.7	0	0.353	0.0286	0.014	1.4821	6.81E-04	1.98
4-0644	ERDF	699-35-69A	49.8	0	0.394	0.0557	0.0076	1.8353	3.24E-05	1.89
4-0791	ERDF	699-35-65A	63.2	0	0.338	0.0256	0.0226	2.2565	6.81E-04	1.60
4-1076	ERDF	699-35-61A	76.4	0	0.357	0	0.0293	1.7015	1.23E-03	1.74
4-1111	200-UP-1	699-38-68A	56.9	1	0.394	0.0497	0.0093	1.4342	5.80E-05	1.69
4-1112	200-UP-1	699-38-68A	66.0	0	0.4346	0	0.0054	1.4985	2.49E-05	1.73

ERDF = Environmental Restoration Disposal Facility
RFtf = Ringold Formation Taylor Flat Unit

Table 16. Van Genuchten Parameters, Fitted Saturated Hydraulic Conductivity, and Measured Bulk Density Data for the Ringold RFWie Unit (WCH-464).

Sample	Site/ Operable Unit	Borehole Number	Depth (m)	Percent Gravel	θ_s (cm^3/cm^3)	θ_r (cm^3/cm^3)	α (1/cm)	N (-)	Fitted K_s (cm/s)	Bulk Density (g/cm^3)
4-0792	ERDF	699-35-65A	75.4	71	0.100	0.0084	0.03	1.5858	3.42E-04	2.32
4-1012	ERDF	699-35-69A	73.9	55	0.147	0	0.0076	1.5109	4.50E-05	2.19
4-1013	ERDF	699-35-69A	77.9	65	0.139	0.0127	0.0065	1.5656	1.06E-06	2.20
4-1079	ERDF	699-35-61A	90.9	61	0.163	0	0.014	1.3079	1.18E-04	2.06
4-1080	ERDF	699-35-61A	93.5	43	0.178	0	0.0074	1.3819	8.11E-06	2.00
3-0668	241-T-106	299-W10-196	38.9	62	0.175	0	0.0192	1.6124	1.63E-04	2.13
3-0682	241-T-106	299-W10-196	46.1	51	0.224	0	0.0166	1.6577	2.37E-04	2.14
3-0688	241-T-106	299-W10-196	48.5	49	0.199	0	0.0043	1.5321	2.60E-05	2.17
3-0689	241-T-106	299-W10-196	52.2	28	0.236	0	0.0025	1.4747	4.58E-05	1.93
3-0690	241-T-106	299-W10-196	53.7	53	0.1819	0.0177	0.0046	1.541	4.19E-05	2.19

ERDF = Environmental Restoration Disposal Facility
RFWie = Ringold Formation Wooded Island Unit E

Composite water-retention curves were calculated by fitting a single curve to all of the measured data available per geologic unit (Figure 10). The van Genuchten-Mualem parameters were determined for the composite curve as shown in Table 17 (WCH-464).

Due to small data sets (only 4 to 12 samples per geologic unit), the following approach was taken to determine uncertainty in each parameter for each geologic unit:

- First, the minimum and maximum value is determined for each parameter (based on information presented in Tables 12 through 16). Based on this information a uniform distribution is considered for each parameter as shown in Table 18. Because K_s was found to vary by several orders of magnitude within each unit, a log-uniform distribution was considered for this parameter.

- Each parameter distribution is sampled independently because the available sample subsets are deemed too small to infer robust correlation functions between parameters. For instance, Figure 11 shows scatter plots of different water retention parameters for the Hf2 unit, which has the largest data set of 12 samples. Poor correlations are observed among parameters (coefficient of determination <0.3 and thereby do not support a more sophisticated approach.

- As some of the van Genuchten parameter should be correlated based on soil moisture retention relationship, but because they are independently sampled from the uniform distributions, it is possible that the resulting soil moisture characteristic curve may become inconsistent with the observed dataset. To build confidence in the approach, 50 realizations were simulated by sampling the parameter distributions (using the Monte-Carlo methodology) and producing soil-moisture characteristic curves. An increased number of realizations produced similar results and so 50 realizations were deemed sufficient for the purpose of illustration. The simulated soil-moisture retention curves and the unsaturated conductivity curves corresponding to each realization are compared to those derived from the experimental data and the composite curve for each geologic unit (Figures 12 and 13). Figure 12 shows that all of the soil-moisture retention curves produced by 50 realizations fall

within or around the observed range of variation of the measured water retention curves and the composite curve falls approximately in the middle of the range produced by 50 realizations. This provides confidence in the sampling approach for independently sampling the van Genuchten parameters and still deriving reasonable soil moisture characteristic curves. Similar results are obtained for the unsaturated hydraulic conductivity curves (Figure 13); however, the uncertainty range at higher water tension (under very dry conditions) is relatively larger than the observed dataset. This is unlikely to have any appreciable effect as the magnitude of unsaturated hydraulic conductivity value is very small.

The Monte-Carlo sampling methodology will be used to generate a set of unsaturated hydraulic conductivity curves (as a function of water tension) based on a sampled set of van Genuchten parameters and K_s values (Figure 13). The combination of vadose zone parameters that lead to unsaturated hydraulic conductivity curves near their mean (composite), maximum, and minimum values among the set of hydraulic conductivity curves generated previously will be considered for propagation of uncertainty in the STOMP-based models (see Section 4.3).

Diffusive porosity is defined in STOMP as all interconnected pore space, and all saturations are defined with respect to the diffusive porosity. It is equivalent to the sum of the effective porosity (interconnected pore space associated with gross fluid flow) and residual moisture content. For the purpose of modeling, the diffusive porosity will be considered equal to the effective porosity, and it will be assumed that the fitted saturated water content (θ_s) represents a good estimate of these parameters.

Figure 10. Observed Distributions of the Water-Retention Parameters for Hanford Formation 2 (12 Samples).

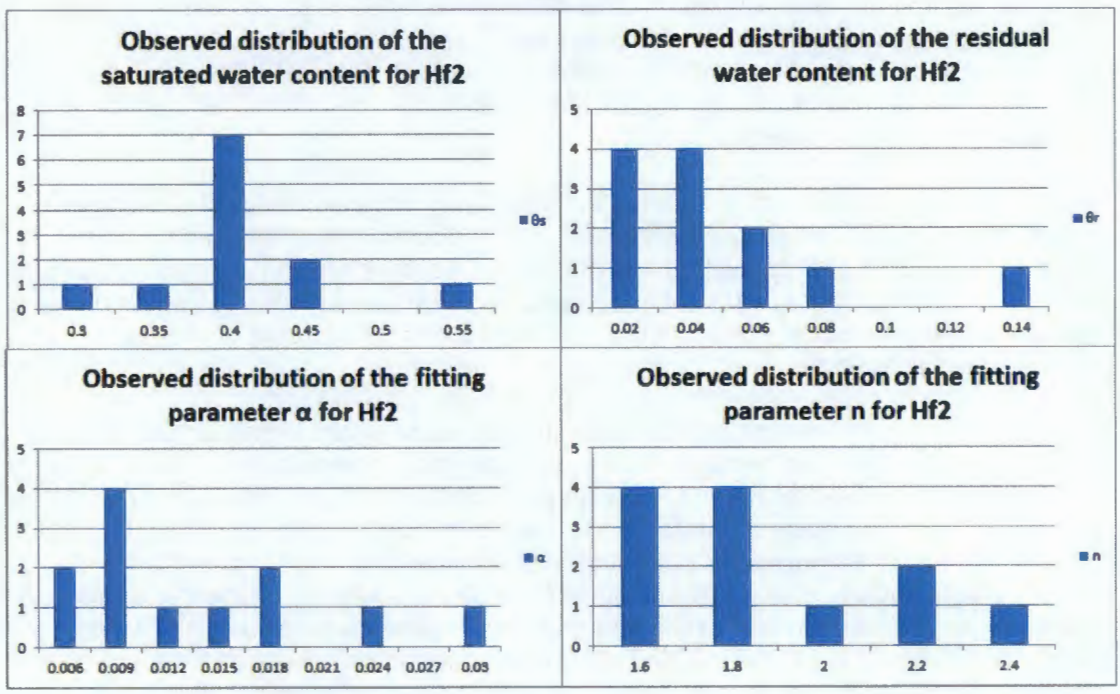

Table 17. Composite van Genuchten-Mualem Parameters for Each ERDF Vadose Zone Unit Based on All Moisture Retention and Unsaturated Conductivity Measurements Available Per Unit (WCH-464).

Geologic Unit	Number of Samples	θ_s	θ_r	A (1/cm)	n	ℓ	Fitted K_s (cm/s)
Hf1 (gravel-dominated)	11	0.2126	0.0032	0.0141	1.3730	0.5	2.62E-04
Hf2 (sand-dominated)	12	0.3819	0.0443	0.0117	1.6162	0.5	9.88E-05
Cold Creek CCuz (silt-dominated) and CCuc (caliche)	4	0.4349	0.0665	0.0085	1.8512	0.5	2.40E-04
Ringold RFtf	12	0.3819	0.0443	0.0117	1.6162	0.5	9.88E-05
Ringold RFWie	10	0.1380	0.0100	0.0210	1.374	0.5	5.60E-04

Hf1 = Hanford formation 1
Hf2 = Hanford formation 2
CCuc = Cold Creek Caliche (carbonate-dominated unit)
CCuz = Cold Creek silt-dominated unit
RFtf = Ringold Formation Taylor Flat Unit
RFWie = Ringold Formation Wooded Island Unit E

Table 18. Upper and Lower Bounds of the Distributions Selected for Each van Genuchtem/Mualem Parameter of Each ERDF Vadose Zone Unit.

Geologic Unit	Number of Samples	θ_s		θ_r		A (1/cm)		n		Fitted K_s (cm/s)	
		Min	Max	Min	Max	Min	Max	Min	Max	Min	Max
Hf1 (gravel-dominated)	11	0.175	0.28	0	0.029	0.0025	0.0438	1.3253	1.7674	2.38E-5	2.43E-3
Hf2 (sand-dominated)	12	0.29	0.5026	0	0.1301	0.0054	0.0293	1.4342	2.2565	1.55E-5	1.23E-3
Cold Creek CCuz (silt-dominated) and CCuc (caliche)	4	0.352	0.489	0	0.0608	0.0037	0.0066	1.6486	2.3247	2.81E-5	2.30E-4
Ringold RFtf	12	0.29	0.5026	0	0.1301	0.0054	0.0293	1.4342	2.2565	1.55E-5	1.23E-3
Ringold RFWie	10	0.1	0.236	0	0.0177	0.0025	0.03	1.3079	1.6577	1.06E-6	3.42E-4

Hf1 = Hanford formation 1
Hf2 = Hanford formation 2
CCuc = Cold Creek Caliche (carbonate-dominated unit)
CCuz = Cold Creek silt-dominated unit
RFtf = Ringold Formation Taylor Flat Unit
RFWie = Ringold Formation Wooded Island Unit E

Figure 11. Some Observed Correlations Between Water Retention Parameters for Hf2 (12 samples).

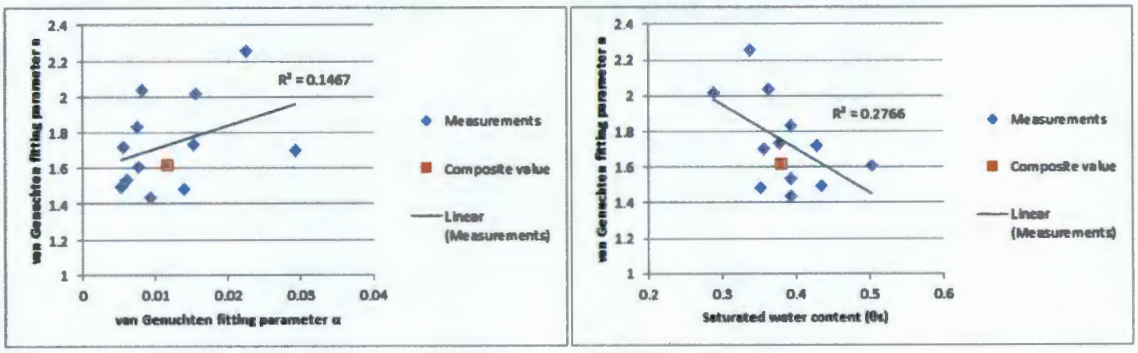

Figure 12. Water Retention Curves of the Hf1 Unit Obtained (i) by a Fit on Observed Retention Data for Each Hf1 Sample (in Red), (ii) by 50 Realizations of Sampled Parameters (in Gray) and (iii) Composite Water Retention Curve (in Black) Obtained by a Simultaneous Fit on All the Available Retention Data of the Hf1 Unit.

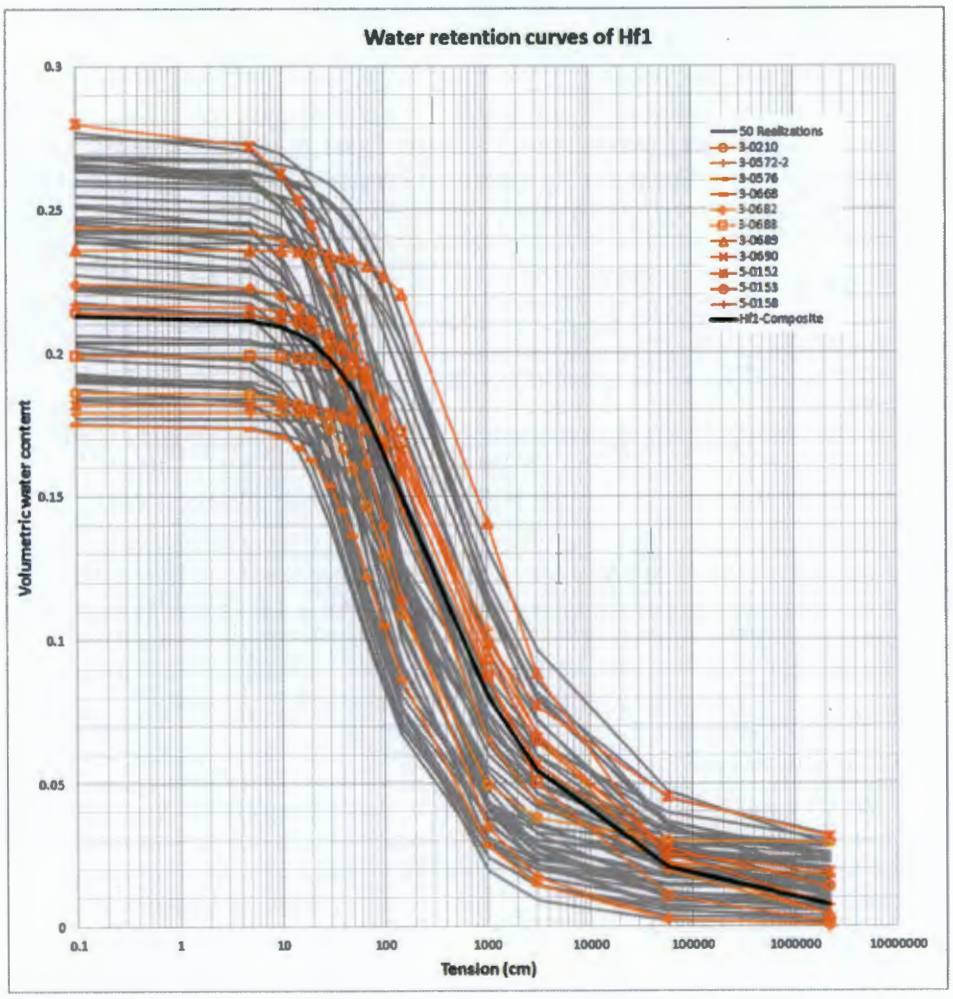

Figure 13. Unsaturated Hydraulic Conductivity Curves for Hf1 Unit Obtained (i) By a Fit on Observed Retention and Conductivity Data for Each Hf1 Sample (Red), (ii) By 50 Realizations of Sampled Parameters (In Gray) and (iii) Composite Water Retention Curve (In Black) Obtained By a Simultaneous Fit on All the Available Retention and Conductivity Data of the Hf1 Unit.

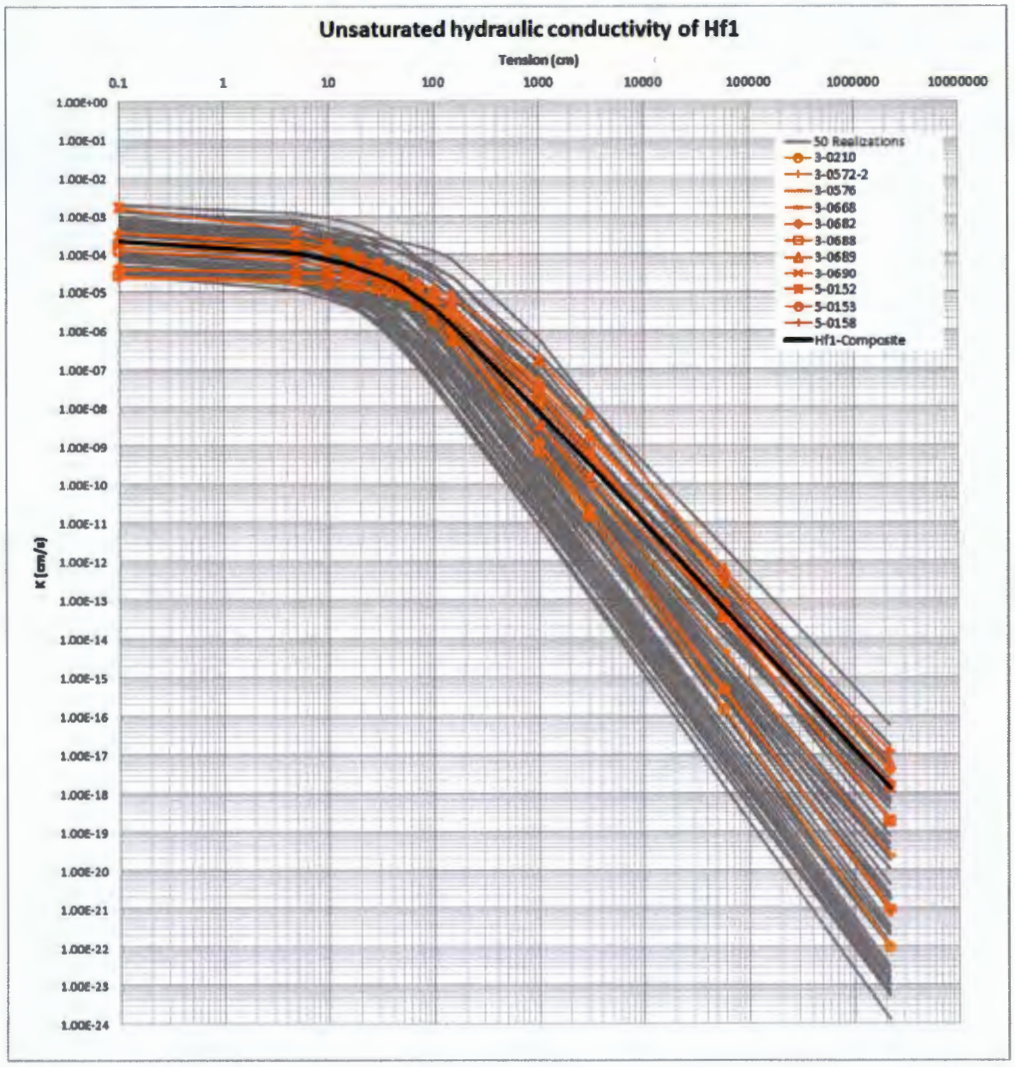

In order to develop an uncertainty range for diffusive porosity, the range of the fitted saturated water content (θ_s) presented earlier for each geologic unit is considered (Table 19). Because of limited information and small variations observed in saturated water content, a uniform distribution is considered for representing the diffusive porosity as shown in Table 19.

Table 19. Upper and Lower Bounds of the Saturated Water Content (θ_s) Used as Diffusive Porosity Estimates for Each ERDF Vadose Zone Unit (WCH-464).

Geologic Unit	Number of Samples	θ_s	
		Min	Max
Hf1 (gravel-dominated)	11	0.175	0.28
Hf2 (sand-dominated)	12	0.29	0.5026
Cold Creek CCuz (silt-dominated) and CCuc (caliche)	4	0.352	0.489
Ringold RFtf	12	0.29	0.5026
Ringold RFWie	10	0.1	0.236

Hf1 = Hanford formation 1
Hf2 = Hanford formation 2
CCuc = Cold Creek Caliche (carbonate-dominated unit)
CCuz = Cold Creek silt-dominated unit
RFtf = Ringold Formation Taylor Flat Unit
RFWie = Ringold Formation Wooded Island Unit E

4.2.3 Anisotropy

Moisture- or tension-dependent anisotropy provides a framework for up-scaling small-scale measurements to effective (up-scaled) properties for application to field-scale models. A stochastic model based on the Polmann (1990) approach is described in WCH-464 (Section 2.1.1) to evaluate the variable tension-dependent anisotropy for sediments at the ERDF site. The following parameters are first estimated using measured data:

- $<LnK_s>$, mean of log saturated conductivity
- σ^2_{LnKs}, variance of log saturated conductivity
- σ^2_{LnK}, variance of log unsaturated conductivity (which depends on mean tension)
- $<h>$, mean tension (positive) or absolute value of matric potential (negative)
- p, slope of the β versus LnK_s regression line, where β is the slope of the unsaturated conductivity curve and approximated locally based on the exponential model from Gardner (1958)
- σ_δ, standard deviation of the residuals in the β versus LnK_s regression
- ζ, $\sigma_\delta / \sigma_{LnKs}$
- A, mean slope, β, for LnK vs. h
- λ, vertical correlation lengths for LnK_s (assumed to be same as that of β).

The vertical correlation length, λ, for LnK_s was derived from fitting a spherical variogram on saturated conductivity estimates provided at about 30-cm (11.8-in.) intervals for a depth of 18 m (59 ft) within the Hanford formation (WCH-464). This data set corresponds to a site located about 0.8 km (0.5 mi) east of the Integrated Disposal Facility (IDF) site in the 200 East Area.

As no such data exist for the other units, the same correlation length was used for all the sandy units and a smaller value was considered for the gravelly units Hf1 and RFWie. This is supported by the fact that a much higher variance of LnK_s was found for the gravelly soils than for the sandy soils.

The macroscopic parameter estimates obtained in WCH-464 are reported in Table 20, together with the mean tension range (cm) for which they were estimated. Equivalent unsaturated horizontal (K_h^{eq}) and vertical (K_v^{eq}) conductivities for the mean tension (<*h*> in cm) are calculated according to the following Polmann's equations:

$$<LnK> = <LnK_s> - A<h> - \sigma^2_{LnKs}\lambda[p - p^2<h> - \zeta^2<h>]/(1+A\lambda)$$

$$\sigma^2_{LnK} = \sigma^2_{LnKs}[(1-p<h>)^2 + \zeta^2<h>^2]/(1+A\lambda)$$

$$K_h^{eq} = \exp[<LnK> + (\sigma^2_{LnK}/2)]$$

$$K_v^{eq} = \exp[<LnK> - (\sigma^2_{LnK}/2)]$$

Table 20. Macroscopic Anisotropy Parameter (Composite Values) Based on Polmann (1990) Equations for Various Geologic Units at the ERDF Site (WCH-464).

Geologic Unit	Number of Samples	<LnK_s>	$\sigma^2_{LnK_s}$	p	ζ	λ (cm)	A	Mean tension range (cm)
Hf1 (gravel-dominated)	11	-14.85	1.94	-2.6E-4	2.50E-4	30	0.00368	700 – 1000
Hf2 (sand-dominated)	12	-14.6	1.50	-7.2E-4	6.55E-4	50	0.00620	500 – 700
Cold Creek CCuz (silt-dominated) and CCuc (caliche)	4	-10.43	1.01	2.4E-3	9.34E-4	50	0.0104	300 – 400
Ringold RFtf	12	-14.6	1.50	-7.2E-4	6.55E-4	50	0.00620	500 – 700
Ringold RFWie	10	-15.76	3.56	-1.1E-4	1.84E-4	30	0.00371	700 – 1000

Hf1 = Hanford formation 1
Hf2 = Hanford formation 2
CCuc = Cold Creek Caliche (carbonate-dominated unit)
CCuz = Cold Creek silt-dominated unit
RFtf = Ringold Formation Taylor Flat Unit
RFWie = Ringold Formation Wooded Island Unit E

The following approach was considered to propagate the uncertainty associated with the vadose zone parameters (i.e., van Genuchten parameters and fitted K_s) through the Polmann equations in order to quantify the impact of this uncertainty on the upscaled anisotropy ratio:

- A total of 100 realizations of the unsaturated hydraulic conductivity curve for the sandy unit Hf1 was generated considering the uniform distribution of the van Genuchten parameters and the log-uniform distribution of fitted K_s previously presented in Section 0
- For the minimum and maximum hydraulic conductivity curves (bounding curves from the 100 realizations), the Polmann parameters A and LnK_s were calculated for the mean tension range of Hf1 (700<h<1,000 cm) (i.e., the straight part of the unsaturated conductivity curve using the model from Gardner [1958])
- Additionally, the Polmann parameters σ^2_{LnKs} (variance of log saturated conductivity), ζ (σ_δ / σ_{LnKs}), and p (slope of the regression line) were calculated for the 100 realizations
- The anisotropy ratio was then calculated with the Polmann equations considering the following six combinations of the Polmann parameters:
  - The parameters calculated with the 100 realizations, together with LnK_s and A obtained with the minimum unsaturated hydraulic conductivity curve of the 100 realizations
  - The parameters calculated with the 100 realizations, together with LnK_s and A obtained with the maximum unsaturated hydraulic conductivity curve of the 100 realizations
  - The parameters calculated with the 100 realizations, together with the composite values of LnK_s and A (first row in Table 20)
  - The composite parameters (Table 20), together with LnK_s and A obtained with the minimum unsaturated hydraulic conductivity curve of the 100 realizations
  - The composite parameters (Table 20), together with LnK_s and A obtained with the maximum unsaturated hydraulic conductivity curve of the 100 realizations
  - The composite parameters together with the composite values of LnK_s and A (all from Table 20).

The results of the anisotropy ratio calculations are reported in Table 21. They show that the range in anisotropy ratio remains small (for the mean tension range of 700<h<1,000 cm for Hf1) even when the unsaturated hydraulic conductivity is varied over the full range of uncertainty. Consequently, the Polmann parameters will be kept fixed during the analyses at the best estimate values (i.e., the composite values) reported in Table 20.

Table 21. Anisotropy Ratios of Hf1 Calculated Over the Mean Tension Range (700 through 1,000 cm) Considering Range of Unsaturated Hydraulic Conductivity Curves.

Unsaturated Hydraulic Conductivity Curve Considered to Estimate A and LnK_s for the Mean Tension Range (700 < h < 1000 cm) of Hf1	Composite Polmann Parameters		Polmann Parameters Calculated from 100 Realizations	
	h = 700 cm	h = 1000 cm	h = 700 cm	h = 1000 cm
Minimum unsaturated hydraulic conductivity curve	11.7	17.1	9.9	11.3
Maximum unsaturated hydraulic conductivity curve	12.0	17.7	10.1	11.6
Composite unsaturated hydraulic conductivity curve	12.1	17.9	10.2	11.7

Hf1 = Hanford formation 1

4.3 PROPAGATION OF UNCERTAINTY IN FLOW-FIELD USING PROCESS-LEVEL STOMP MODEL

Different combinations of vadose zone hydraulic parameter values will be generated from their distributions (Section 4.2) and will be used to run a process-level model developed using STOMP multiple times. The number of runs performed will be based on the judgment of the modelers and will depend on the evaluation of results and the availability of computational resources. The results generated with these simulations will provide the plausible range of flow rates through the vadose zone over time. It is expected that the calculations would include, at a minimum, estimates of flow rates based on evaluation of the following:

- The best estimate recharge rates and vadose zone properties in order to get the best estimate of the flow rates through the vadose zone
- The maximum estimates of the recharge rate together with the set of vadose zone parameters that result in maximum unsaturated hydraulic conductivity, in order to get the maximum estimate of the flow rates through the vadose zone
- The minimum estimates of the recharge rate together with the set of vadose zone parameters that result in the minimum unsaturated hydraulic conductivity, in order to get the minimum estimate of the flow rates through the vadose zone.

When possible, further simulations would be performed by selecting parameter values from different percentiles of the parameter distributions (e.g., the 25th and 75th percentiles). The results given by these simulations will be analyzed in order to abstract the flow-field for use in the GoldSim-based model.

4.4 ABSTRATION OF FLOW-FIELD FOR GOLDSIM-BASED MODEL

In order to abstract the vadose zone flow-field derived from multiple STOMP simulations, the results will be analyzed in order to identify the following two hydraulic regimes:

- The transient flow-field in the early part of the simulations
- The steady-state flow-field once a stable velocity is reached over time in the long-term part of the simulations.

For each of these regimes, a probability distribution function of the vadose flow rates and associated water contents through time may be built. The uncertainty in the flow-field can be propagated in GoldSim-based abstraction model by sampling the distribution.

5.0 SATURATED ZONE FLOW-FIELD

As the water table mainly flows through the Ringold Formation Unit E below ERDF, the saturated zone parameters will be defined for this unit only. Both STOMP- and GoldSim-based models can use these parameters, as the saturated zone flow rates can be determined based on parameter values and by applying the Darcy's law. Several Hanford documents informally refer to Ringold Formation Unit E as Ringold E. For convenience we will also use this abbreviated terminology.

5.1 SATURATED HORIZONTAL HYDRAULIC CONDUCTIVITY

Several past studies have focused on evaluating the horizontal hydraulic conductivity of the Ringold E in the Central Plateau. According to pump test analysis and calibration results (Table 22) summarized within the Central Plateau Groundwater Model Data Package (CP-47631), this parameter can range from 0.1 to more than 2,500 m/d. An updated review of Ringold E properties, conducted for the development of the 200-ZP-1 Model (DOE/RL-2007-28) showed that this parameter more usually ranges from 1 to 100 m/d, according to slug tests and sediment sample analysis (Figure 14).

In order to evaluate the ERDF-specific uncertainty associated with this parameter, we will focus on slug test results obtained by PNNL-19482, *Slug Test Characterization Results for Multi-Test/Depth Intervals Conducted During the Drilling of CERCLA Operable Unit OU UP-1 Wells 299-W19-48, 699-30-66, and 699-36-70B,* and calibrated results from the Central Plateau model in the vicinity of ERDF. These are shown in Figure 15. PNNL-19482 performed slug tests at different test depth intervals within three UP-1 wells located less than 1 km (0.6 mi) from the ERDF site. These results are compared in Figure 16 with the calibrated value of 5 m/d (16.4 ft/d) from the Central Plateau model for Ringold E. The comparison shows that the saturated horizontal hydraulic conductivity of Ringold E is expected to vary from 0.1 to 10 m/d (0.32 to 32.8 ft/d) with 5 m/d as the most probable value. Consequently, in order to represent the uncertainty associated with the saturated horizontal hydraulic conductivity of Ringold E, a uniform distribution between 0.1 and 10 m/d (0.32 to 32.8 ft/d) is considered so that higher weight is given to the upper end of the range and the mean value is near 5 m/d.

Table 22. Review of Ringold E Horizontal Hydraulic Conductivity (m/d) (CP-47631).

Geologic Unit	PNL-10886	PNNL-13641	PNNL-14398	PNNL-14753
	Experimental Data	Experimental Data	Calibration	Calibration
Ringold Formation Unit E	0.1 – 200	0.1 – 560	3 – 10	0.24 – 2562

Figure 14. Observed Distribution of the Saturated Hydraulic Conductivity of Ringold Formation Unit E Considering Slug Tests and Sediment Sample Analyses for the 200-ZP-1 Model (DOE/RL-2007-28).

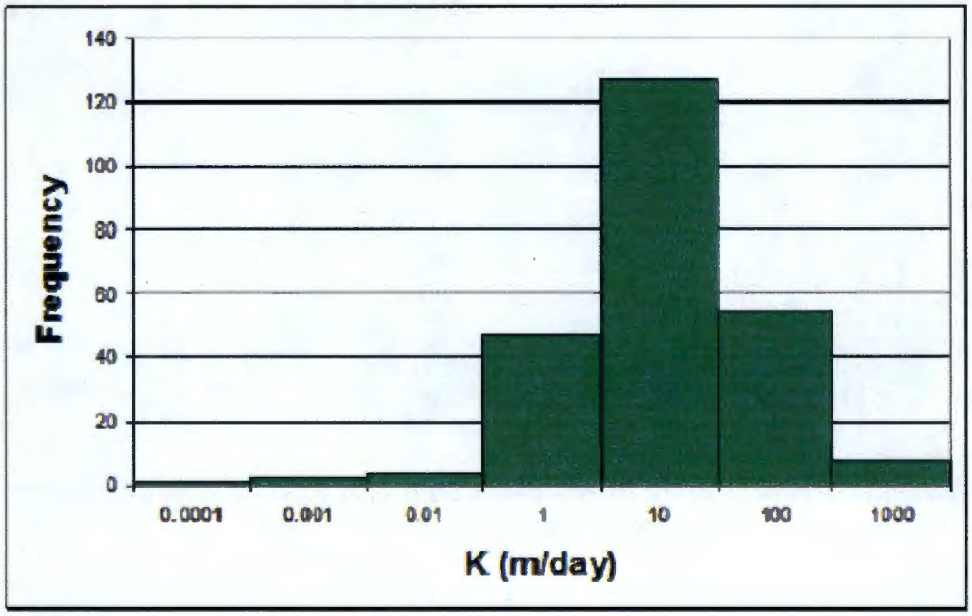

Figure 15. Location of the Tested Wells Near the ERDF and Calibrated Horizontal Hydraulic Conductivity Field Given by the Central Plateau Model V3.4 in the ERDF Area for the Ringold Formation Unit E.

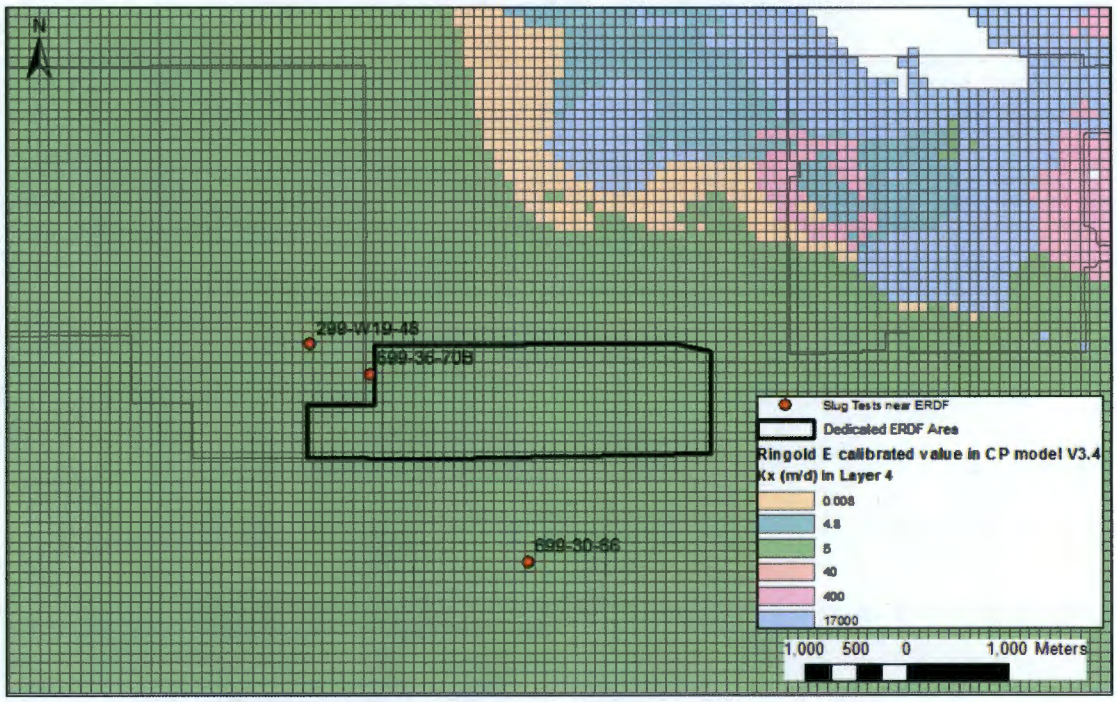

Figure 16. Comparison of PNNL-19482 Slug Test Results with Central Plateau Model Calibration in the ERDF Area.

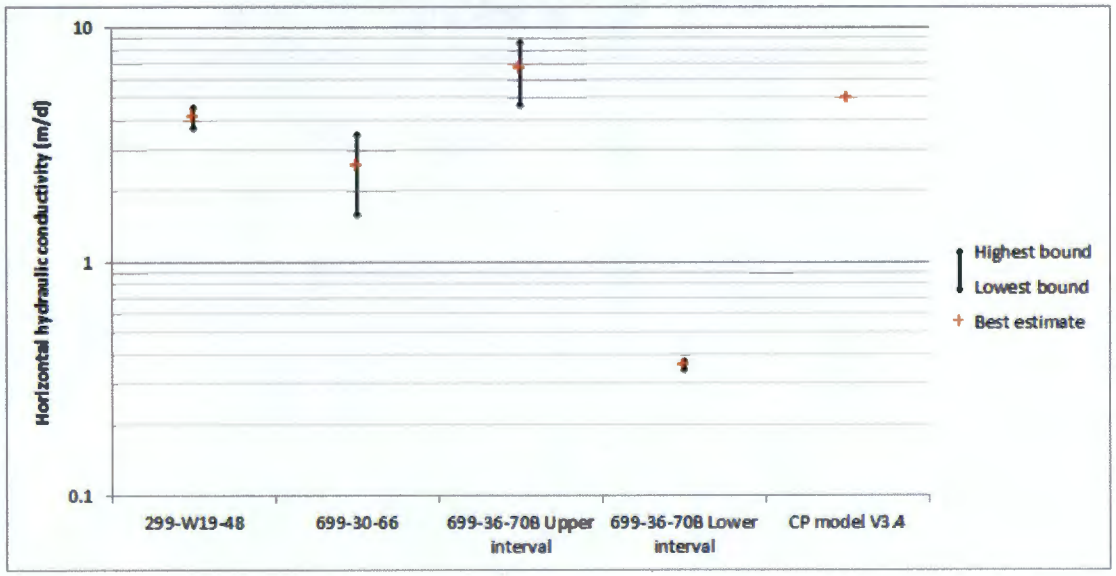

5.2 ANISOTROPY IN SATURATED HYDRAULIC CONDUCTIVITY

Anisotropy in saturated hydraulic conductivity, defined here as the ratio of vertical to horizontal hydraulic conductivity, for Ringold E has been estimated from pumping tests, which indicate values ranging from 0.01 to 0.1 (PNL-10886, *Development of a Three-Dimensional Ground-Water Model of the Hanford Site Unconfined Aquifer System: FY 1995 Status Report*) and 0.015 to 0.5 (DOE/RL-2007-28) for post-year 2000 testing. On the other hand, in the Central Plateau model, a vertical anisotropy of 0.1 was considered (CP-46731). This value was consistent with the previous modeling analyses (e.g., PNNL-14398, *Transient Inverse Calibration of the Site-Wide groundwater Flow Model (ACM-2): FY 2003 Progress Report,* and PNNL-14753, *Groundwater Data Package for Hanford Assessments*) prior to the development of the Central Plateau groundwater model.

Several studies have found the model calibration relatively insensitive to vertical anisotropy. This is largely because of the large horizontal scale and the relatively small vertical extent of the modeling analyses.

Even if this parameter is not likely to have a significant impact on modeling results, its associated uncertainty may be considered in the following triangular distribution, according to the plausible values suggested in the literature:

- A minimum value of 0.01
- A maximum value of 0.5
- A mode of 0.1.

This leads to a mean of 0.2.

5.3 HYDRAULIC GRADIENT

According to the Central Plateau groundwater model (CP-47631), the hydraulic heads around ERDF will continue to slowly decline until their stabilization around year 2200 at 125.8 m (412.7 ft) in the western part of the facility and 121.6 m (398.9 ft) in the eastern part (Figure 17). This evolution will lead to a stabilization of the west-to-east and northeast hydraulic gradient to the long-term value of 0.00145, which is close to the one observed prior to start of Hanford operations (Figure 17).

It should be noted that the predicted evolution of hydraulic head includes the influence of the pump-and-treat remedial actions currently under way and planned for 200-ZP-1 Groundwater Operable Unit. The planned shutdown of ZP-1 pumping wells in year 2034 may likely have a minor effect on the simulated heads (Figure 17) and hydraulic gradient (Figure 18) as shown for the monitoring well 699-35-70 located near ERDF. The water table elevation could increase by about 17 cm (6.7 in.) over a 5-year period following shutdown, and the hydraulic gradient would change to 0.0016 for a short period of time.

Figure 17. Predictive Heads (m) Below the ERDF Given by the Central Plateau Model Version 3.4 Until 2200.

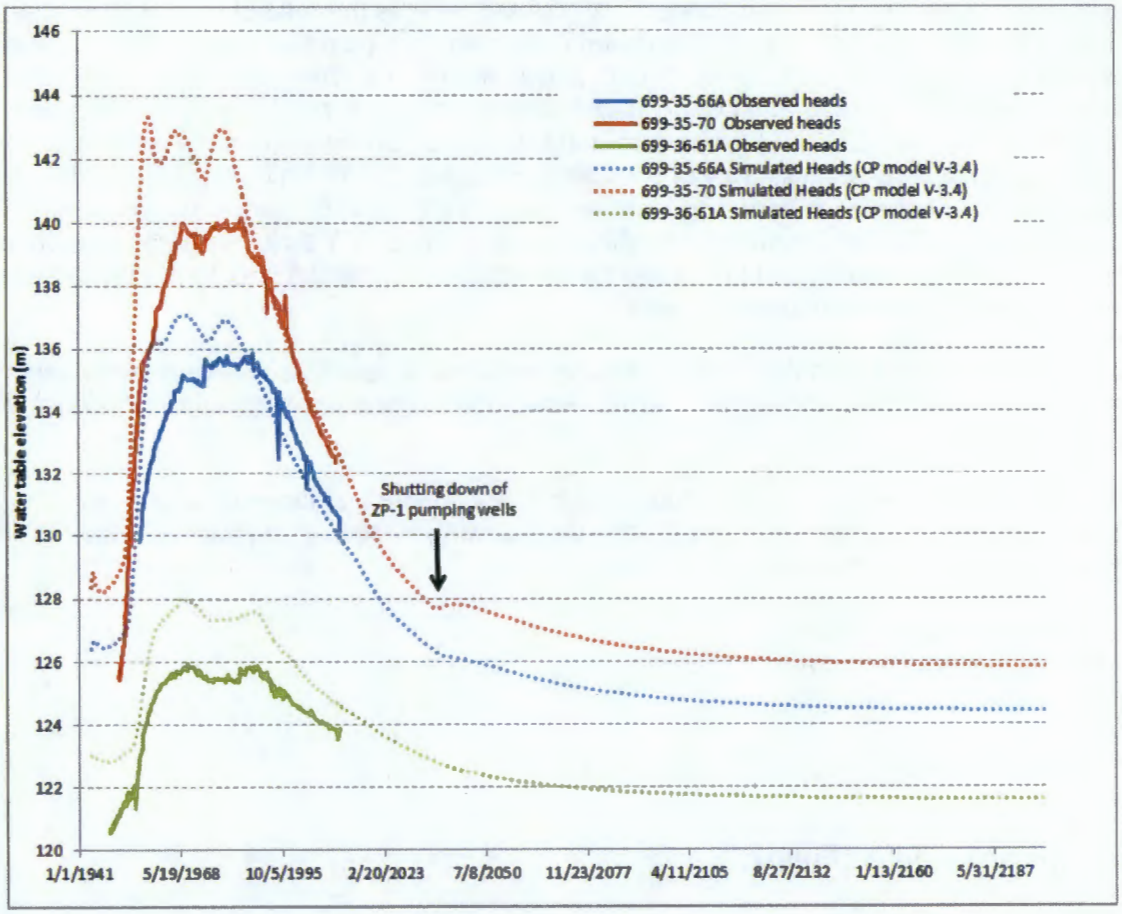

Figure 18. Observed and Simulated W-NE Hydraulic Gradient (%) Through the ERDF Given by the Central Plateau Model Version 3.4 Until 2300.

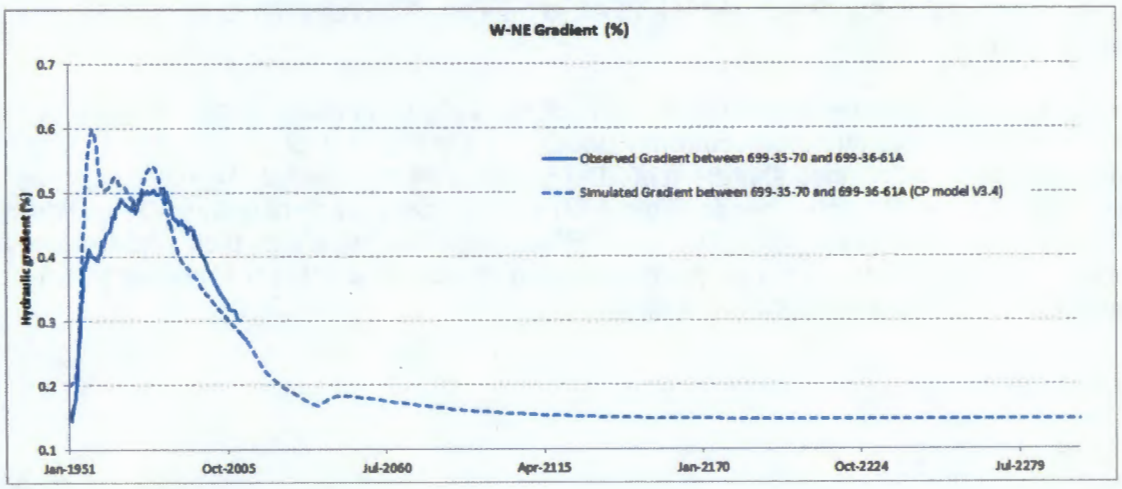

The changes in hydraulic gradient are expected to occur early in the simulation (within the first 200 years) and may not influence the transport of contaminants because of long travel times in the vadose zone. It is expected that by the time the mobile contaminants (that have zero retardation) reach the water table the hydraulic gradient will be nearly stable. Consequently, the hydraulic gradient will not be treated as a stochastic variable and its value is fixed at 0.0015, which is the long-term value given by the Central Plateau model.

5.4 SPECIFIC STORAGE

PNNL-19482 provides specific storage values for the three wells located in 200-UP-1 Groundwater Operable Unit near ERDF. Multiple stress-level slug tests were conducted at different depth intervals in the unconfined Ringold Unit E aquifer. Specific storage and hydraulic conductivity estimates were derived from evaluating the results using standard, linear response based analytical methods (either the Bouwer and Rice or standard type-curve method). The specific storage values range from 5E-6 to 3.5E-3 m^{-1}. The results are summarized in Table 23.

Uncertainty in specific storage is unlikely to affect the modeling results as near steady-state conditions are expected to exist in the unconfined aquifer for the duration of the PA analysis. No pumping is expected within the ERDF footprint and the effect of any pump-and-treat remedial action in the 200-UP-1 Groundwater Operable Unit is expected to be short-term and much earlier than the expected contaminant arrival times in the unconfined aquifer. Consequently, a log-uniform distribution over the specific storage range is considered and the fixed mean value of 1.32E-4 m^{-1} is recommended for use in the analysis.

Table 23. Slug-Test Analysis Result (PNNL-19482).

Test Well	Test Zone Depth (m) Below Ground Surface	Specific Storage (m^{-1})
299-W19-48	86.53 to 89.27 m	5.0E-6 to 1.0E-5
699-30-66	75.7 to 89.0 m	5.0E-6 to 3.0E-5
699-36-70B	81.91 to 83.33 m	2.5E-3 to 3.5E-3
	112.58 to 114.12 m	1.0E-4
	124.11 to 125.43 m	8.0E-4

6.0 TRANSPORT PARAMETERS FOR MODELING

This section focuses on quantifying the uncertainty associated with the parameters used to represent transport of radionuclides and their chemical interactions with geologic materials along a migration pathway from the ERDF through the vadose zone and into the underlying aquifer.

A summary of modeling input parameters that will affect the chemical interactions between radionuclides and geologic materials below the ERDF is provided in WCH-476, *Chemical Reactivity of Radionuclides with Waste Material and Subsurface Soils during Release and*

Migration from the Environmental Restoration Disposal Facility. The standard modeling approach being considered for describing the chemical reactivity of contaminants in the ERDF PA modeling analyses is based on the radioelement-specific retardation factor R defined as:

$$R=1+K_d*(\rho/\theta)$$

where K_d is the aqueous/solid partitioning ratio, ρ is the sediment bulk density, and θ the porosity in saturated media (aquifer) or volumetric moisture content in unsaturated media (vadose zone).

We will discuss first the parameter values that affect the retardation factor (i.e., K_d and bulk density) and then other transport parameters (e.g., macrodispersivity).

6.1 AQUEOUS/SOLID PARTITIONING RATIO (K_d)

The literature data available to implement an empirical K_d approach in the ERDF PA modeling analyses has been summarized in WCH-476. As the majority of the K_d experiments currently available corresponds to measurements performed on fine-grained fraction of the sediments, extrapolation of these results to the ERDF-specific HSUs requires gravel correction, and changes in reactivity based on the carbonate or silt content. We have identified following four groups of ERDF HSUs for which a specific K_d value is presented:

- Sandy units that have negligible gravel content (Hf2 and RFtf)
- Gravely units that have a significant gravel content (Hf1 and RFwie)
- Silt-dominated unit of Cold Creek (CCuz)
- Carbonate-dominated unit corresponding to Cold Creek Caliche (CCuc).

The choice of K_d values (and uncertainty range) are guided by the chemistry of the leachate that could emanate from ERDF wastes. Six waste chemistry types were defined by PNNL-11800, *Composite Analysis for Low-Level Waste Disposal in the 200 Area Plateau of the Hanford Site,* in order to differentiate chemically distinct waste streams that impact the sorption of contaminants. PNNL-14702 reviewed this classification and defined semi-quantitative chemical concentrations for each waste stream category in order to provide a less ambiguous and more technically defensible approach for the assignment of K_d values (Table 24).

ERDF leachate samples were found to contain detectable concentrations of common metals, anions, and mobile radionuclides under near neutral conditions (WCH-295, *Groundwater and Leachate Monitoring and Sampling at ERDF, CY 2007*, WCH-315, *Groundwater and Leachate Monitoring and Sampling at ERDF, CY 2008*). An average pH of 7.4 was measured over the period from June 2006 to December 2008 in leachate samples. Based on the categories presented in Table 24, the ERDF leachate chemistry is judged to belong to category 4 (i.e., Low-Salt/Near-Neutral category).

The unconfined aquifer below the ERDF was also found to belong to this category because of near-neutral, low-salt, and low-organic conditions in the groundwater (WCH-295, WCH-315). Even if leachate chemistry were to evolve in the future as new ERDF cells become filled with other wastes, it is not expected to increase or decrease the pH or salt concentrations significantly in ERDF leachates, to the point of modifying the waste stream designation.

Table 24. Waste Stream Designation and Assumed Compositions for Determination of K_d Values (PNNL-14702).

Category	Waste Stream Description	Composition
1	Very acidic	1.0 M HNO_3
2	High salt/very basic	2 M NaOH, 4 M $NaNO_3$, 2 M $NaNO_2$
3	Chelates/high-salt	1.0 M $NaNO_3$, 0.05 M EDTA, pH 12
4	Low-salt/near-neutral	Same as Hanford Groundwater
5	Integrated Disposal Facility vitrified waste	High pH, high ionic strength
6	Integrated Disposal Facility cementitious waste	High pH, medium ionic strength

Additionally, as no known Hanford operations-period contamination has impacted the ERDF vadose zone prior to its construction, the "no impact" classification for the vadose zone sediments will be considered for selecting a K_d value for each radionuclide of concern.

The radionuclides for which K_d values are derived for the ERDF PA are selected depending on the ERDF inventory estimate (WCH-479). Radionuclides that are unlikely to impact the dose estimates because of either their short half-life or small initial inventory have been screened out (as detailed in Section 0). This selection process can be summarized as follows:

- All radionuclides with half-lives greater than 6 years and/or inventories (currently disposed and forecast wastes decayed to 2011) greater than 1 Ci have been selected (as presented in Table 5-1 of WCH-479).
- ^{41}Ca and ^{133}Ba are excluded because ^{41}Ca has a very low inventory (0.3 Ci decayed to 2011) and ^{133}Ba will decay relatively quickly to a small activity due to its short half-life of 10.6 years (e.g., it will decay from 5 Ci in 2011 to 1 Ci in 2035 at ERDF closure).
- ^{60}Co, ^{126}Sn, ^{243}Cm, and ^{243}Am are included in the list of radionuclides for the ERDF PA due to relatively large initial inventory or because of decay to radionuclides that can impact the dose.
- The final list of radionuclides of concern for the ERDF PA corresponds to the following 40 radioactive isotopes: ^{108m}Ag, ^{241}Am, ^{14}C, ^{113m}Cd, ^{36}Cl, ^{244}Cm, ^{137}Cs, ^{152}Eu, ^{154}Eu, ^{3}H, ^{129}I, ^{40}K, ^{93}Mo, ^{93m}Nb, ^{94}Nb, ^{59}Ni, ^{63}Ni, ^{237}Np, ^{238}Pu, ^{239}Pu, ^{240}Pu, ^{241}Pu, ^{242}Pu, ^{226}Ra, ^{79}Se, ^{151}Sm, ^{121m}Sn, ^{90}Sr, ^{99}Tc, ^{232}Th, ^{233}U, ^{234}U, ^{235}U, ^{236}U, ^{238}U, ^{93}Zr, ^{60}Co, ^{126}Sn, ^{243}Cm, and ^{243}Am.

The sections below provide radionuclide-specific K_d distribution functions for sandy, gravely, silty, and carbonated HSUs for a low-salt/near-neutral waste stream and geologic materials not impacted by waste. These K_d values are deemed relevant for representing chemical reactivity of the contaminants during their migration through the vadose zone as well as through the unconfined aquifer.

6.1.1 K_d for Sandy and Gravelly Units

In an attempt to choose an internally consistent set of K_d values representative of the ERDF-specific geologic material, a single source of reference is desirable. Based on review of literature, values suggested by PNNL-17154, *Geochemical Characterization Data Package for the Vadose Zone in the Single-Shell Tank Waste Management Areas at the Hanford Site,* for sand-size sediments not impacted by waste were selected, as shown in Table 25. Where data/information gaps were found the K_d values were taken from additional references (also listed in Table 25).

For ^{14}C, the possible maximum K_d value of 100 mL/g and the best estimate of 5 mL/g recommended by both PNNL-14702 and PNNL-17154 was lowered in order to be consistent with results presented by *Multiphase Carbon-14 Transport in Near-Field-Scale Unsaturated Column of Natural Sediments* (INEEL 2004), which show that for silty and carbonated sediments (a more favorable substrate for ^{14}C sorption than sand-dominated layers), the ^{14}C K_d value range from 0.8 to 2.4 mL/g (more details are presented in Section 6.1.3). Consequently, we chose a best estimate of 0.5 mL/g for sandy units Hf2 and RFtf (lower value than 0.8 mL/g for carbonated silty clay described by INEEL 2004), a minimum value 0 mL/g, and a maximum value of 2.4 mL/g.

The K_d values reported in Table 25 are not corrected for gravel content as they are given for sediment materials <2 mm (0.8 in.) in size. For materials that contain significant amounts of gravel (notably Hf1 and Ringold E), K_d values are typically lower than those determined with <2-mm (0.8-in.) size material because the surface area and corresponding quantity of adsorption sites is much lower (PNNL-17154).

The two following equations, recommended by PNNL-17154, are used for gravel correction, depending on minimum K_d value:

- For minimum $K_d \geq 10$ mL/g:

$$K_d(gc) = (1-0.77f)\ K_d(<2mm)$$

- For minimum $K_d < 10$ mL/g:

$$K_d(gc) = (1-f)\ K_d(<2mm)$$

Where $K_d(gc)$ is the gravel-corrected K_d value of K_d contaminants, *f* the weight fraction gravel, and K_d (<2 mm [0.8 in.]) is the K_d determined for <2-mm (0.8-in.) size fraction of sediment material.

Table 25. Aqueous/Solid Partitioning Ratio (K_d in mL/g) Estimates for Low-Organic/ Low-Salt/Near-Neutral Waste Chemistry, not Impacted Sand (<2 mm Size Fraction).

Analyte	Not Impacted Sand (< 2 mm Size)			Reference[a]
	Best Value	Minimum Value	Maximum Value	
^{3}H	0	0	0	1
^{36}Cl	0	0	0	1
$^{99}Tc(VII)$	0	0	0.1	1
^{129}I	0.2	0	2	1
^{14}C	0.5	0	2.4	2
$^{60}Co(II,III)$	10	0	2000	1
U(VI), all isotopes	0.8	0.2	4	1
$^{237}Np(V)$	10	2	30	1
$^{79}Se(VI,IV)$	5	3	10	1
$^{226}Ra(II)$	20	10	50	1
^{90}Sr	20	10	50	1
$^{126}Sn(IV)$, all isotopes	50	50	250	1
^{63}Ni, all isotopes	300	50	2500	1
^{241}Am, all isotopes	300	60	2000	1
Eu(III), all isotopes	300	60	2000	1
Pu, all isotopes	600	200	2000	1
^{137}Cs	2000	200	10000	1
^{108m}Ag, all isotopes	400	10	30000	3 Not specific for sand (soil/water values)
Nb, all isotopes	0	0	0.1	4
^{113m}Cd	300	80	1000	5 Not specific for sand (soil/water value for 7<pH<8)
^{232}Th	1000	40	2500	4
Cm, all isotopes	300	60	1300	4
^{93}Zr	1000	40	2500	4
^{151}Sm	300	60	2000	Assumed equivalent to Eu
^{93}Mo	0	0	0	No relevant information
^{40}K	0	0	0	No relevant information

[a]Reference:
1: PNNL-17154
2: INEEL 2004
3: EPA/600/R-05/074
4: PNNL-16663
5: EPA 402-R-99-004B

The average gravel content for each HSU is summarized in Table 26 based on measured values (Tables 12 through 16). According to the equations presented above, K_d values for the gravel-dominated sequences Hf1 (41.4% of gravel) and RFwie (53.8% of gravel) were corrected for the gravel fraction, and the resulting corrected values are presented in Table 27. The K_d for sand reported in Table 25 will be used without further modification for Hf2 and RFtf, as their gravel content is close to zero (Table 26).

A triangular distribution is chosen to represent uncertainty in K_d. The distribution will be bounded by the maximum and minimum values with best value assigned to the mode of the distribution.

6.1.2 K_d for Silt-Dominated Cold Creek (CCuz)

For the silt-dominated layer of the Cold Creek unit, K_d estimates suggested by PNNL-17154 for silt-size sediments not impacted by waste are considered (Table 28). A triangular distribution is chosen to represent uncertainty in K_d. The distribution will be bounded by the maximum and minimum values with best value assigned to the mode of the distribution.

For ^{14}C, in order to be consistent with results presented by INEEL (2004), a minimum value and best estimate value of 0.8 mL/g is considered for K_d (same as the minimum value observed for carbonated silty clay; more details are presented in Section 6.1.3). A maximum value of 2.4 mL/g is considered for K_d (same as the maximum value observed for carbonated silty clay).

Where no information is available for sorption of radionuclides on silt-size sediments, the values developed for sand (Table 25) will be used.

Table 26. Average Percent Gravel Measured on Each Unit (According to WCH-464).

Geologic Unit	Number of Samples	Percent Gravel (%)
Hf1 (gravel-dominated)	11	41.4
Hf2 (sand-dominated)	12	Rounded to 0
Cold Creek CCuz (silt-dominated) and CCuc (caliche)	4	Rounded to 0
Ringold RFtf	12	Rounded to 0
Ringold RFWie (Ringold E)	10	53.8

Hf1 = Hanford formation 1
Hf2 = Hanford formation 2
CCuc = Cold Creek Caliche (carbonate-dominated unit)
CCuz = Cold Creek silt-dominated unit
RFtf = Ringold Formation Taylor Flat Unit
RFWie = Ringold Formation Wooded Island Unit E

Table 27. Aqueous/Solid Partitioning Ratio (K_d in mL/g) Estimates Corrected for Gravel for Hf1 and RFwie.

Analyte	Hf1 (41.4% of Gravel)			RFwie (53.8% of Gravel)		
	Best Value	Minimum Value	Maximum Value	Best Value	Minimum Value	Maximum Value
^{3}H	0.0	0.0	0.0	0.0	0.0	0.0
^{36}Cl	0.0	0.0	0.0	0.0	0.0	0.0
$^{99}Tc(VII)$	0.0	0.0	0.1	0.0	0.0	0.0
^{129}I	0.1	0.0	1.2	0.1	0.0	0.9
^{14}C	0.3	0.0	1.4	0.2	0.0	1.1
$^{60}Co(II,III)$	5.9	0.0	1172.0	4.6	0.0	924.0
U(VI), all isotopes	0.5	0.1	2.3	0.4	0.1	1.8
$^{237}Np(V)$	5.9	1.4	17.6	4.6	1.2	13.9
$^{79}Se(VI,IV)$	2.9	2.0	5.9	2.3	1.8	4.6
$^{226}Ra(II)$	13.6	6.8	34.1	11.7	5.9	29.3
^{90}Sr	13.6	6.8	34.1	11.7	5.9	29.3
$^{126}Sn(IV)$, all isotopes	34.1	34.1	170.3	29.3	29.3	146.4
^{63}Ni, all isotopes	204.4	34.1	1703.1	175.7	29.3	1464.4
^{241}Am, all isotopes	204.4	40.9	1362.4	175.7	35.1	1171.5
Eu(III), all isotopes	204.4	40.9	1362.4	175.7	35.1	1171.5
Pu, all isotopes	408.7	136.2	1362.4	351.4	117.1	1171.5
^{137}Cs	1362.4	136.2	6812.2	1171.5	117.1	5857.4
^{108m}Ag, all isotopes	272.5	6.8	20436.6	234.3	5.9	17572.2
Nb, all isotopes	0.0	0.0	0.1	0.0	0.0	0.0
^{113m}Cd	204.4	54.5	681.2	175.7	46.9	585.7
^{232}Th	681.2	27.2	1703.1	585.7	23.4	1464.4
Cm, all isotopes	204.4	40.9	885.6	175.7	35.1	761.5
^{93}Zr	681.2	27.2	1703.1	585.7	23.4	1464.4
^{151}Sm	204.4	40.9	1362.4	175.7	35.1	1171.5
^{93}Mo	0.0	0.0	0.0	0.0	0.0	0.0
^{40}K	0.0	0.0	0.0	0.0	0.0	0.0

Hf1 = Hanford formation 1
RFWie = Ringold Formation Wooded Island Unit E

Table 28. Aqueous/Solid Partitioning Ratio (K_d in mL/g) Estimates for Low-Organic/Low-Salt/Near-Neutral Waste Chemistry, Not Impacted Silt-Size Sediments.

Analyte	Silt-Size Sediments – No Impact PNNL-17154		
	Best Value	Minimal Value	Maximal Value
^{3}H	0	0	0
^{36}Cl	0	0	0
$^{99}Tc(VII)$	0	0	0.2
^{129}I	0.2	0	5
$^{60}Co(II,III)$	10	0	2000
U(VI)	1.5	0.2	20
$^{237}Np(V)$	20	5	60
$^{79}Se(VI,IV)$	5	3	30
$^{226}Ra(II)$	40	20	200
^{90}Sr	40	20	200
Pb(II)	100	30	2000
$^{126}Sn(IV)$	100	50	250
^{63}Ni	300	50	2500
^{241}Am	300	200	4000
Eu(III)	300	200	4000
Pu (all isotopes)	600	200	4000
^{137}Cs	2000	600	10000

Note: Where no radionuclide specific information is available for sorption the K_d values developed for sand (Table 25) is used.

6.1.3 K_d for Carbonate-Dominated Cold Creek (CCuc)

For the carbonate-dominated layer of the Cold Creek unit (caliche), K_d estimates suggested by PNNL-17154 for carbonate-dominated sediments not impacted by waste are presented in Table 29, except for ^{14}C for which the K_d was derived from INEEL (2004) based on meso-scale column experiment (2.6 m [8.5 ft] high by 0.9 m [2.9 ft] in diameter) filled with playa-derived calcareous silty-clays under near-neutral pH conditions. They derived a K_d range for ^{14}C from 0.8 to 2.4 mL/g, with an average of 1.6 mL/g. Much higher values (83 mL/g) and a dependence on contact time were previously observed by Allard et al. (1981). However, the lower K_d values measured by INEEL (2004) after 1 year under steady-state geochemical and hydraulic conditions are deemed more reliable to represent sorption in the Cold Creek caliche unit. Consequently, a uniform distribution bounded by 0.8 and 2.4 mL/g will be considered to represent the uncertainty associated with this parameter in this unit.

Where no radionuclide specific information is available for sorption on carbonate in PNNL-17154, the K_d values developed for sand (Table 25) will be used.

Table 29. Aqueous/Solid Partitioning Ratio (K_d in mL/g) Estimates Given by PNNL-17154 for Low Organic/Low Salt/Near Neutral Waste Chemistry, Not Impacted Carbonate-Dominated Sediments.

Analyte	Carbonate-dominated Sediments – No Impact PNNL-17154		
	Best Value	Minimal Value	Maximal Value
^{3}H	0	0	0
^{36}Cl	0	0	0
$^{99}Tc(VII)$	0	0	0.2
^{129}I	0.2	0	2
$^{60}Co(II,III)$	15	3	2000
U(VI)	4	3	20
$^{237}Np(V)$	10	2	30
$^{79}Se(VI,IV)$	5	3	30
$^{226}Ra(II)$	40	20	200
^{90}Sr	40	20	200
Pb(II)	50	10	500
$^{126}Sn(IV)$	50	50	250
^{63}Ni	300	50	2500
^{241}Am	150	60	2000
Eu(III)	150	60	2000
Pu (all isotopes)	300	200	2000
^{137}Cs	2000	200	10000

Note: Where no radionuclide specific information is available for sorption the K_d values developed for sand (Table 25) is used.

A triangular probability distribution is chosen to represent uncertainty in K_d. The distribution will be bounded by the maximum and minimum values with best value assigned to the mode of the distribution. For ^{14}C a uniform distribution bounded by 0.8 and 2.4 mL/g is considered.

6.2 EFFECTIVE BULK DENSITIES

In order to take into account the uncertainty associated with effective bulk densities, we will consider uniform distributions of this parameter, which will be bounded by the minimum and maximum bulk densities measured for each unit (Tables 12 through 16). These bounds are summarized in Table 30.

Table 30. Minimum and Maximum Bulk Densities (g/cm^3) Measured for Each Geologic Unit (WCH-464).

Geologic Unit	Number of Samples	Bulk Density (g/cm^3)	
		Min.	Max.
Hf1 (gravel-dominated)	11	1.85	2.19
Hf2 (sand-dominated)	12	1.60	1.98
Cold Creek CCuz (silt-dominated) and CCuc (caliche)	4	1.60	1.72
Ringold RFtf	12	1.60	1.98
Ringold RFWie	10	1.93	2.32

Hf1 = Hanford formation 1
Hf2 = Hanford formation 2
CCuc = Cold Creek Caliche (carbonate-dominated unit)
CCuz = Cold Creek silt-dominated unit
RFtf = Ringold Formation Taylor Flat Unit
RFWie = Ringold Formation Wooded Island Unit E

6.3 EFFECTIVE DIFFUSION COEFFICIENT

It is assumed that the effective large-scale diffusion coefficients for all strata at the ERDF site are a function of volumetric moisture content, θ, and can be expressed using the Millington-Quirk (1961) empirical relation:

$$D_e(\theta) = D_0 \frac{\theta^{10/3}}{\theta_s^2}$$

where $D_e(\theta)$ is the effective diffusion coefficient of an ionic species, and D_0 is the effective diffusion coefficient for the same species in free water. The molecular diffusion coefficient for all species in pore water is assumed to be 2.5×10^{-5} cm^2/sec (WHC-SD-WM-EE-004, *Performance Assessment of Grouted Double-Shell Tank Waste Disposal at Hanford*). This parameter will not be treated as a stochastic variable as its effect on transport through the vadose zone and saturated zone is expected to be negligible.

6.4 VADOSE ZONE MACRODISPERSIVITIES

In WCH-464, the Gelhar and Axness (1983) model is recommended to estimate asymptotic values of macrodispersivity. However, to account for the effects of unsaturated flow, the following modified version is suggested for ERDF:

$$A_L(< h >) = \sigma_{LnK}^2 \lambda$$

where the longitudinal macrodispersivity A_L depends on the mean tension $< h >$ through σ_{LnK}^2 the variance of log unsaturated conductivity and λ the correlation length of log unsaturated conductivity (*LnK*).

Assuming a correlation length of 30 cm (11.8 in.) for all five units and an anisotropy ratio of 10, the macrodispersivities (Table 31) were estimated for nonreactive species in the vadose zone (WCH-464).

Vadose zone macrodispersivities are not expected to affect significantly the transport of contaminants below the facility. These parameters will thus not be treated as stochastic variables and the values reported in Table 31 will be kept fixed in uncertainty analyses.

Table 31. Nonreactive Macrodispersivities Estimates for Various Geologic Units at the ERDF Site (WCH-464).

Geologic Unit	A_L cm	A_T cm
Backfill Hf1 (gravel-dominated)	~150	15
Hf2 (sand-dominated)	~150	15
Cold Creek CCuz (silt-dominated) and CCuc (caliche)	~50	5
Ringold RFtf	~150	15
Ringold RFWie	~150	15

Hf1 = Hanford formation 1
Hf2 = Hanford formation 2
CCuc = Cold Creek Caliche (carbonate-dominated unit)
CCuz = Cold Creek silt-dominated unit
RFtf = Ringold Formation Taylor Flat Unit
RFWie = Ringold Formation Wooded Island Unit E

6.5 SATURATED ZONE MACRODISPERSIVITIES

In order to define a plausible range for longitudinal saturated macrodispersivities (α_L) below the ERDF, three general relationships quantifying the dependence of this parameter on measurement scale (L_s) were extracted from literature (Table 32). The application of these relationships for a scale of about 100 m (328.1 ft) (corresponding to the ERDF modeling scale) leads to the following longitudinal macrodispersivity estimates (Table 33). As shown in Table 33, the saturated longitudinal macrodispersivity can range from 3 to 17 m (9.8 to 55.7 ft) for transport scale of 100 m (328 ft). A uniform distribution ranging from 1 to 20 m (3.2 to 65.6 ft) is considered. The ratio between longitudinal and transverse macrodispersivity will be assumed to be uniformly distributed between 5 and 10 (ratios considered in 200 Area modeling approaches, cf. Khaleel et al. 2006 and van der Kamp et al. 1994, "Field Study of a Long and Very Narrow Contaminant Plume").

Table 32. Relationship Between Saturated Longitudinal Macrodispersivity (α_L) and Scale of Measurement (L_s).

Reference	Relationship	Origin
Neuman (1990)	$\alpha_L \approx 0.017 L_s^{1.5}$	"Universal relationship" established considering both field and laboratory data (excluding modeling results)
Schulze-Makuch (2005)	$\alpha_L \approx 0.085 L_s^{0.81}$	Established considering field and modeling results (all reliabilities) and excluding laboratory data
Xu and Eckstein (1995)	$\alpha_L \approx 0.94(\log_{10} L_s)^{2.693}$	Established considering the same data set as Neuman (1990) including numerical model results

Table 33. Estimates of Saturated Longitudinal Macrodispersivities Deduced from Three Literature Relationships Considering a Length Scale of 100 m.

Reference	Saturated Longitudinal Macrodispersivity Estimate (m) for a Scale ≈ 100 m
Neuman (1990)	17
Schulze-Makuch (2005)	3.5
Xu and Eckstein (1995)	6

7.0 POST-CLOSURE ERDF INVENTORY

The inventory of various radionuclides in waste disposed at ERDF is described in detail in WCH-479. The inventory estimates are separated into the following two components:

- Currently disposed at the ERDF (as of August 2010)
- Currently forecast to be disposed at the ERDF (before its assumed closure in 2035).

These two radionuclide inventory estimates are decay corrected to a common date and combined in order to develop the post-closure inventory for the PA calculations. Uncertainty ranges for radionuclide inventory is also developed based on the guidance in WCH-479.

The mass and activities of radionuclides from waste sites where remedial decisions are pending, but where some waste could be potentially considered for disposal at ERDF once the decisions are made, have also been estimated in WCH-479 to provide bounding estimates for ERDF post-closure inventory. However, these bounding estimates are not deemed to be reliable at this stage and have potentially large uncertainties. Therefore, inventory estimates from bounding calculations are not considered in the ERDF PA calculations.

The uncertainty estimates for the currently disposed and currently forecasted inventory is used to develop a best, minimum, and maximum value. These estimates are reported in Table 34. As a starting point, all radionuclides with half-lives greater than 6 years and/or inventories (currently disposed and forecast wastes decayed to 2011) greater than 1 Ci have been selected (same as Table 5-1 of WCH-479). This list of radionuclides is further modified by excluding or including the following radionuclides:

- ^{41}Ca and ^{133}Ba are excluded because ^{41}Ca has a very low inventory (0.3 Ci decayed to 2011) and ^{133}Ba will decay relatively quickly to a small activity due to its short half-life of 10.6 years (e.g., it will decay from 5 Ci in 2011 to 1 Ci in 2035 at assumed ERDF closure).

- ^{60}Co, ^{126}Sn, ^{243}Cm and ^{243}Am are included in the list of radionuclides for the ERDF PA due to relatively large initial inventory or because of decay to radionuclides that can impact the dose.

The final list of radionuclides of concern for the ERDF PA corresponds to the following 40 radionuclides: ^{108m}Ag, ^{241}Am, ^{14}C, ^{113m}Cd, ^{36}Cl, ^{244}Cm, ^{137}Cs, ^{152}Eu, ^{154}Eu, ^{3}H, ^{129}I, ^{40}K, ^{93}Mo, ^{93m}Nb, ^{94}Nb, ^{59}Ni, ^{63}Ni, ^{237}Np, ^{238}Pu, ^{239}Pu, ^{240}Pu, ^{241}Pu, ^{242}Pu, ^{226}Ra, ^{79}Se, ^{151}Sm, ^{121m}Sn, ^{90}Sr, ^{99}Tc, ^{232}Th, ^{233}U, ^{234}U, ^{235}U, ^{236}U, ^{238}U, ^{93}Zr, ^{60}Co, ^{126}Sn, ^{243}Cm, and ^{243}Am.

In order to represent uncertainty in the radionuclide inventory, a triangular distribution is considered for the currently disposed and currently forecast wastes (Table 34). The best values are assigned to the mode of the distribution with minimum and maximum set at their estimated values.

Table 34. Best, Minimum, and Maximum Estimates of Total Mass or Activity for Each Radionuclide Considered in the ERDF PA Uncertainty Analyses. (2 Pages)

Radionuclides	Half-Life (yr)	Specific-Activity (Ci/g)	Activity (Ci) Currently Disposed Decayed to 2035			Activity (Ci) Currently Forecast Decayed to 2035			Total Activity (Ci) Decayed to 2035		
			Best	Min	Max	Best	Min	Max	Best	Min	Max
^{108m}Ag	418	7.926	238.32	166.83	357.49	0.77	0.54	1.15	239.09	167.37	358.64
^{241}Am	432.9	3.427	524.45	367.12	786.68	317.56	222.29	476.34	842.01	589.41	1263.02
^{14}C	5729.2	4.455	1882.53	1495.65	2492.75	458.67	458.67	917.33	2341.2	1954.32	3410.08
^{113m}Cd	13.7	231.1	0.89	0.62	1.34	0.48	0.33	0.71	1.37	0.95	2.05
^{36}Cl	301987.5	0.03291	0.00	0.00	0.00	0.02	0.01	0.04	0.02	0.01	0.04
^{244}Cm	18.1	80.93	0.64	0.45	0.96	11.17	7.82	16.75	11.81	8.27	17.71
^{137}Cs	30.2	86.55	8416.35	6917.55	10952.78	247878.76	178703.29	299760.36	256295.1	185620.8	310713.1
^{152}Eu	13.5	174	1411.50	988.05	2117.25	5.83	4.08	8.75	1417.33	992.13	2126
^{154}Eu	8.6	270.3	195.10	136.57	292.65	24.57	17.20	36.85	219.67	153.77	329.5
^{3}H	12.3	9613	2014.47	1603.30	2585.98	5947.74	4137.56	9050.91	7962.21	5740.86	11636.89
^{129}I	15688772	0.0001768	0.02	0.01	0.03	0.00	0.00	0.01	0.02	0.01	0.04
^{40}K	1279881867	6.989E-06	0.00	0.00	1.00	0.00	0.00	0.00	0	0	1
^{93}Mo	3011.6	1.278	0.50	0.35	0.75	0.03	0.02	0.04	0.53	0.37	0.79
^{93m}Nb	16.1	238.6	1.71	1.20	2.56	0.07	0.05	0.11	1.78	1.25	2.67
^{94}Nb	19985.7	0.1905	0.30	0.21	0.45	0.08	0.06	0.12	0.38	0.27	0.57
^{59}Ni	75988	0.07982	189.96	132.97	284.94	109.98	76.98	164.96	299.94	209.95	449.9
^{63}Ni	99	57.38	12223.38	8556.37	18335.07	464.93	329.68	929.86	12688.31	8886.05	19264.93
^{237}Np	2139896.6	0.0007047	0.40	0.28	0.60	0.03	0.02	0.04	0.43	0.3	0.64
^{238}Pu	87.7	17.12	34.74	27.79	45.17	41.36	33.09	62.04	76.1	60.88	107.21
^{239}Pu	24111.5	0.06202	259.82	207.86	337.77	1199.17	959.34	1798.76	1458.99	1167.2	2136.53
^{240}Pu	6562.6	0.2269	119.70	95.76	155.61	299.24	239.39	448.86	418.94	335.15	604.47
^{241}Pu	14.4	103	1606.40	1285.12	2088.32	251.98	201.59	377.98	1858.38	1486.71	2466.3
^{242}Pu	373602.6	0.003954	0.70	0.56	0.91	0.02	0.02	0.03	0.72	0.58	0.94
^{226}Ra	1599.9	0.9885	0.89	0.62	1.34	0.79	0.55	1.19	1.68	1.17	2.53
^{79}Se	64992.3	0.06969	0.10	0.07	0.15	0.05	0.03	0.07	0.15	0.1	0.22
^{151}Sm	90	26.32	215.29	150.70	322.94	51.54	36.08	77.31	266.83	186.78	400.25

Table 34. Best, Minimum, and Maximum Estimates of Total Mass or Activity for Each Radionuclide Considered in the ERDF PA Uncertainty Analyses. (2 Pages)

Radionuclides	Half-Life (yr)	Specific-Activity (Ci/g)	Activity (Ci) Currently Disposed Decayed to 2035			Activity (Ci) Currently Forecast Decayed to 2035			Total Activity (Ci) Decayed to 2035		
			Best	Min	Max	Best	Min	Max	Best	Min	Max
^{121m}Sn	55	53.76	12.56	8.79	18.84	0.03	0.02	0.04	12.59	8.81	18.88
^{90}Sr	28.6	138.8	6372.24	5030.72	8384.53	111793.72	55896.86	134152.47	118166	60927.58	142537
^{99}Tc	211296.2	0.01711	21.00	17.00	32.00	32.00	22.00	63.99	53	39	95.99
^{232}Th	14050498137	1.097E-07	1.10	0.77	1.65	0.20	0.14	0.30	1.3	0.91	1.95
^{233}U	159264.3	0.009633	14.60	11.68	18.98	0.01	0.00	0.01	14.61	11.68	18.99
^{234}U	245709.4	0.006217	13.50	10.80	17.55	4.00	2.80	8.00	17.5	13.6	25.55
^{235}U	703792430.4	2.161E-06	7.60	6.08	9.88	0.30	0.21	0.60	7.9	6.29	10.48
^{236}U	23417496.9	6.468E-05	0.40	0.32	0.52	0.10	0.07	0.20	0.5	0.39	0.72
^{238}U	4468020382	3.361E-07	67.50	54.00	87.75	20.00	14.00	40.00	87.5	68	127.75
U Total[a]			202.00	160.00	260.00	60.00	42.00	120.00	262.00	202.00	380.00
^{93}Zr	1529900.9	0.002515	16.00	11.20	24.00	2.00	1.40	3.00	18	12.6	27
^{60}Co	5.3	1131	236.18	165.33	354.27	1300.07	910.05	1950.10	1536.25	1075.38	2304.37
^{126}Sn	100007.6	0.02839	0.20	0.14	0.30	0.07	0.05	0.10	0.27	0.19	0.4
^{243}Cm	30	49.03	0.06	0.04	0.09	0.46	0.32	0.69	0.52	0.36	0.78
^{243}Am	7364.3	0.1997	0.60	0.42	0.90	0.20	0.14	0.30	0.8	0.56	1.2

[a] Results are in Metric Tons (not Ci) under Activity heading.
ERDF = Environmental Restoration Disposal Facility
PA = performance assessment

8.0 CONCLUSION

In conclusion, we summarize in the following tables the distribution functions suggested in this report for recharge (Table 35), vadose zone parameters (Tables 36 and 37), saturated zone parameters (Table 38), nonreactive (Table 39), and reactive (Table 40) transport parameters and inventory (Table 41) that will be considered in the ERDF PA uncertainty and sensitivity analyses.

Table 35. Summary of the Recharge Distribution Functions that will be Considered for the ERDF PA Uncertainty and Sensitivity Analyses.

Period	Zone	Distribution Type	Value (mm/yr)
Pre-operation (before 1996)	Undisturbed zone (Rupert sand with vegetation)	Triangular	Mean: 1.7 Min: 0.26 Max: 4 Mode: 0.9
Operation (1996-2035)	Undisturbed zone (Rupert sand with vegetation)	Triangular	Mean: 1.7 Min: 0.26 Max: 4 Mode: 0.9
	Disturbed zone (Rupert sand without vegetation)	Triangular	Mean: 45 Min: 22.5 Max: 90 Mode: 22.5
	Under construction zone (ERDF cells)	Fixed value	Best estimate: 0
Early Post-Closure (2035-2535)	Undisturbed zone (Rupert Sand with vegetation)	Triangular	Mean: 1.7 Min: 0.26 Max: 4 Mode: 0.9
	Side slopes (compacted silt)	Fixed value	Best estimate: 2
	Side slopes from 2135 to 2535 (degraded gravel with vegetation)	Fixed value	Best estimate: 2
	Top portion of the barrier from 2035 to 2135	Fixed value	Best estimate: 0
	Top portion of the barrier from 2135 to 2535	Triangular	Mean: 0.5 Min: 0.05 Max: 1 Mode: 0.5
Late Post-Closure (2535 End of Simulation)	Undisturbed zone (Rupert Sand with vegetation)	Triangular	Mean: 1.7 Min: 0.26 Max: 4 Mode: 0.9
	Degraded side slopes with vegetation	Fixed value	Best estimate: 2
	Degraded top portion of the barrier	Triangular	Mean: 1 Min: 0.1 Max: 2 Mode: 1

ERDF = Environmental Restoration Disposal Facility
PA = performance assessment

Table 36. Summary of the Vadose Zone Parameter Distributions that will be Considered for the ERDF PA Uncertainty and Sensitivity Analyses.

Geologic Unit	Number of Samples	θ_s		θ_r		A (1/cm)		n		Fitted K_s (cm/s)	
		Uniform Distribution		Uniform Distribution		Uniform Distribution		Uniform Distribution		Log-uniform Distribution	
		Min	Max	Min	Max	Min	Max	Min	Max	Min	Max
Hf1 (gravel-dominated)	11	0.175	0.28	0	0.029	0.0025	0.0438	1.3253	1.7674	2.38E-5	2.43E-3
Hf2 (sand-dominated)	12	0.29	0.5026	0	0.1301	0.0054	0.0293	1.4342	2.2565	1.55E-5	1.23E-3
Cold Creek CCuz (silt-dominated) and CCuc (caliche)	4	0.352	0.489	0	0.0608	0.0037	0.0066	1.6486	2.3247	2.81E-5	2.30E-4
Ringold RFtf	12	0.29	0.5026	0	0.1301	0.0054	0.0293	1.4342	2.2565	1.55E-5	1.23E-3
Ringold RFWie	10	0.1	0.236	0	0.0177	0.0025	0.03	1.3079	1.6577	1.06E-6	3.42E-4

Note: Diffusive porosity is assumed to be equivalent to the saturated water content. Same uncertainty range is applied.

ERDF = Environmental Restoration Disposal Facility
Hf1 = Hanford formation 1
HF2 = Hanford formation 2
CCuc = Cold Creek Caliche (carbonate-dominated unit)
CCuz = Cold Creek silt-dominated unit
PA = performance assessment
RFtf = Ringold Formation Taylor Flat Unit
RFWie = Ringold Formation Wooded Island Unit E

Table 37. Summary of the Polmann Parameters that will be Considered for the ERDF PA Uncertainty and Sensitivity Analyses.

Geologic Unit	Number of Samples	$\langle LnK_s \rangle$	$\sigma^2_{LnK_s}$	p	ζ	λ (cm)	A	Mean tension range (cm)
Hf1 (gravel-dominated)	11	-14.85	1.94	-2.6E-4	2.50E-4	30	0.00368	700 – 1000
Hf2 (sand-dominated)	12	-14.6	1.50	-7.2E-4	6.55E-4	50	0.00620	500 – 700
Cold Creek CCuz (silt-dominated) and CCuc (caliche)	4	-10.43	1.01	2.4E-3	9.34E-4	50	0.0104	300 – 400
Ringold RFtf	12	-14.6	1.50	-7.2E-4	6.55E-4	50	0.00620	500 – 700
Ringold RFWie	10	-15.76	3.56	-1.1E-4	1.84E-4	30	0.00371	700 – 1000

ERDF = Environmental Restoration Disposal Facility
Hf1 = Hanford formation 1
HF2 = Hanford formation 2
CCuc = Cold Creek Caliche (carbonate-dominated unit)
CCuz = Cold Creek silt-dominated unit
PA = performance assessment
RFtf = Ringold Formation Taylor Flat Unit
RFWie = Ringold Formation Wooded Island Unit E

Table 38. Summary of the Saturated Zone Parameter Distributions that will be Considered for the ERDF PA Uncertainty and Sensitivity Analyses.

Parameter	Distribution Type	Distribution Features
Saturated horizontal hydraulic conductivity of Ringold E	Uniform	Min: 0.1 m/d Max: 10 m/d
Saturated vertical anistropy	Triangular	Min: 0.01 Max: 0.5 Mode: 0.1 (Mean: 0.2)
Specific storage	Fixed value	1.32E-4 m^{-1}
Hydraulic gradient	Fixed value	0.00145

ERDF = Environmental Restoration Disposal Facility
PA = performance assessment

Table 39. Summary of the Transport Parameter Distributions that will be Considered for the ERDF PA Uncertainty and Sensitivity Analyses.

Parameter		Distribution	Hf1	Hf2	CCuz	CCuc	RFtf	RFwie
Bulk density (g/cm3)	Min Max	Uniform	1.85 2.19	1.60 1.98	1.60 1.72	1.60 1.72	1.60 1.98	1.93 2.32
Effective Diffusion Coefficient (cm^2/s)	Best	Fixed value	2.5E-5					
Vadose zone longitudinal dispersivity (cm)	Best	Fixed value	150	150	50	50	150	150
Vadose zone transverse dispersivity (cm)	Best	Fixed value	15	15	5	5	15	15
Saturated zone longitudinal dispersivity (m)	Min Max	Uniform	NA	NA	NA	NA	NA	1 20
Ratio longitudinal/transverse dispersivity (-)	Min Max	Uniform	NA	NA	NA	NA	NA	5 10

ERDF = Environmental Restoration Disposal Facility
Hf1 = Hanford formation 1
HF2 = Hanford formation 2
CCuc = Cold Creek Caliche (carbonate-dominated unit)
CCuz = Cold Creek silt-dominated unit
PA = performance assessment
RFtf = Ringold Formation Taylor Flat Unit
RFWie = Ringold Formation Wooded Island Unit E

Table 40. Summary of the K_d (mL/g) Distributions that will be Considered for the ERDF PA Uncertainty and Sensitivity Analyses. (2 Pages)

K_d (mL/g)		Distribution	Hf1	Hf2	CCuz	CCuc	RFtf	RFwie
^{3}H	Best	Fixed value	0	0	0	0	0	0
^{36}Cl	Best	Fixed value	0	0	0	0	0	0
$^{99}Tc(VII)$	Mode	Triangular	0	0	0	0	0	0
	Min		0	0	0	0	0	0
	Max		0.1	0.1	0.2	2	0.1	0
^{129}I	Mode	Triangular	0.1	0.2	0.2	0.2	0.2	0.1
	Min		0	0	0	0	0	0
	Max		1.2	2	5	2	2	0.9
^{14}C	Mode	Triangular (uniform for CCuc)	0.3	0.5	0.8		0.5	0.2
	Min		0	0	0.8	0.8	0	0
	Max		1.4	2.4	2.4	2.4	2.4	1.1
$^{60}Co(II,III)$	Mode	Triangular	5.9	10	10	15	10	4.6
	Min		0	0	0	3	0	0
	Max		1172	2000	2000	2000	2000	924
U(VI), all isotopes	Mode	Triangular	0.5	0.8	1.5	4	0.8	0.4
	Min		0.1	0.2	0.2	3	0.2	0.1
	Max		2.3	4	20	20	4	1.8
$^{237}Np(V)$	Mode	Triangular	5.9	10	20	10	10	4.6
	Min		1.4	2	5	2	2	1.2
	Max		17.6	30	60	30	30	13.9
$^{79}Se(VI,IV)$	Mode	Triangular	2.9	5	5	5	5	2.3
	Min		2	3	3	3	3	1.8
	Max		5.9	10	30	30	10	4.6
$^{226}Ra(II)$	Mode	Triangular	13.6	20	40	40	20	11.7
	Min		6.8	10	20	20	10	5.9
	Max		34.1	50	200	200	50	29.3
^{90}Sr	Mode	Triangular	13.6	20	40	40	20	11.7
	Min		6.8	10	20	20	10	5.9
	Max		34.1	50	200	200	50	29.3
$^{126}Sn(IV)$, all isotopes	Mode	Triangular	34.1	50	100	50	50	29.3
	Min		34.1	50	50	50	50	29.3
	Max		170.3	250	250	250	250	146.4
^{63}Ni, all isotopes	Mode	Triangular	204.4	300	300	300	300	175.7
	Min		34.1	50	50	50	50	29.3
	Max		1703.1	2500	2500	2500	2500	1464.4
^{241}Am, all isotopes	Mode	Triangular	204.4	300	300	150	300	175.7
	Min		40.9	60	200	60	60	35.5
	Max		1362.4	2000	4000	2000	2000	1171.5
Eu(III), all isotopes	Mode	Triangular	204.4	300	300	150	300	175.7
	Min		40.9	60	200	60	60	5.5
	Max		1362.4	2000	4000	2000	2000	1171.5
Pu, all isotopes	Mode	Triangular	408.7	600	600	300	600	351.4
	Min		136.2	200	200	200	200	117.1
	Max		1362.4	2000	4000	2000	2000	1171.5
^{137}Cs	Mode	Triangular	1362.4	2000	2000	2000	2000	1171.5
	Min		136.2	200	600	200	200	117.1
	Max		6812.2	1000	10000	10000	1000	5857.4

Table 40. Summary of the K_d (mL/g) Distributions that will be Considered for the ERDF PA Uncertainty and Sensitivity Analyses. (2 Pages)

K_d (mL/g)		Distribution	Hf1	Hf2	CCuz	CCuc	RFtf	RFwie
^{108m}Ag, all isotopes	Mode Min Max	Triangular	272.5 6.8 20436	400 10 30000	400 10 30000	400 10 30000	400 10 30000	243.3 5.9 17572
Nb, all isotopes	Mode Min Max	Triangular	0 0 0.1	0 0 0.1	0 0 0.1	0 0 0.1	0 0 0.1	0 0 0
^{113m}Cd	Mode Min Max	Triangular	204.4 54.5 681.2	300 80 1000	300 80 1000	300 80 1000	300 80 1000	175.7 46.9 585.7
^{232}Th	Mode Min Max	Triangular	681.2 27.2 1703	1000 40 2500	1000 40 2500	1000 40 2500	1000 40 2500	585.7 23.4 1464.4
Cm, all isotopes	Mode Min Max	Triangular	204.4 40.9 885.6	300 60 1300	300 60 1300	300 60 1300	300 60 1300	175.7 35.1 761.5
^{93}Zr	Mode Min Max	Triangular	681.2 27.2 1703	1000 40 2500	1000 40 2500	1000 40 2500	1000 40 2500	585.7 23.4 1464.4
^{151}Sm	Mode Min Max	Triangular	204.4 40.9 1362.4	300 60 2000	300 60 2000	300 60 2000	300 60 2000	175.7 35.1 1171.5
^{93}Mo	Best	Fixed value	0	0	0	0	0	0
^{40}K	Best	Fixed value	0	0	0	0	0	0

ERDF = Environmental Restoration Disposal Facility
Hf1 = Hanford formation 1
HF2 = Hanford formation 2
CCuc = Cold Creek Caliche (carbonate-dominated unit)
CCuz = Cold Creek silt-dominated unit
PA = performance assessment
RFtf = Ringold Formation Taylor Flat Unit
RFWie = Ringold Formation Wooded Island Unit E

Table 41. Summary of the Radionuclide Inventory (Curies or Metric Tons) that will be Considered for the ERDF PA Uncertainty and Sensitivity Analyses. (2 Pages)

Radionuclides	Total Inventory (Ci) (Currently Disposed + Forecasted) Decayed to 2035			Distribution
	Best	Min	Max	
^{108m}Ag	239.09	167.37	358.64	Triangular
^{241}Am	842.01	589.41	1263.02	
^{14}C	2341.2	1954.32	3410.08	
^{113m}Cd	1.37	0.95	2.05	
^{36}Cl	0.02	0.01	0.04	
^{244}Cm	11.81	8.27	17.71	
^{137}Cs	256295.1	185620.8	310713.1	
^{152}Eu	1417.33	992.13	2126	
^{154}Eu	219.67	153.77	329.5	
^{3}H	7962.21	5740.86	11636.89	
^{129}I	0.02	0.01	0.04	
^{40}K	0	0	1	
^{93}Mo	0.53	0.37	0.79	
^{93m}Nb	1.78	1.25	2.67	
^{94}Nb	0.38	0.27	0.57	
^{59}Ni	299.94	209.95	449.9	
^{63}Ni	12688.31	8886.05	19264.93	
^{237}Np	0.43	0.3	0.64	
^{238}Pu	76.1	60.88	107.21	
^{239}Pu	1458.99	1167.2	2136.53	
^{240}Pu	418.94	335.15	604.47	
^{241}Pu	1858.38	1486.71	2466.3	
^{242}Pu	0.72	0.58	0.94	
^{226}Ra	1.68	1.17	2.53	
^{79}Se	0.15	0.1	0.22	
^{151}Sm	266.83	186.78	400.25	
^{121m}Sn	12.59	8.81	18.88	
^{90}Sr	118166	60927.58	142537	
^{99}Tc	53	39	95.99	
^{232}Th	1.3	0.91	1.95	
^{233}U	14.61	11.68	18.99	
^{234}U	17.5	13.6	25.55	
^{235}U	7.9	6.29	10.48	
^{236}U	0.5	0.39	0.72	
^{238}U	87.5	68	127.75	

Table 41. Summary of the Radionuclide Inventory (Curies or Metric Tons) that will be Considered for the ERDF PA Uncertainty and Sensitivity Analyses. (2 Pages)

Radionuclides	Total Inventory (Ci) (Currently Disposed + Forecasted) Decayed to 2035			Distribution
	Best	Min	Max	Triangular
^{93}Zr	18	12.6	27	
^{60}Co	1536.25	1075.38	2304.37	
^{126}Sn	0.27	0.19	0.4	
^{243}Cm	0.52	0.36	0.78	
^{243}Am	0.8	0.56	1.2	

[a] Results are in Metric Tons (not Ci).

ERDF = Environmental Restoration Disposal Facility

PA = performance assessment

9.0 REFERENCES

Allard, B., B. Torstenfelt, K. Anderson, 1981, "Sorption Studies of H14CO on Some Geologic Media and Concrete," In J. G. Moore (ed.) *Scientific Basis for Nuclear Waste Management III*, Plenum Publ. Corp, New York, p. 465–472.

BHI-00007, 1994, *Prototype Hanford Surface Barrier: Design Basis Document*, Bechtel Hanford, Inc., Richland, Washington.

BNWL-243, 1966, *Soil Survey Hanford Project in Benton County, Washington*, Pacific Northwest Laboratory, Richland, Washington.

CP-47631, 2011, Model Package Report: Central Plateau Groundwater Model Version 3.3, Rev. 0, CH2M HILL Plateau Remediation Company, Richland, Washington.

DOE, 2005, *Technical Guidance Document for Tank Closure Environmental Impact Statement Vadose Zone and Groundwater Revised Analyses*, Rev. 0, Richland, Washington.

DOE/ORP-2005-01, 2006, *Initial Single-Shell Tank System Performance Assessment for the Hanford Site*, Rev. 0, U.S. Department of Energy, Office of River Protection, Richland, Washington.

DOE/RL-93-33, 1996, *Focused Feasibility Study of Engineered Barriers for Waste Management Units in the 200 Areas*, Rev. 0, U.S. Department of Energy, Richland Operations Office, Richland, Washington.

DOE/RL-2007-28, 2008, *Feasibility Study for the 200-ZP-1 Operable Unit*, U.S. Department of Energy, Richland Operations Office, Richland, Washington.

DOE/RL-2010-11, 2010, *Hanford Site Groundwater Monitoring and Performance Report for 2009 – Vol. 1 & 2*, Rev. 1, U.S. Department of Energy, Richland Operations Office, Richland, Washington.

DOE G 435.1-1, 1999, *Implementation Guide for Use with DOE M 435.1-1*, U.S. Department of Energy, Washington, D.C.

DOE M 435.1-1, 1999, *Low-Level Waste Disposal Facility Federal Review Group Manual,* U.S. Department of Energy, Washington, D.C.

Enfield, C. G., J. J. C. Hsieh and A. W. Warrick, 1973, "Evaluation of Water Flux Above a Deep Water Table Using Thermocouple Psychrometers," *Soil Sci. Soc. Am. P.* 37:968–970.

EPA 402-R-99-004B, 1999, *Understanding Variation in Partition Coefficient, K_d, Values. Volume II: Review of Geochemistry and Available K_d Values for Cadmium, Cesium, Chromium, Lead, Plutonium, Radon, Strontium, Thorium, Tritium (3H), and Uranium*, U.S. Environmental Protection Agency, Office of Air and Radiation, Washington, D.C.

EPA/600/R-02/099, 2002, *Assessment and Recommendations for Improving the Performance of Waste Containment Systems*, U.S. Environmental Protection Agency National Risk Management Research Laboratory, Cincinnati, Ohio.

EPA/600/R-05/074, 2005, *Partition Coefficient for Metals in Surface Water, Soil and Waste*, U.S. Environmental Protection Agency, Office of Research and Development, Washington, D.C.

EPA/630/R-97/001, 1997, *Guiding Principles for Monte Carlo Analysis*, Risk Assessment Forum, Washington, D.C.

Fayer, M. J. and G. W. Gee, 2006, "Multiple-Year Water Balance of Soil Covers in a Semiarid Setting," *J Environ. Qual.* 35:366-377.

Gardner, W. R., 1958, "Some Steady-State Solutions of the Unsaturated Moisture Flow Equation with Applications to Evaporation from a Water Table," *Soil Sci.* 85:228-232.

Gee, G. W., M. J. Fayer, M. L. Rockhold and M. D. Campbell, 1992, "Variations in Recharge at the Hanford Site," *Northwest Sci.* 66:237–250.

Gelhar, L. W. and C. L. Axness, 1983, "Three-Dimensional Analysis of Macrodispersion in a Stratified Aquifer," *Water Resources Research*, Vol. 19, pp. 161-180.

GoldSim Technology Group, 2009. *GoldSim Contaminant Transport Module User's Guide*, Version 5.0, Issaquah, Washington.

Harr, M. E., 1987, *Reliability-Based Design in Civil Engineering*, McGraw-Hill, New York.

Helton, J. C., 1993, "Uncertainty and Sensitivity Analysis Techniques for Use in Performance Assessment for Radioactive Waste Disposal," *Reliability Engineering & System Safety* 42:327–367.

Hoffman F. O., 1996, "The Effect of Distribution Choice for Uncertain Parameters in a Monte Carlo Analysis." Presented at Society of Risk Analysis Annual Meeting, Workshop on Quantitative Techniques for Analysis of Variability and Uncertainty in Exposure and Risk Assessment, New Orleans, December 8.

INEEL, 2004, *Multiphase Carbon-14 Transport in Near-Field-Scale Unsaturated Column of Natural Sediments*, INEEL/EXT-04-01793, Idaho National Engineering and Environmental Laboratory, Bechtel BWXT Idaho, LLC.

Keller, J. M., M. J. Fayer, R. J. Serne, and M. M. Valenta, 2007, "Assessment of the Chloride Mass Balance Technique: Accounting for Gravel Content," In Hartman, M. J., L. F. Morasch, and W. D. Webber (eds.), *Hanford Site Groundwater Monitoring for Fiscal Year 2006*, PNNL-16346, Pacific Northwest National Laboratory, Richland, Washington.

Khaleel, R., M. P. Connelly, and W. J. McMahon, 2006, *Modeling Data Package for an Initial Assessment of Closure of the S and SX Tank Farms*, RPP 17209, Rev. 1, CH2M HILL Hanford Group, Inc., Richland, Washington.

Koerner and Hsuan, 2003, Proceedings Assoc. of State Dam Safety Officials Conference, Lake Harmony, Pennsylvania, June 4-6.

Millington, R. J. and J. P. Quirk, 1961, "Permeability of Porous Solids," *Trans. Faraday Soc.* 57:1200-1207.

Mishra, S., 2002, "Assigning Probability Distributions to Input Parameters of Performance Assessment Models," SKB Technical Report TR-02-11, Swedish Nuclear Fuel and Waste Management Co., Stockholm, 49 p.

Mishra, S., 2007, "Uncertainty and Sensitivity Analysis Techniques for Hydrologic Modeling," International Workshop on Advances in Hydroinformatics 4 – 7 June 2007, Niagara Falls, Canada.

Mualem Y., 1976, "A New Model for Predicting the Hydraulic Conductivity of Unsaturated Porous Media," *Water Resources Research*, Vol. 12, p. 513-522.

Murphy, E. M., T. R. Ginn, and J. L. Phillips, 1996, "Geochemical Estimates of Paleorecharge in the Pasco Basin: Evaluation of the Chloride Mass-Balance Technique," *Water Resour. Res.* 32(9):2853–2868.

Neuman, S. P., 1990, "Universal Scaling of Hydraulic Conductivities and Dispersivities in Geologic Media," *Water Resources Research*, Vol. 26, No. 8, p. 1749-1758.

PNNL-6415, 2005, *Hanford Site National Environmental Policy Act (NEPA) Characterization*, Rev. 17, Pacific Northwest National Laboratory, Richland, Washington.

PNL-10872, 1995, *Hanford Prototype-Barrier Status Report: FY 1995*, Pacific Northwest National Laboratory, Richland, Washington.

PNL-10886, 1995, *Development of a Three-Dimensional Ground-Water Model of the Hanford Site Unconfined Aquifer System: FY 1995 Status Report*, Pacific Northwest Laboratory, Richland, Washington.

PNNL-11800, 1998, *Composite Analysis for Low-Level Waste Disposal in the 200 Area Plateau of the Hanford Site*, Pacific Northwest National Laboratory, Richland, Washington.

PNNL-12030, 2000, *STOMP Subsurface Transport Over Multiple Phases: Theory Guide*, Pacific Northwest National Laboratory, Richland, Washington.

PNNL-13033, 1999, *Recharge Data Package for the Immobilized Low-Activity Waste 2001 Performance Assessment*, Pacific Northwest National Laboratory, Richland, Washington.

PNNL-13641, 2001, *Uncertainty Analysis Framework – Hanford Site-Wide Groundwater Flow and Transport Model*, Pacific Northwest National Laboratory, Richland, Washington.

PNNL-14398, 2003, *Transient Inverse Calibration of the Site-Wide Groundwater Flow Model (ACM-2): FY 2003 Progress Report*, Pacific Northwest National Laboratory, Richland, Washington.

PNNL-14702, 2006, *Vadose Zone Hydrogeology Data Package for Hanford Assessments*, Pacific Northwest National Laboratory, Richland, Washington.

PNNL-14744, 2004, *Recharge Data Package for the 2005 Integrated Disposal Facility Performance Assessment*, Pacific Northwest National Laboratory, Richland, Washington.

PNNL-14753, 2006, *Groundwater Data Package for Hanford Assessments*, Pacific Northwest National Laboratory, Richland, Washington.

PNNL-16663, 2007, *Geochemical Processes Data Package for the Vadose Zone in the Single-Shell Tank Waste Management Areas at the Hanford Site*, Pacific Northwest National Laboratory, Richland, Washington.

PNNL-16688, 2007, *Recharge Data Package for Hanford Single-Shell Tank Waste Management Areas*, Pacific Northwest National Laboratory, Richland, Washington.

PNNL-17154, 2008, *Geochemical Characterization Data Package for the Vadose Zone in the Single-Shell Tank Waste Management Areas at the Hanford Site*, Pacific Northwest National Laboratory, Richland, Washington.

PNNL-18845, 2011, *200-BP-1 Prototype Hanford Barrier – 15 Years of Performance Monitoring*, Rev. 1, Pacific Northwest National Laboratory, Richland, Washington.

PNNL-18934, 2009, *The Effects of Fire on the Function of the 200-BP-1 Engineered Surface Barrier*, Pacific Northwest National Laboratory, Richland, Washington.

PNNL-19482, 2010, *Slug Test Characterization Results for Multi-Test/Depth Intervals Conducted During the Drilling of CERCLA Operable Unit OU UP-1 Wells 299-W19-48, 699-30-66, and 699-36-70B*, Pacific Northwest National Laboratory, Richland, Washington.

Polmann, D. J., 1990, Application of Stochastic Methods to Transient Flow and Transport in Heterogeneous Unsaturated Soils, Ph.D. Thesis, Massachusetts Institute of Technology, Cambridge, Massachusetts.

Prych, E. A., 1998, *Using Chloride and Chlorine-36 as Soil-Water Tracers to Estimate Deep Percolation at Selected Locations on the U.S. Department of Energy Hanford Site, Washington*, Water-Supply Paper 2481, U.S. Geological Survey, Tacoma, Washington.

Resource Conservation and Recovery Act of 1976, 42 U.S.C. 6901, et seq., as amended.

Rowe, R. K., 2005, "Long-Term Performance of Contaminant Barrier Systems," *Geotechnique* 55(9), 631-678.

Schulze-Makuch, D., 2005, "Longitudinal Dispersivity Data and Implications for Scaling Behavior," *Ground Water*, Vol. 43, No. 3, p. 443–456.

van der Kamp, G., L. D. Luba, J. A. Cherry, and H. Maathuis, 1994, "Field Study of a Long and Very Narrow Contaminant Plume," *Ground Water,* Vol. 32, No. 6, p. 1008–1016.

van Genuchten, M. T., 1980, "A closed-form solution for predicting the conductivity of unsaturated soils," *Soil Sci. Soc. Am. J.*, 44, 892-898.

WCH-295, 2008, *Groundwater and Leachate Monitoring and Sampling at ERDF, CY 2007*, Rev. 0, Washington Closure Hanford, Richland, Washington.

WCH-315, 2009, *Groundwater and Leachate Monitoring and Sampling at ERDF, CY 2008*, Rev. 0, Washington Closure Hanford, Richland, Washington.

WCH-462, 2013, *ERDF Performance Assessment Modeling Approach*, Draft Rev. B, Washington Closure Hanford, Richland, Washington.

WCH-463, 2013, *Hydrogeologic Model for the Environmental Restoration Disposal Facility, Hanford Site*, Draft Rev. A, Washington Closure Hanford, Richland, Washington.

WCH-464, 2013, *Hydrologic Data Package in Support of Environmental Restoration Disposal Facility Performance Assessment Modeling*, Washington Closure Hanford, Richland, Washington.

WCH-476, 2013, *Chemical Reactivity of Radionuclides with Waste Material and Subsurface Soils During Release and Migration from the Environmental Restoration Disposal Facility*, Washington Closure Hanford, Richland, Washington.

WCH-479, 2013, *Inventory Data Package for ERDF Waste Disposal*, Draft Rev. A, Washington Closure Hanford, Richland, Washington.

WHC-EP-0883, 1995, *Variability and Scaling of Hydraulic Properties for 200 Area Soils, Hanford Site*, Westinghouse Hanford Company, Richland, Washington.

WHC-SD-WM-EE-004, 1995, *Performance Assessment of Grouted Double-Shell Tank Waste Disposal at Hanford,* Rev. 1, Westinghouse Hanford Company, Richland, Washington.

Xu, M. and Y. Eckstein, 1995, "Use of Weighted Least-Squares Method in Evaluation of the Relationship Between Dispersivity and Filed Scale," *Ground Water*, Vol. 33, No. 6, p.905-908.

APPENDIX A

PROPAGATION OF UNCERTAINTY IN VADOSE ZONE FLOW PARAMETERS

APPENDIX A

PROPAGATION OF UNCERTAINTY IN VADOSE ZONE FLOW PARAMETERS

The uncertainty in recharge rates was derived from sampling the probability distributions listed in Table 11 for parameters that vary spatially and temporally. To cover the parameter range the values were selected at five different percentiles from each probability distribution function: 0th percentile (minimum), 25th percentile (lower quartile), 50th percentile (median), 75th percentile (upper quartile), and 100th percentile (maximum). The five sampled values were judged adequate in order to balance the computational burden without sacrificing the full range of uncertainty. Table A-1 presents the selected recharge parameter values for the uncertainty analysis along with the value chosen as the best estimate for the compliance calculation (deterministic case).

Table A-1. Uncertainty in Recharge Rate Parameters.

Recharge Zone	Unit	Distribution	Min	25th Percentile	Median	75th Percentile	Max	Compliance Value
Undisturbed zone/natural conditions (for all times)	mm/yr	Triangular	0.26	1.05	1.59	2.30	4	1.7
Disturbed zone (bare soil) from 1996 to 2035	mm/yr	Triangular	22.5	31.54	42.27	56.25	90	45
Below side slopes of surface barrier and berm (for all times)	mm/yr	Fixed value	2	2	2	2	2	2
Below intact liner (construction area) from 2035 to 2135	mm/yr	Fixed value	0	0	0	0	0	0
Below the top portion of the surface barrier from 2135 to 2535 (degraded liner)	mm/yr	Triangular	0.05	0.38	0.52	0.66	1	0.5
Below the degraded top portion of the surface barrier after 2535 (degraded liner)	mm/yr	Triangular	0.1	0.75	1.03	1.31	2	1

The uncertainty in the vadose zone hydraulic parameter was considered by evaluating the combination of parameter values that lead to uncertainty in unsaturated hydraulic conductivity (the primary parameter that affects moisture content when recharge is constant) as a function of soil matric potential. A family of 200 unsaturated hydraulic conductivity curves as a function of soil matric potential (water tension) are generated based on sampling the uncertainty in van Genuchten-Mualem parameters listed in Table 18 for each hydrostratigraphic unit. The results are presented in Figure A-1. The uncertainty range in unsaturated hydraulic conductivity curves

is evaluated around -700 cm, which is within the expected soil matric potential range of about -600 cm to about -1,000 cm in the vadose zone sediments in the vicinity of ERDF under post-closure recharge conditions, as shown in Figure A-2 (generated from preliminary flow model calculations).

An empirical cumulative distribution function is created from 200 synthetic data points and the hydraulic parameter set corresponding to the 0th (minimum), 25th (lower quartile), 50th (median), 75th (upper quartile), and 100th percentile (maximum) unsaturated hydraulic conductivity curves are selected. Table A-2 provides the selected hydraulic parameter values for the uncertainty analyses. It is important to note that the percentile vadose zone hydraulic parameter values refer to collective sets of parameter values (i.e., saturated moisture content, van Genuchten α and n, and residual saturation) associated with the selected unsaturated hydraulic conductivity-matric potential characteristic curve, and not to the properties individually. Each set of parameters produces a unique characteristic curve, and the percentile values are determined according to the magnitude of the unsaturated hydraulic conductivity at -700 cm matric potential. Thus, a maximum vadose zone hydraulic parameter value does not necessarily represent the largest value of that particular parameter, but the value associated with the maximum unsaturated hydraulic conductivity curve, and the corresponding set of parameters.

In order to derive the uncertainty range in flow field, the recharge rates sampled for the given percentile are combined with the vadose zone hydraulic parameters for the corresponding percentile. For example, the 75th percentile recharge rate values from Table A-1 and 75th percentile vadose zone hydraulic parameter values from Table A-2 are used as input to the flow model. As a result five flow fields are generated for the purpose of evaluating uncertainty.

Figure A-1. Family of Unsaturated Hydraulic Conductivity Curves as a Function of Matric Potential for the Hydrostratigraphic Units at ERDF.

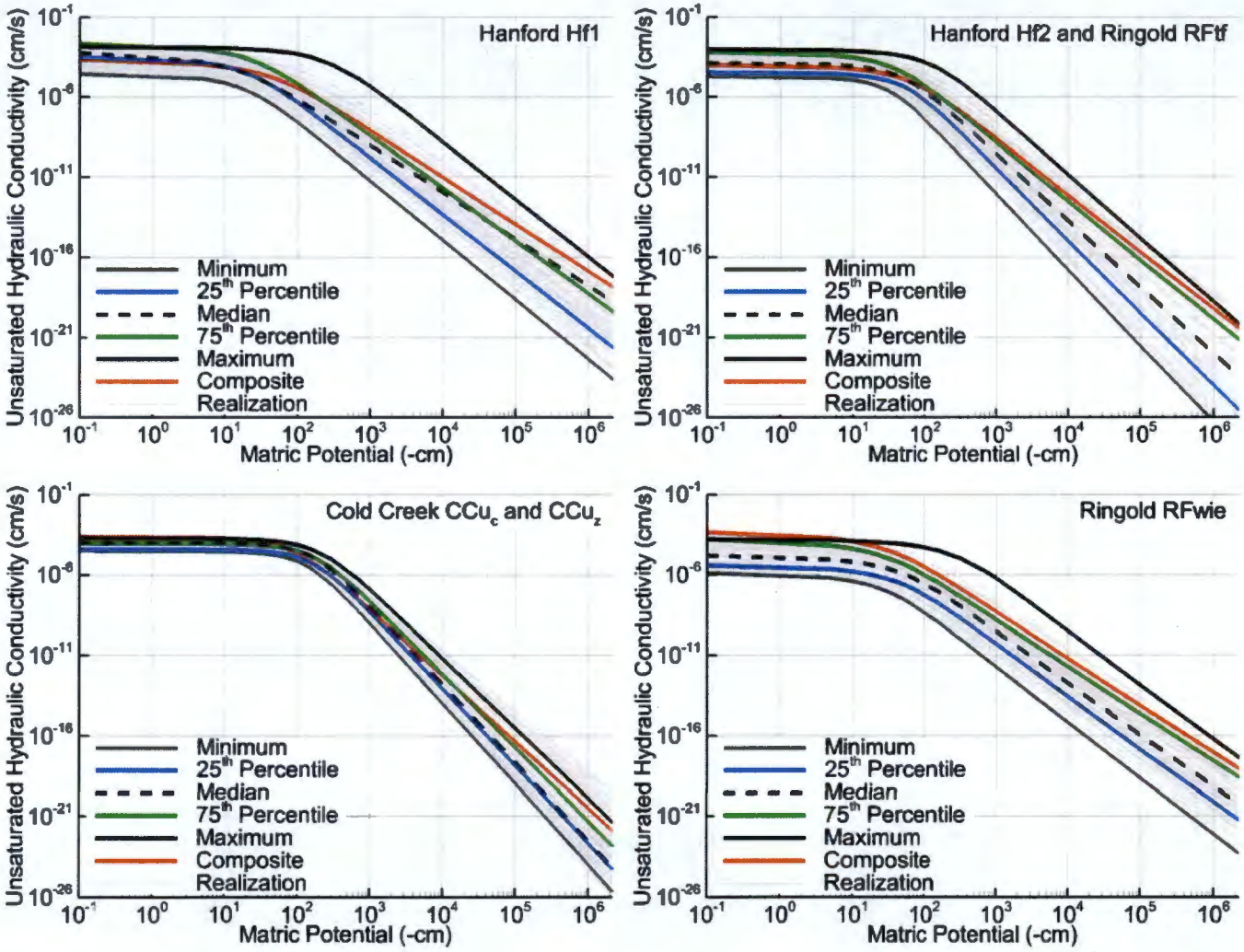

Table A-2. Percentile Values of van Genuchten-Mualem Parameters for Various Strata at the ERDF Site [a].

Strata	Percentile	θ_s	θ_r	α (1/cm)	n	Fitted K_s (cm/s)
Hanford Hf1 (gravel-dominated)[b]	Minimum	0.2335	0.0224	0.0398	1.6796	2.89E-05
	25th Percentile	0.2729	0.0055	0.0388	1.7527	1.05E-03
	Median	0.2016	0.0107	0.0286	1.7051	1.20E-03
	75th Percentile	0.2079	0.0217	0.0111	1.5827	1.15E-04
	Maximum	0.2033	0.0049	0.0027	1.6380	1.42E-03
	Compliance	0.2126	0.0032	0.0141	1.3730	2.62E-04
Hanford Hf2 (sand-dominated)[c]	Minimum	0.4084	0.1004	0.0270	2.0932	1.86E-05
	25th Percentile	0.3310	0.0956	0.0149	2.0258	2.85E-05
	Median	0.3675	0.1293	0.0122	1.9314	5.00E-05
	75th Percentile	0.3526	0.1034	0.0083	2.0028	6.19E-05
	Maximum	0.3515	0.0238	0.0062	1.7888	9.14E-04
	Compliance	0.3819	0.0443	0.0117	1.6162	9.88E-05
Cold Creek CCu_z (silt-dominated) and CCu_c (caliche)	Minimum	0.4283	0.0469	0.0063	2.1904	3.07E-05
	25th Percentile	0.3603	0.0233	0.0060	2.0896	9.09E-05
	Median	0.4358	0.0281	0.0050	2.1405	1.02E-04
	75th Percentile	0.3843	0.0114	0.0045	2.0279	9.27E-05
	Maximum	0.3916	0.0111	0.0038	1.9401	1.99E-04
	Compliance	0.4349	0.0665	0.0085	1.8512	2.40E-04
Ringold RFtf	Minimum	0.4084	0.1004	0.0270	2.0932	1.86E-05
	25th Percentile	0.3310	0.0956	0.0149	2.0258	2.85E-05
	Median	0.3675	0.1293	0.0122	1.9314	5.00E-05
	75th Percentile	0.3526	0.1034	0.0083	2.0028	6.19E-05
	Maximum	0.3515	0.0238	0.0062	1.7888	9.14E-04
	Compliance	0.3819	0.0443	0.0117	1.6162	9.88E-05
Ringold RFwie	Minimum	0.1757	0.0137	0.0274	1.5882	1.35E-06
	25th Percentile	0.1264	0.0069	0.0186	1.5838	8.52E-06
	Median	0.2059	0.0130	0.0131	1.3288	8.59E-06
	75th Percentile	0.1172	0.0022	0.0151	1.4800	8.43E-05
	Maximum	0.1366	0.0030	0.0026	1.5553	1.74E-04
	Compliance	0.1380	0.0100	0.0210	1.374	5.60E-04

[a] The connectivity parameter ℓ is assumed to be 0.5 for all strata and all percentile values.

[b] The parameters for the Hanford Hf1 (gravel-dominated) unit are applied to the ERDF waste soil and ERDF berm material.

[c] The parameters for the Hanford Hf2 (sand-dominated) unit are applied to the ERDF composite liner material.

Figure A-2. Steady-state Moisture Content and Matric Potential of the Vadose Zone Units Under Post-Closure Recharge Rate of 1 mm/yr

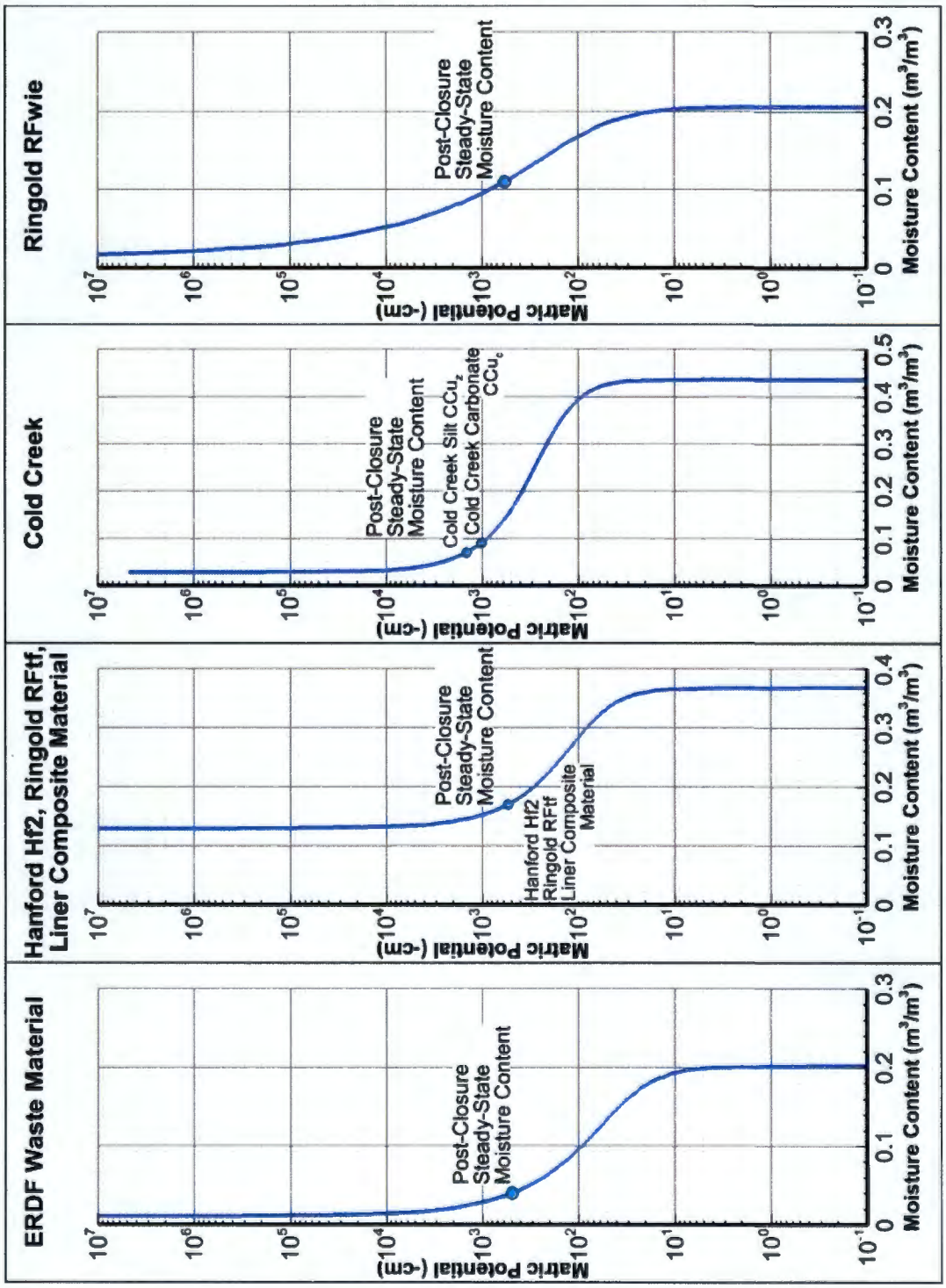

Note: ERDF Waste Material is given hydraulic properties of Hanford Hf1 unit

DISTRIBUTION

U.S. Department of Energy
Richland Operations Office

R. D. Hildebrand (1 CD only)	A6-38
O. C. Robertson (10 CDs only)	A3-04

Washington Closure Hanford

J. F. Armatrout	T2-03
W. A. Borlaug	T2-03
M. A. Casbon	T2-03
R. J. Landon	H4-21
B. L. Lawrence	T2-03

CH2MHILL Plateau Remediation Company

S. Mehta (1 CD only)	H8-51

Document Control	H4-11